

# Chapter 1

## Microscopy

### **Introduction**

Since the first microscope setting up, the world of microscopy has revolutionized biology and it remains not only an essential tool in that science, but also an important research methodology in many other sciences, including material science, numerous engineering disciplines, and food sciences. Three branches of microscopy are well-known: optical, electron and scanning probe microscopy.

Optical and electron microscopy are based on the diffraction, reflection, or refraction of electron beam interacting with the subject of study, and the subsequent collection of this scattered radiation in order to build up an image. This process may be carried out by wide-field irradiation of the sample (for example, standard light microscopy and transmission electron microscopy) or by scanning of a fine beam over the sample (for example, confocal laser scanning microscopy and scanning electron microscopy).

Scanning probe microscopy involves the interaction of a scanning probe with the surface or object of interest (Abramowitz and Davidson, 2007).

### *1.1 Optical microscopy*

In optical microscopy, visible light is transmitted through or reflected from the sample through a single or multiple lenses to allow a magnified view of the sample (Abramowitz and Davidson, 2007). The resulting image can be detected directly by the eye, imaged on a photographic plate or captured digitally. The

single lens with its attachments, or the system of lenses and imaging equipment, along with the appropriate lighting equipment, sample stage and support, makes up the basic light microscope. The most recent development is the digital microscope which uses a CCD camera to focus on the exhibit of interest. The image is shown on a computer screen since the camera is connected, so eye-pieces are unnecessary. The technique can only image dark or strongly refracting objects effectively.

Conventional optical microscope (i.e. bright field microscopy) presents two main limitations: out of focus light from points outside the focal plane reduces image clarity and diffraction limits resolution to approximately 0.25 micrometers. Indeed, a light microscope, even one with perfect lenses and perfect illumination, simply cannot be used to distinguish objects that are smaller than half the wavelength of light. White light has an average wavelength of 0.55 micrometers, half of which is 0.275 micrometers. Any two lines that are closer together than 0.275 micrometers will be seen as a single line, and any object with a diameter smaller than 0.275 micrometers will be invisible or, at best, show up as a blur. To see nano-particles under a microscope, scientists must bypass light altogether and use a different sort of "illumination," one with a shorter wavelength.

## *1.2 Fluorescence Microscope*

A fluorescence microscope is a light microscope that uses the fluorescence phenomenon to study properties of the observed organic or inorganic substances (Spring and Davidson, 2008). It is the most popular method for studying the dynamic behavior exhibited in live cell imaging. In a conventional reflected fluorescence light microscope, the light emitted from a mercury arc lamp provides a mixture of wavelength from UV to red. Each component in the substrate can absorb a specific wavelength. An emission filter is necessary to isolate the desired wavelength. Many cellular components are colorless and cannot be clearly distinguished under a microscope, thus usually the component of interest is previously labeled with a specific dye. The fundamental idea is to bind the dye to molecules of interest, so that the spatial distribution of these molecules is revealed from the location of the dye. In the conventional fluorescence microscope the entire specimen is flooded in light from a light source. All parts of the specimen in

the optical path are excited and the resulting fluorescence is detected by the microscope photodetector as background signal. To go over this limitation, an evolution of this kind of microscope has been set up and it is represented by the confocal microscope.

### *1.3 Confocal Laser Scanning Microscope*

Confocal microscopy is a relatively recent non-destructive testing (NDT) method which offers an attractive opportunity for the 3D insight of the inner structure of several kind of substrates. Originally invented by Marvin Minsky in 1957 to overcome some limitation of wide-field fluorescence microscopes, CLSM has been significantly improved and nowadays it is used in many fields, from biological to material and food sciences and for industrial applications, when a correlation is required between the macroscopic behaviour of matter and its microscopic properties.

CLSM becomes even more powerful if different stages are connected. They allow to induce changes in the substrates structure directly under the microscopes. Several type of stages are available: time-temperature and tensile are two of the most used (Lorén et al, 2007)

The basic components forming a CLSM system (Figure 1.1) are the laser source, which provides light at discrete band of wavelength and has very high intensity, a beam splitter, the objective, the pinhole, which only selects the fluorescence light emitted by the in-focus plane hitting the detection system, to collect the emitted light emerging from the sample, and the sample positioning stages (Blonk and Van Aalst 1993).

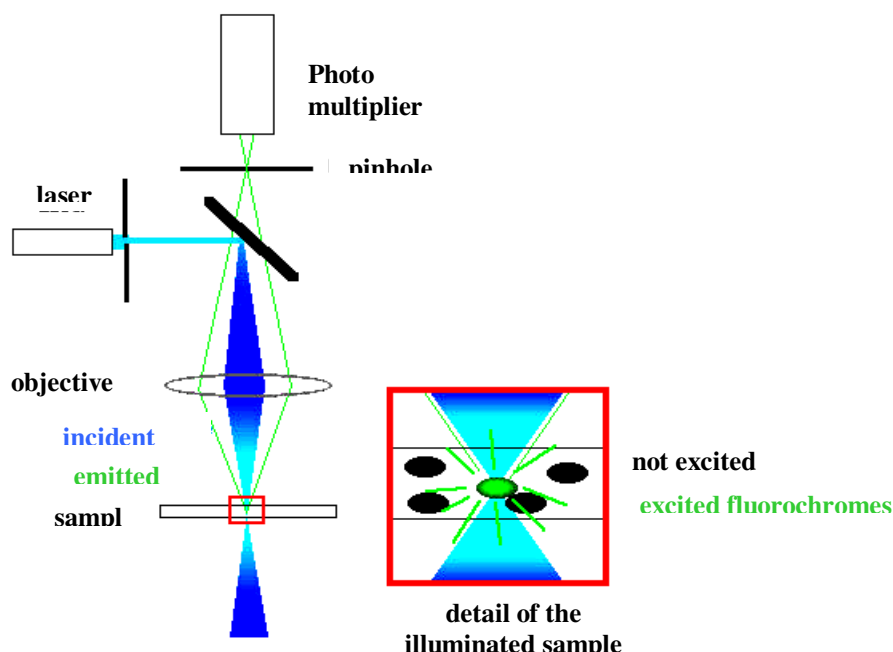


**Figure.1.1.** Main components in a Confocal Laser Scanning Microscopy.

Lasers that can deliver well-defined wavelengths, have a number of unique properties, such as high degree of monochromaticity and spatial and temporal coherence, small divergence, high brightness, plane-polarised emission, and a Gaussian beam profile that make them an almost ideal light source for use in a CLSM (Gratton and Van Deven, 1995). Since different fluorochromes require different excitation wavelengths, more than one laser is needed to cover the most essential wavelengths for multiple staining components. The laser power transmitted from each laser is controlled by an acousto-optical tunable filter (AOTF), which mixes the proportion of light coming from each laser and transmits it to the specimen almost instantaneously. The beam splitter directs the incoming laser light towards the specimen and the re-emitted fluorescent light towards the detector. The beam splitter is made of a filter, which consists of wavelength-discriminating mirrors or an acousto-optic beam splitter (AOBS). The wavelength-discriminating mirrors are dichroics and trichroics, that reflect light with certain wavelengths and allow light with other wavelengths to pass (Lorén et al. 2007).

The objective is the most important instrumental component in determining the information content of an image (Keller, 1995). The role of the objective is to focus the laser beam and to ensure constructive interference at the focal point. The resolved details in the specimen, the contrast at which details are presented, the

depth through the specimen from which useful information can be obtained and the diameter of the useful scanned region are all limited by the performance of the objective. The most important parameters that a CLSM user must consider are the magnification, the numerical aperture and the working distance of the objective. Basically, the numerical aperture determines how much of the re-emitted fluorescent light is collected by the objective. Spatial resolution is defined as the minimum spatial separation required between two points to distinguish them as two separate objects. The lateral and axial resolutions can be estimated as:

$$R_{lateral} \approx \frac{0.4\lambda_e}{NA} \qquad R_{axial} \approx \frac{1.4\lambda_e}{NA^2}$$

Where  $\lambda_e$  is the wavelength of the detected light and NA is the numerical aperture (Jonkman and Stelzer, 2002). A very important factor that a CLSM user should consider is the refractive index. Objective are made for a specific immersion medium, which could be water or oil. Using the correct medium is crucial in order to obtain the maximum performance from the microscope.

CLSM is based on the same physical principles of fluorescence microscope but it takes the advantage of a rejection of out of focus fluorescent light and it provides a better resolution either in vertical and horizontal planes. In a confocal microscope, the point source of light illuminates just a small conical region of the specimen, the emitted light is collected from the objective and focused on the pinhole and a confocal point detector, which is usually a photo multiplier tube (PMT), simultaneously acquires light from the same illuminated region (Sheppard and Shotton, 1997). The dimension of the illuminated area is determined by the effects of diffraction and aberration of the ocular and it is usually 0.5  $\mu$ m. Fluorescence light emanating from region above or below the in-focus plane is blocked by the pinhole and totally prevented from reaching the detector. The primary component in the detector is the photomultiplier tube (PMT), which counts the number of photons. However, just a fraction of all photons that reach the PMT becomes registered because of various PMT properties like quantum efficiency, responsivity, spectral response, inherent noise, response time and linearity, which differ from one PMT to another (Art, 1995). From several slices recorded at different depths by moving the specimen in the axial direction and

through specific mathematical algorithm, a volume can be rendered and 3D information can be available (Diaspro, 2002).

### *1.4 CLSM Techniques*

CLSM can be utilised for many type of sophisticated fluorescence-based microscopy techniques such as Fluorescence Recovery After Photobleaching (FRAP), Fluorescence Correlation Spectroscopy (FCS), Fluorescence Loss In Photobleaching (FLIP), Fluorescence In-Situ Hybridization (FISH), Fluorescence Resonance Energy Transfer (FRET), and Fluorescence Lifetime Imaging Microscopy (FLIM) (Navratil et al, 2005; Nath and Jonhson, 2000; Bastiaens and Squire, 1999).

FRAP in connection with CLSM is a versatile technique that has been used to study many different phenomena and materials such as intracellular molecules (Braga et al, 2004), binding interactions between cellular molecules (Sprague and McNally, 2005), polymer solutions and gels (Burke et al, 2000), protein dynamics in living cells (Lippincott-Schwartz et al., 2003) and whey protein diffusion (Weinbreck et al., 2004). The main idea of FRAP is to quickly destroy part of the fluorochromes irreversibly due to photon-induced chemical damage in a certain local region of the specimen using high intensity laser beam. As a consequence of this process, called photobleaching, the concentration of fluorochromes that can emit light, and consequently, pixel intensity in the bleached region decrease. However, new fresh fluorochromes from adjacent region immediately start to diffuse out from the bleached region, which results in a recovery of the pixel intensity. The rate of the recovery is proportional to the diffusion rate of the fluorochromes. Basically, higher mobility of the molecules result in a shorter time of recovery and vice versa.

FCS is a technique in which spontaneous fluorescence intensity fluctuations are measured in a microscopic detection volume of about  $1\text{ }\mu\text{m}^3$  defined by tightly focused laser beam in the CLSM. Fluorescence intensity fluctuations represent changes in either the number or the fluorescence quantum yield of molecules resident in the observed volume. Small, rapidly diffusing molecules produce rapidly fluctuating intensity patterns, whereas larger molecules produce more sustained bursts of fluorescence (Hess et al, 2002).

In a FLIP experiment, a small fluorescent region in the sample is repeatedly photobleached while the rest is repeatedly imaged. Any regions that are connected to the bleached area will gradually lose fluorescence due to lateral movement of mobile fluorochromes into this area. By contrast, the fluorescence in unconnected regions will not be affected. FLIP is useful to determine mass transport in cells. FLIP can also be used to assess whether a protein moves uniformly across a particular cell compartment or undergoes interactions that impede this motion (Lippincott-Schwartz et al., 2003).

FISH is a technique used to detect and localize the presence or absence of specific DNA sequences on chromosomes. FISH uses fluorescent probes that bind to only those parts of the chromosome with which they show a high degree of sequence similarity. Fluorescence microscopy can be used to find out where the fluorescent probe binds to the chromosomes. FISH is often used for finding specific features in DNA for use in genetic counseling and species identification (Nath J., K.L. Jonsson. 2000). Biofilms, for example, are composed of complex multi-species bacterial organizations. Preparing DNA probes for one species and performing FISH with this probe allows to visualize the distribution of this specific species within the biofilm. Preparing probes (in two different colors) for two species allows to visualize/study co-localization of these two species in the biofilm, and can be useful in determining the fine architecture of the biofilm (Moter and Göbel, U., 2000). FISH can also be used to detect and localize specific mRNAs within tissue samples. In this context, it can help defining the spatial-temporal patterns of gene expression within cells and tissues.

FLIM is a new fluorescence microscopy technology. In addition to multi-color staining, fluorescence lifetime imaging can also be utilized to visualize the factors that affect the fluorescence lifetime properties of the dye molecule, that is the state of the environment around the molecule. With this technique, five or six dyes in the wavelength range from ultra violet to near infrared can be used simultaneously under microscopy with no confusion between colours. Each fluorescent dye has its own lifetime in the excited state. By detecting differences in lifetime, it is possible to distinguish even dyes having the same fluorescent colour as well as to identify autofluorescence. Furthermore, images showing high signal-to-noise ratio can be obtained by using a probe with very long lifetime compared to that of the fluorescent dyes normally used. For instance, platinum coproporphyrin has a

lifetime of millisecond order while the lifetimes of ordinary fluorescent dyes are of nanosecond order. Such relatively long-lived fluorescent dyes will soon be used as probes for DNA detection on chips.

Fluorescence lifetime imaging also makes it possible to obtain information on the molecules while observing a living cell. The factors affecting the fluorescence lifetime include ion intensity, hydrophobic properties, oxygen concentration, molecular binding, and molecular interaction by energy transfer when two proteins approach each other. Lifetime is, however, independent of dye concentration, photobleaching, light scattering and excitation light intensity. Therefore, fluorescence lifetime imaging allows us to perform accurate ion concentration measurement. For instance, FLIM allows quantitative  $\text{Ca}^{2+}$  imaging using visible-wavelength illumination (Lakowicz, J.R. and Szmacinski, 1996).

In confocal laser scanning microscopy, as well as in molecular biology, FRET is a useful tool to quantify molecular dynamics in biophysics and biochemistry, such as protein-protein interactions, protein-DNA interactions, and protein conformational changes. For monitoring the complex formation between two molecules, one of them is labelled with a donor and the other with an acceptor, and these fluorophore-labelled molecules are mixed. When they are dissociated, the donor emission is detected upon the donor excitation. On the other hand, when the donor and acceptor are in proximity (1-10 nm) due to the interaction of the two molecules, the acceptor emission is predominantly observed because of the intermolecular FRET from the donor to the acceptor. For monitoring protein conformational changes, the target protein is labeled with a donor and an acceptor at two loci. When a twist or bend of the protein brings the change in the distance or relative orientation of the donor and acceptor, FRET change is observed. If a molecular interaction or a protein conformational change is dependent on ligand binding, this FRET technique is applicable to fluorescent indicators for the ligand detection.

FRET quantification is most often based on measuring changes in fluorescence intensity or fluorescence lifetime upon changing the experimental conditions. For instance, a microscope image of donor emission is taken with the acceptor being present. The acceptor is then bleached, such that it is incapable of accepting energy transfer and another donor emission image is acquired. A pixel-based quantification using the second equation in the theory section above is then

possible. An alternative way of temporarily deactivating the acceptor is based on its fluorescence saturation. Exploiting polarisation characteristics of light, a FRET quantification is also possible with only a single camera exposure (Cardullo and Parpura, 2003).

## **Conclusions**

Microscopy allows direct visualization of microstructure. Sophisticated instrumentation is expensive but it provides an opportunity to understand structure at basic molecular level and allow us to predict structural development.

By this introductory chapter I gave an overview of the optical microscopy world, especially focusing on CLSM: Its main components and the physical background of the laser interaction with matter were also briefly pointed out.

It is well known that CLSM can provide better images than the conventional fluorescence microscope, due to the many advantages of the pinhole system. Indeed, this little aperture is an ideal tool to eliminate the out of focus light and to obtain higher quality images. Then, it also allows to perform quantitative studies about the sample components distribution, dimension and organization.

Optical sections, acquired at different depths of the samples, can be combined by a specific software into a three-dimensional representation of the microstructure.

Many extra components of the CLSM (i.e. time-temperature, tensile, shear and flow stages) offer the possibility to manipulate the structure directly under the microscope, even though this development is still in its infancy.

CLSM can be used for many sophisticated fluorescence-based microscopy techniques like FRAP, FRET, FLIM and FLIP in a wide range of experiments.

# Chapter 2

## Fluorescence

### Introduction

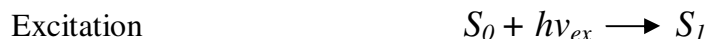
Fluorescence illumination and observation is the most rapidly expanding microscopy technique in biological sciences. In contrast to other methods of optical microscopy that are based on macroscopic specimen features, such as phase gradients and light absorption, fluorescence microscopy is capable of imaging the distribution of a single molecular species based solely on the properties of fluorescence emission. Most specimens studied with confocal microscopy are labelled with fluorescent substances which can emit light in some area of the spectrum. Thus, the precise location of labeled intracellular components can be monitored, as well as their associated diffusion coefficients, transport characteristics, and interactions with other biomolecules. In addition, fluorescence enables the investigation of pH, viscosity, refractive index, ionic concentrations, membrane potential, and solvent polarity (Slavik, 1996).

Since the introduction of immunofluorescence, many fluorescent probes, constructed around synthetic aromatic organic chemicals, are designed to bind with a specific biological macromolecule. Fluorescent dyes are also useful in monitoring cellular integrity (live versus dead and apoptosis), protein trafficking, and enzymatic activity. Moreover, fluorescent probes have been widely applied to genetic mapping and chromosome analysis in the field of molecular genetics (Allan, 2000). One of the most important fluorescent probes is the Green Fluorescent Protein (GFP), which has revolutionized optical imaging, letting the observation of real-time dynamic processes in their natural environment.

Photomicrography under fluorescence illumination conditions can present a unique set of circumstances posing some problems for the microscopist. Exposure times are often exceedingly long, the specimen's fluorescence may fade during exposure, and totally black backgrounds often signal light meters to suggest overexposure. That is the reason why the fluorophores should be chosen accurately and the microscope should to be used appropriately.

## 2.1 Basic concepts of Fluorescence

Fluorescence is a luminescence phenomenon, which occurs when a molecule, atom or nanostructure relaxes to its ground state after being electrically excited.



$h\nu$  is a generic term for photon energy:  $h$  = Planck's constant and  $\nu$  = frequency of light.

Electronic Ground State of the fluorescent molecule is called  $S_0$  and  $S_1$  is the first (electronically) excited state.

The Jablonski Diagram (Figure 2.1) shows a number of possible routes by which an excited molecule can return to its ground state via unstable triplet states. A rapid return results in fluorescence and a delayed return results in phosphorescence (Elumalai et al., 2002). If the spin state of the initial and final energy levels are different (e.g.  $T_1 \neq S_0$ ), the emission is called phosphorescence (shown in longer wavelength red).

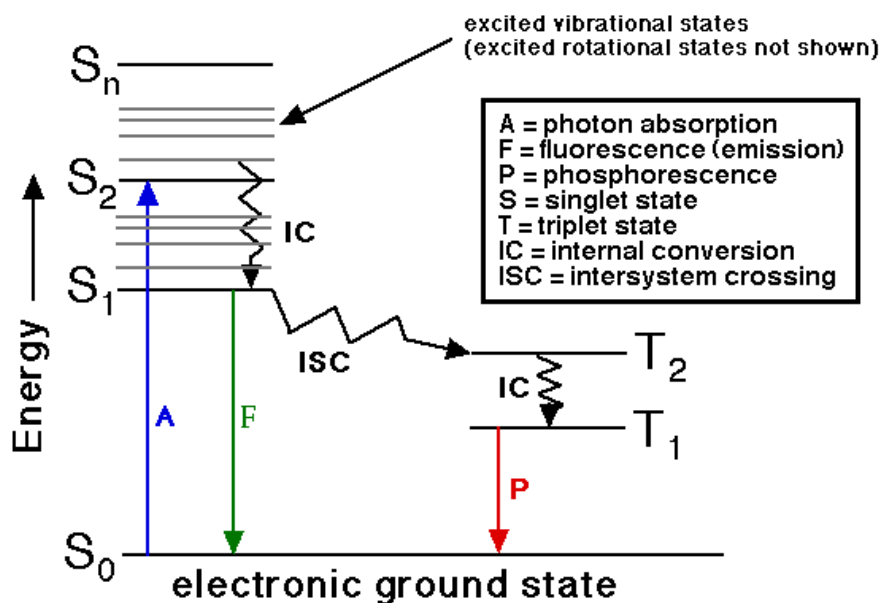


**Figure 2.1.** Jablonski Diagram illustrates the electronic states of a molecule and the transitions between them.

A molecule in its excited state ( $S_1$ ) can relax by various competing pathways. Excited molecules can relax via conversion to a triplet state which may subsequently relax via phosphorescence or by a secondary non-radiative relaxation step. Relaxation of an  $S_1$  state can also occur through interaction with a second molecule through fluorescence quenching or photobleaching. Molecular oxygen ( $O_2$ ) is an extremely efficient quencher of fluorescence because of its unusual triplet ground state. Molecules that are excited through light absorption can transfer energy to a second 'sensitized' molecule, which is converted to its excited state and it can then fluoresce. In contrast to quenching, photobleaching (also termed fading) occurs when a fluorophore permanently loses the ability to fluoresce due to photon-induced chemical damage and covalent modification (Figure 2.2).

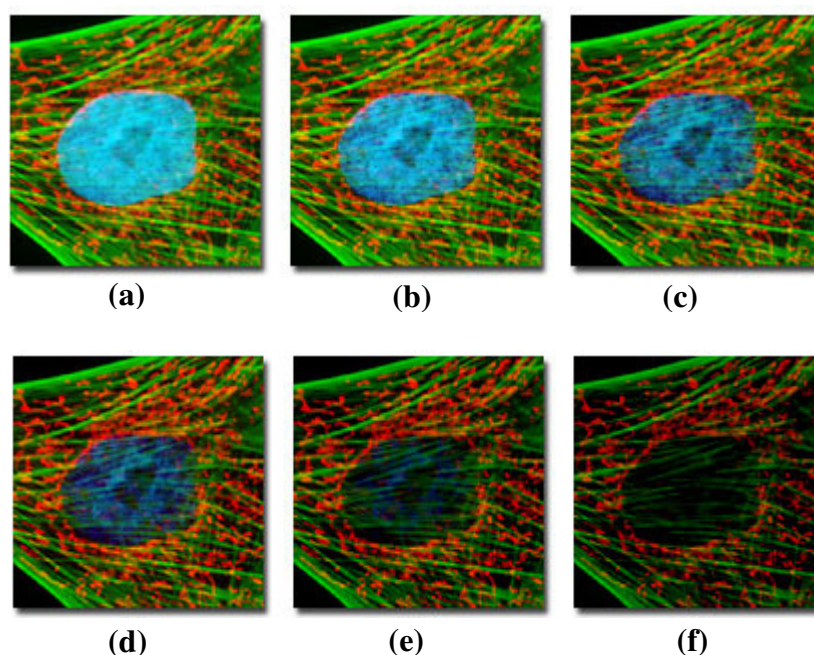


**Figure 2.2.** Photobleaching rates in a multiply stained specimen.

Upon transition from an excited singlet state to the excited triplet state, fluorophores may interact with another molecule to produce irreversible covalent modifications. The triplet state is relatively long-lived with respect to the singlet state, thus allowing excited molecules a much longer timeframe to undergo chemical reactions with components in the environment. The average number of excitation and emission cycles that occur for a particular fluorophore before photobleaching is dependent upon the molecular structure and the local environment. Some fluorophores bleach quickly after emitting only a few photons,

while others that are more robust can undergo thousands or millions of cycles before bleaching.

Molecules can also undergo 'non-radiative relaxation' in which the excitation energy is dissipated as heat (vibrations) released to the solvent. As a result, the emission spectrum is shifted to longer wavelengths than the excitation spectrum. This phenomenon is known as *Stokes Law* or *Stokes shift*. The greater the Stokes shift, the easier it is to separate excitation light from emission light. The emission intensity peak is usually lower than the excitation peak, and the emission curve is often a mirror image of the excitation curve, but shifted to longer wavelengths. In order to achieve maximum fluorescence intensity, the fluorochrome is usually excited at the wavelength at the peak of the excitation curve, and the emission detection is usually selected at the peak wavelength of the emission curve (Figure 2.3).

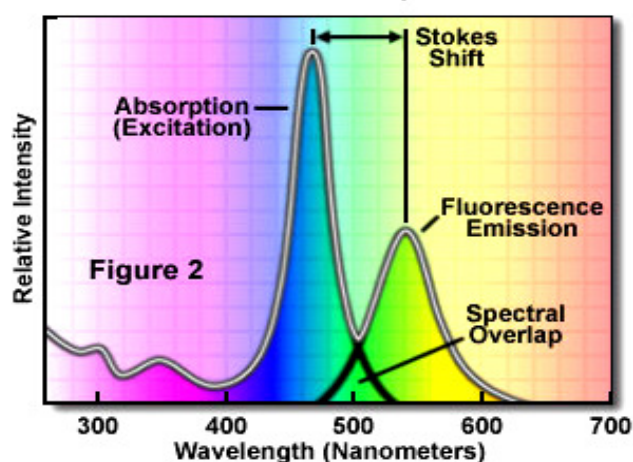


Figure 2.3. Typical fluorochrome absorption-emission spectral profile.

An important parameter of fluorescence is the quantum yield which gives the efficiency of the fluorescence process. It is defined as the ratio of the number of photons emitted to the number of photons absorbed.

$$\Phi = \frac{\text{\# photons emitted}}{\text{\# photons absorbed}}$$

The maximum fluorescence quantum yield is 1.0 (100%): every photon absorbed results in a photon emitted. Compounds with quantum yields of 0.10 are

still considered quite fluorescent (Lakowicz, 2006). **Quantum yield should be known to choose the best dye to use.**

Other rates of excited state decay are caused by mechanisms other than photon emission and are therefore often called "non-radiative rates", which can include: dynamic collisional quenching, near-field dipole-dipole interaction (or resonance energy transfer), internal conversion and intersystem crossing. Thus, if the rate of any pathway changes, this will affect both the excited state lifetime and the fluorescence quantum yield. Choosing a dye means knowing the fluorescence lifetime. This refers to the average time the molecule stays in its excited state before emitting a photon. The delay between absorption and emission is negligible, generally on the order of nanoseconds.

More formally, various radiative and non-radiative processes can de-populate the excited state. In such case the total decay rate is the sum over all rates:

$$\Gamma_{tot} = \Gamma_{rad} + \Gamma_{nrad}$$

$\Gamma_{tot}$  is the total decay rate

$\Gamma_{rad}$  the radiative decay rate

$\Gamma_{nrad}$  the non-radiative decay rate.

Extinction coefficient, quantum yield, mean luminous intensity of the light source, and fluorescence lifetime are all important factors contributing to the intensity and utility of fluorescence emission. In addition, the localized environment surrounding the fluorochrome plays a primary role in determining the characteristics of fluorescence emission. Variables such as solvent viscosity, ionic concentrations, pH, and hydrophobicity in the environment can have profound effects on both the fluorescence intensity and the lifetime of the excited state (Lakowicz, 2006). Greenspan et al. (1985) shows that the fluorescence intensity of Nile Red in n-heptane is nearly 80 times greater than that in acetone and ~2,000 times greater than that in ethanol.

## 2.2 Fluorophores

Hundreds of fluorophores are available with known intensity curves of excitation and emission. In selecting a fluorophore, it is important to choose one that can be excited by the available laser source of the microscope: the absorption peak of the probe should be close to that one of the available laser wavelength (Figure 2.4).

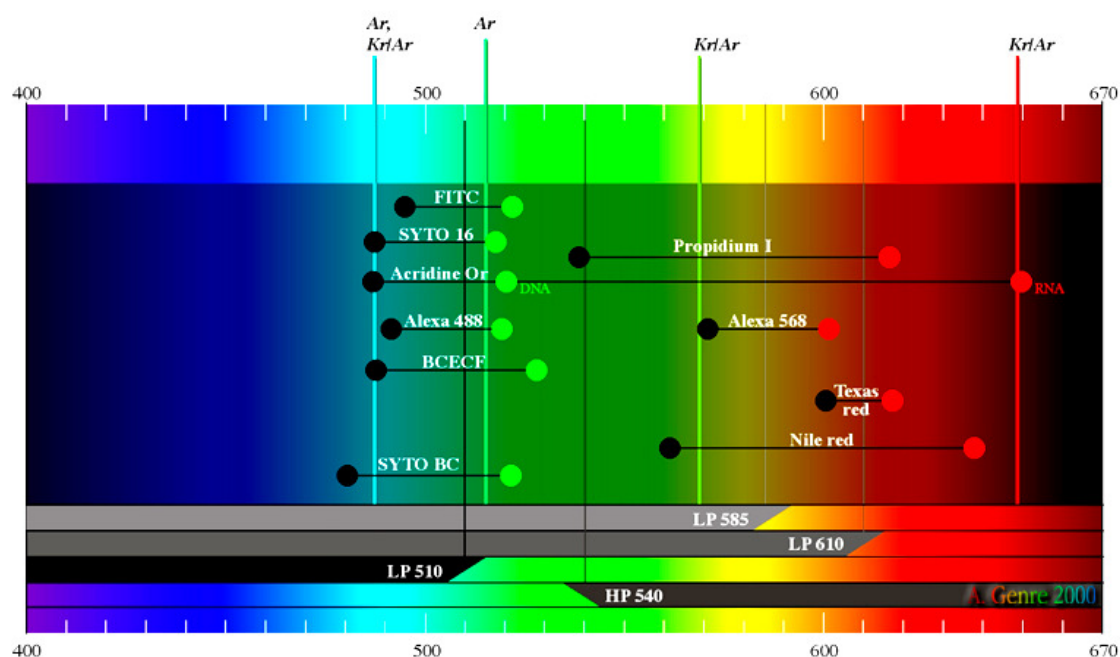


**Figure 2.4.** Absorption and emission wavelengths of some fluorophores, lasers emission wavelength and main filters.

When using more than one probe in the same preparation, the fluorochromes should be chosen with well separated spectra and with a little emission overlap. Usually, probes are unstable in water because they are subject to slow hydrolysis, as sensitive to light and heat than the dry form. It is recommended to always protect a probe in solution from light. One of the most common fluorophores, which has been used in our experiments is Fluorescein Isothiocyanate (FITC), a reactive derivative of fluorescein (Figure 2.5). for several years, it has been one of the most common fluorophores chemically attached to other, non-fluorescent molecules to create new and fluorescent molecules for a variety of applications. FITC is a toxic protein stain, which reacts towards amine and sulfhydryl groups on proteins. It absorbs at 490nm

and emits at 520nm and can be dissolved in different solvents (DMSO, ethanol, acetone). This fluorophore is one of the most used because of the visible light excitation and emission, a high quantum yield, and pH sensitivity in the physiological range.

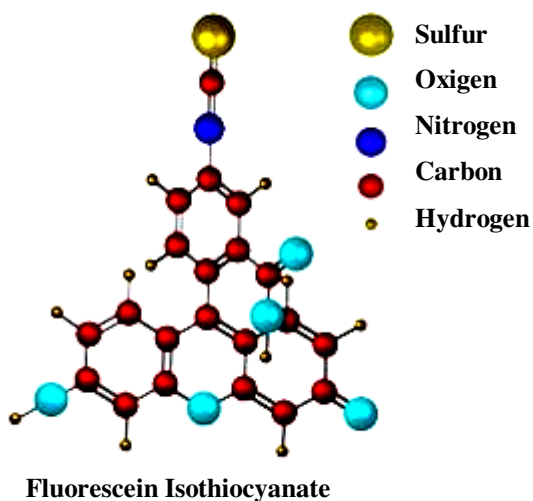


*Figure 2.5. Skeletal formula of fluorescein isothiocyanate.*

With significant advances in detection technology and the discovery of other dyes, however, the limitations of FITC have become apparent:

- Collisional quenching when multiple dyes are attached to a protein or small molecules;
- Fast rates of photobleaching upon exposure to excitation light;
- Quenching under slightly acidic conditions.

These limitations prevent the researcher from getting the brightest conjugates and the most sensitive fluorescence signal.

A recent generation of fluorophores, named Alexa Fluor, has been produced from Molecular Probes® (Figure 2.6).

## Alexa Fluor Synthetic Fluorochromes

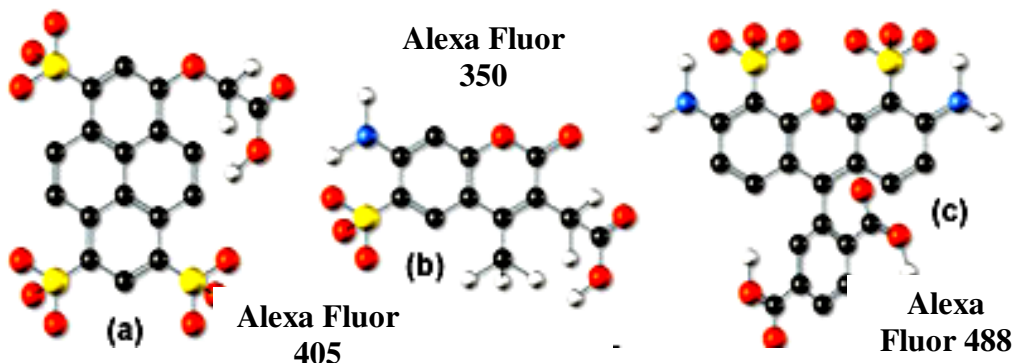


**Figure 2.6.** Alexa Fluor are available in a wide range of fluorescence excitation and emission wavelengths.

It shows nearly identical spectral properties and quantum yield as fluorescein (FITC), produces brighter, more photostable conjugates that are ideal for imaging and other applications requiring increased sensitivity and environmentally insensitive fluorescence detection. Fluorescein conjugates rapidly quench as more fluorophores are added. The Alexa Fluor® 488 dye allows more fluorophores to be attached to the conjugate before self-quenching becomes apparent, leading to significantly brighter conjugates (Figure 2.7). This increased brightness allows to use less conjugate for experiments, reducing background fluorescence.

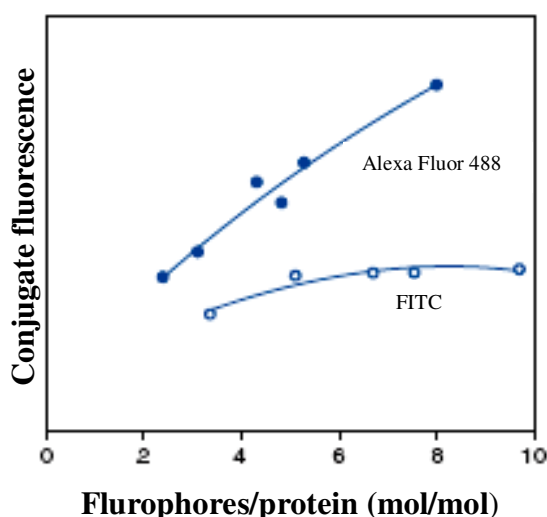


**Figure 2.7.** Comparison of the relative fluorescence of Alexa Fluor® 488 dye and FITC.

The superior photostability of the Alexa Fluor® 488 dye let to have more time on hand for image observation and capture, thereby permitting greater sensitivity

and simplifying the detection of low-abundance targets (Figure 2.8) (Haugland, 2002).

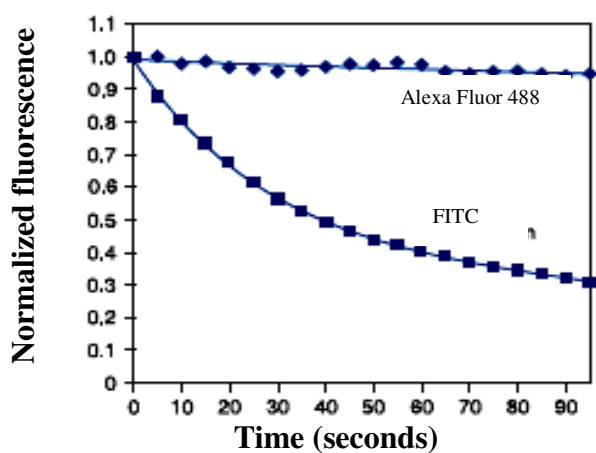


**Figure 2.8.** Photobleaching profiles of cells stained with Alexa Fluor® 488 or FITC.

Other fluorophores tested in our laboratory are Nile Red (Figure 2.9) and Methylene Blue (Figure 2.10).

Nile red is a non-toxic lipophilic stain. Produced by boiling a solution of Nile Blue with sulfuric acid, it dissolves in Dimethyl sulfoxide (DMSO). It stains red intracellular lipid droplets and it absorbs at 560 nm and emits at 640nm.

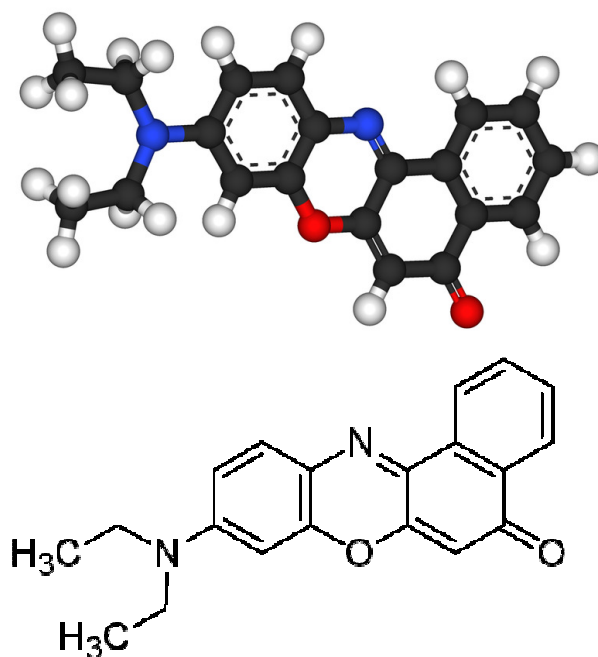


**Figure 2.9.** Structural formula of Nile Red.

Methylene blue is a non-toxic proteins stain. It has been tested to replace FITC in our experiment, once we observed that the FITC and Nile Red spectra do overlap.

It is odourless at room temperature and gives a blue solution when dissolved in water. Nevertheless, it is unstable and photobleaches easily, thus it has never superseded FITC in our laboratory.

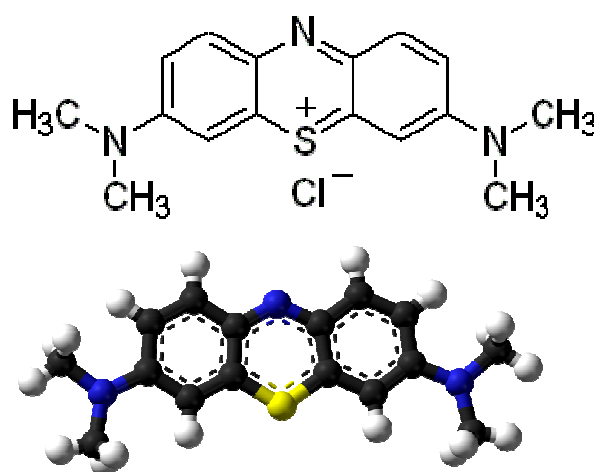


*Figure 2.10. Structural formula of Methylene Blue.*

The excitation and emission spectra of a fluorophore contain important practical information about what wavelengths of light we need to supply and detect, in order to use that fluorophore effectively.

Excitation and emission spectra must be examined carefully, when choosing two or more fluorophores to be used simultaneously in an experiment, so that the fluorophores can be excited in a manner that will generate distinct emissions.

While a given dye's excitation peak may not exactly match the peak of the laser wavelength, the high power of the laser can still produce significant fluorescence from the dye when exciting at a suboptimal wavelength.

If multiple dyes are used in the sample, it is recommended to choose fluorophores that do not overlap their corresponding spectra. Moreover, a bandpass emission filter can be used to isolate the emission from each dye. Careful filter

selection helps to ensure that the detector registers only the light of interest in the fluorescence emitted from the sample.

### 2.3 Immunofluorescence

The fundamental idea of a staining procedure is to bind the fluorophores to molecules of interest, so that the spatial distribution of these molecules is revealed from the location of the fluorophores.

In the past, dyes were not specific, this means that a dye might target all the DNA, or all of the proteins in a substrate. The development of immunolabelling techniques allows to localize specific molecules within the specimen using antibodies and antigens. Immunofluorescence is the labeling of antibodies or antigens with fluorescent labels, designed to target a specific protein or other molecules of interest. Different methodologies have been developed. The most common are direct and indirect methods (Figure 2.11) (Muzi, 1999).

Direct immunofluorescence uses primary antibodies directly labelled with a fluorophore. This direct labeling decreases the number of steps in the staining procedure and, more importantly, often avoids cross-reactivity and high background problems. This type of fluorescent labeling can be performed in less than one hour with readily available labeling kits.

Indirect immunofluorescence employs two sets of antibodies: a primary antibody is used against the antigen of interest; then a secondary ("indirect"), dye-coupled antibody is introduced in order to recognize the primary antibody. Typically this is done by using antibodies of different species.

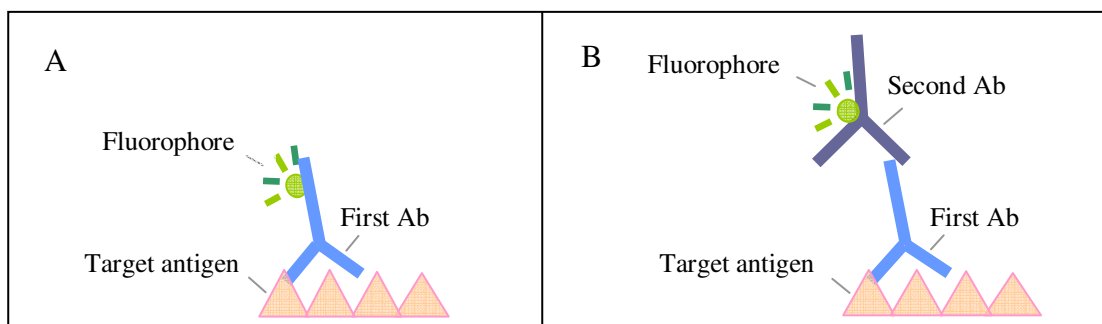


**Figure 2.11.** Direct (A) and indirect (B) methods of immunolabeling.

The major disadvantage of immunofluorescence is that the specimen must be fixed and permeabilized before adding the fluorescently-labelled antibodies. This renders live cell imaging impossible.

## *2.4 Green Fluorescent Protein*

Most of the times, the researcher is interested in looking at the living system in real time and discover the complex processes involved in it. The solution at this problem came with the discovery of the green fluorescent protein (GFP).

Martin Chalfie, Osamu Shimomura and Roger Y. Tsien share the 2008 Nobel Prize in Chemistry for their discovery and development of the green fluorescent protein.

GFP is a fluorescent protein that was first found in the jellyfish *Aequora Victoria*. It has the useful properties that its formation is not species-specific. This mean that it can be fused to any target protein by genetically encoding its DNA as a fusion with the cDNA (complementary DNA) of the target protein. Using GFP, it is possible to operate in living systems. Hence the movement of individual cellular components can now be analyzed across time. There is no requirement to fix or permeablize the cells first. The discovery of GFP has made the imaging of real-time dynamic processes commonplace, and has caused a revolution in optical imaging (Tsien, 1998). GFP exhibits bright green fluorescence when exposed to blue light. It has a major excitation peak at a wavelength of 395 nm and a minor one at 488 nm. Its emission peak is at 509 nm which is in the lower green portion of the visible spectrum (Tsien, 1998).

Due to the potential for widespread usage and the evolving needs of researchers, many different mutants of GFP have been engineered (Tsien, 2005). The first major improvement was a single point mutation (S65T) reported in 1995 in *Nature* (Heim et al, 1995). This mutation sensationally improved the spectral characteristics of GFP, resulting in increased fluorescence, photostability and a shift of the major excitation peak to 488nm with the peak emission kept at 509 nm. This matched the spectral characteristics of commonly available FITC filter sets, increasing the practicality of use by the general researcher.

The revolution of GFP goes further with the development of different colored GFP isoforms, such us YFP (yellow fluorescent protein) fluoresces in the yellow

range, CFP (cyan fluorescent protein) emits lightblue-grey and BFP (blue fluorescent protein) emits in the blue range. This allows more than one protein to be visualized simultaneously in a substrate. Moreover, this development enables new methods of studying protein-protein interactions with FRET (Shaner et al., 2005).

GFP has a typical beta barrel structure, consisting of one  $\beta$ -sheet with alpha helix containing the fluorophore running through the center (Figure 2.12) (Ormö et al., 1996; Yang et al., 1996).

The tightly packed nature of the barrel excludes solvent molecules, protecting the fluorophore fluorescence from quenching by water.

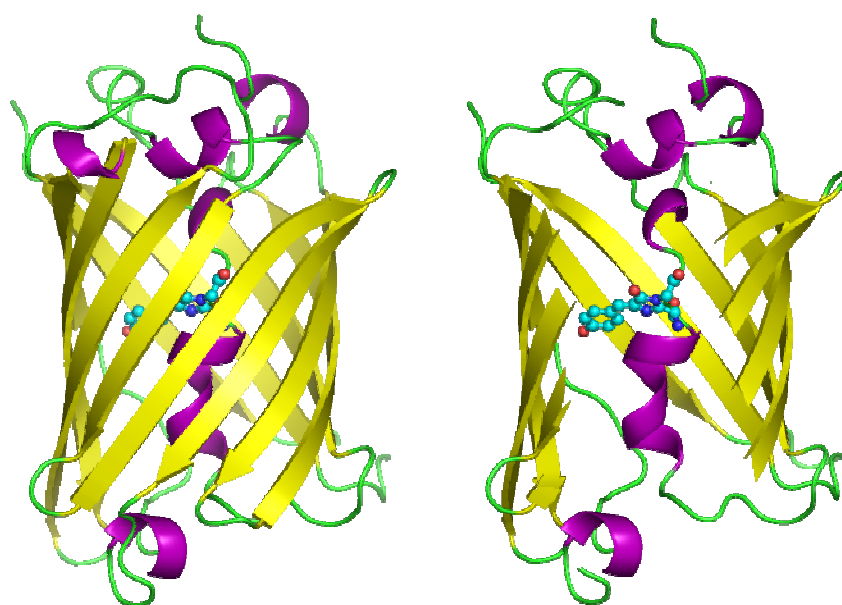


**Figure 2.12.** GFP structure. One wholly-reproduced protein (on the left) and cutaway version to show the fluorophore (on the right).

The availability of GFP and its derivatives has thoroughly redefined fluorescence microscopy and the way it is used in cell biology and other disciplines (Yuste, 2005). While most small fluorescent molecules such as FITC (fluorescein isothiocyanate) are strongly phototoxic when used in live cells, fluorescent proteins such as GFP are usually much less harmful when illuminated in living cells. This has triggered the development of highly automated live cell fluorescence microscopy systems which can be used to observe cells over time, expressing one or more proteins tagged with fluorescent proteins.

## **Conclusions**

Even though the fluorescence phenomenon appears to be almost instantaneous, with current instrumentation the relatively long timeframe between absorption of a photon and the emission of a second photon by a fluorophore opens the door to a considerable number of investigations. Regarding fluorescence techniques, changes in absorption and emission spectra, quantum yield, lifetimes, quenching and photobleaching, solvent effects, diffusion, complex formation, and a host of environmental variables need to be taken into account. When coupled to the optical microscope, fluorescence enables investigators to study a wide spectrum of phenomena in sciences. Many important processes are objectives for investigation using high degree of specificity, sharpness and spatial resolution available with confocal microscopy. For example, fluorescent probes have been employed to monitor the spatial distribution of food elements, intracellular pH and the localized concentration of important ions, and for the study of cell viability and apoptosis. The recent proliferation in the diversity of available fluorescent proteins (i.e., GFP) promises a wide variety of new tools for optical imaging and offers unprecedented opportunities to understand life processes and to manipulate reaction or element organization and distribution within a specimen. In reviewing the large number of applications that benefit from fluorescence analysis, it is apparent why the significant utility of fluorescence and confocal microscopy has driven this technique to the forefront of biological and food research.

# Chapter 3

## Microstructure

### Introduction

Most heterogeneous foods are known as dispersed systems. A heterogeneous system has structural elements, which often are not in thermodynamic equilibrium. Various ways of manufacturing can lead to a variety of structures, that are mainly determined and maintained by the organization of their components and their interactions with each other. Differences in structure usually imply differences in properties. Structure, rheological and sensory properties of food depend on the history of the product, such as processing steps applied, storage conditions, temperature history. Several kinds of structure give the food a certain consistency, which greatly reduce element transport rates in the system. Then, in many foods, elements are fully compartmentalized in cells, emulsion droplets and tissue fragments. This implies that the reactions between those components may be hindered. The compartmentalization may also apply to flavour substances, with the effect of slowing down their release during eating. If the compartments are fairly large, they can lead to fluctuation in flavour release during eating, thereby enhancing flavour because fluctuation can offset adaptation of the senses to flavour stimuli. Thus, a compartmentalized food generally tastes quite different from the same food that has been homogenized (i.e. milk).

Heterogeneous systems are also physically unstable. Indeed, several physical changes can occur during storage, which could be perceived as a change in consistency, colour or a separation into layers. Dispersed systems generally have one or more kinds of interface, often making up a considerable surface area. Then, surface phenomena are of paramount importance. Colloidal interaction forces between structural elements are also essential, as they determine rheological properties and physical stability.

Microstructure is studied to monitor most of the parameters discussed above. Microstructure is a complementary tool of conventional analysis both to monitor food quality, assessing distribution and organization of basic elements, and

removing possible defects, and to create new products that reflect consumers' demand.

### *3.1 Microstructural features and their interactions*

Structure can be defined as the distribution over space of the components in a system. Its properties are determined by its components, their chemical and physical properties, and their interactions. Functionality of most food components (carbohydrates, proteins, lipids, vitamins, minerals, water) is characterized by their organization, shape and size, and the extent to which they interact with each other. The structural building blocks of such a system can be called structural elements, which are regions bounded by a closed surface, where at least some properties within the region are different from those in the rest of the system. Structural elements can be particles, such as air bubbles, oil droplet, crystals, starch granules, and cells. If these particles are separated from each other, the system is called dispersion. In many cases, internal interaction forces act between structural elements. Internal means that the forces have their origin in the material making up the structural elements. Gravity, electric field and flow are excluded. Interaction forces can be attractive or repulsive and the net result always depends on the distance over which they are acting. Net attractive force can cause aggregation into a floc (Aguilera and Stanley, 1999). Structural elements can organise and constitute a phase.

Complex structures can be distinguished in lyophilic or reversible and lyophobic or irreversible systems. Lyophilic heterogeneous systems can be in thermodynamic equilibrium. No energy is spent to build them: they form spontaneously by mixing the components. Important examples are:

- Macromolecular solutions: they are especially formed by polymers. These molecules can be so large that they should be considered as particles. A dilute polymer solution could be treated as homogeneous when considering its dielectric properties or the diffusion of salt through it. However, like other dispersions, polymers can scatter light, and heterogeneity is essential to explain its viscosity.
- Association colloids: formed by fairly small molecules that associate spontaneously into larger structures. Clear examples of the formation of micelles

are shown in Figure 3.1. At high concentration these molecules can form a range of structures, called mesomorphic, of liquid crystalline phases.

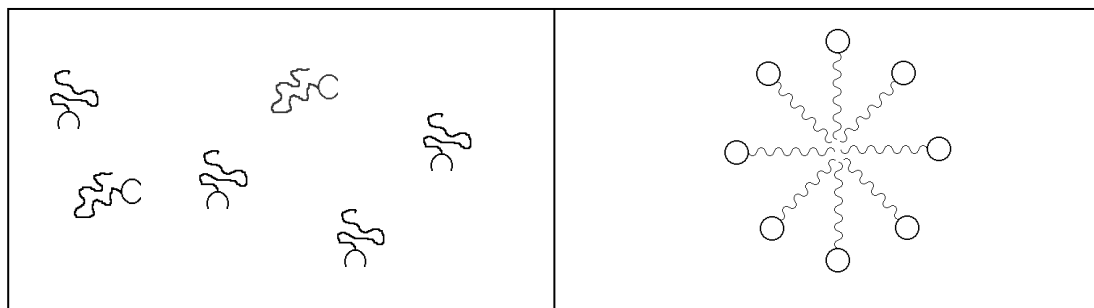


**Figure 3.1.** Schematic picture of micelle formation.

Particles in lyophilic dispersions cannot constitute a phase: they do not have sharp boundaries. On the other hand, lyophobic systems contain particles that do make up a phase. A considerable amount of energy is necessary to make them and they never form spontaneously. A lyophobic dispersion always has a continuous phase, in which other particles are dispersed. According to the state of the two phases, five types of dispersion can be distinguished:

Dispersion type	Dispersed phase	Continuous phase
Foam	Gas	Liquid
Fog, aerosol	Liquid	Gas
Emulsion	Liquid	Liquid
Smoke, powder	Solid	Gas
Suspension	Solid	Liquid

The characteristics of the continuous phase determine many properties of the system. If the continuous phase is liquid, it determines what substances can be dissolved in it. It also affects greatly the interaction forces between the particles and the possibility to loose substances by evaporation. The continuous phase can be solid. This implies that the structural elements are immobilized, which considerably enhances physical stability of the system (Walstra, 2003).

### 3.2 *Microstructure of dairy products*

During the last 30 years, interest in the microstructure of dairy products has grown and at the same time different microscopy techniques (i.e. Electron, Light Microscopy and, since the early 1990's, the newer technique of Confocal Laser Scanning Microscopy) have been developed to visualize nano-features of these products, to examine their size, shape and arrangement, and as complementary methods for quality assessment, defect detection and product development.

Microstructure of dairy products consist of a complex arrangement of fat and protein in aqueous phases. The transition from milk to gel to cheese is defined by the association of casein micelles to form a fibrillar and eventually over time a more amorphous casein network, disrupted by fat globules (Kimber et al., 1974).

Cheese macrostructure, made of curd granules, is the result of microstructural arrangement of its basic components, first of all fat and proteins.

In cheese, fat (triglycerides and phospholipids) is found as small globules ( $\approx 2\mu\text{m}$ ), clusters of globules and large areas of fat (10 - 50  $\mu\text{m}$ ) that are mostly pools of free fat trapped within the protein matrix (Everett and Olson, 2003). Microscopic observations have demonstrated that lipids are not only simple globules but complex biological systems made of triglycerides connected and “protected” from phospholipids, that are the main components of globule membrane and interact with proteins.

The presence of fat is necessary both to preserve the characteristic flavour profile and mouthfeel, and to maintain texture by partially disrupting casein fibrous matrix, softening the product. Banks et al. (1989), demonstrated that reducing fat in Cheddar cheese to less than two thirds results in poor flavour, high firmness in texture and uncharacteristic flavour and bitterness. Conversely, Jameson (1990) reported that Mozzarella cheese, was successfully produced.

Fat contributes to cheese microstructure formation by binding the caseins (small globules) and as an inert filling material by disrupting the protein matrix (large fat globules). Size and structure of fat globules influence the melting point of cheese, free oil formation and texture: large fat globule rupture lubricates caseins, promoting their flow and enhancing melting, pools of free fat contribute to free oil formation on cheese surface, large fat globules with a small Laplace pressure of

deformability decrease cheese firmness, whereas small fat globules are much harder to deform and rupt, and do not disrupt protein matrix, thus contribute to cheese firmness (Everett and Auty, 2008).

Fat globules are often subject to partial coalescence. Globules do not coalesce into one drop, although there is oil-oil contact between them. The mechanism is illustrated in Figure 3.2. Fat globules are made of various lipids and some of them are crystalline at room temperature. Crystals protruding from a globule surface can pierce the film of the closest globule and let the two neighbour fat globules attach. This mechanism can occur among many droplets causing the partial coalescence and the formation of fat clusters. Long heating processes leads to melting of the crystals and clusters can coalesce into large drops.

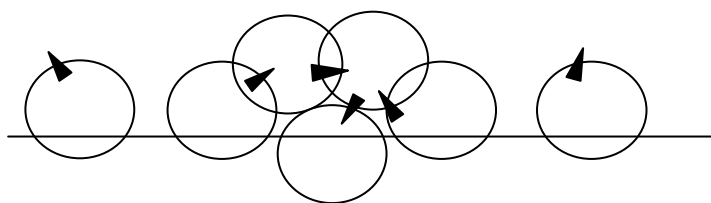


**Figure 3.2.** *Partial coalescence. Protruding crystals pierce the closest globules, especially when lipids roll around one another.*

Proteins in cheese are mainly made of caseins. Schmidt and Büchheim (1992), observed that casein surface is occupied by k-casein. McMahon and Oommen (2008) suggested the supramolecular structure of the casein micelle (Figure 3.3), where calcium phosphate nanoclusters, presumed to be located at the interlocking sites, play an integral role in casein micelle synthesis and in maintaining supramolecule integrity. These calcium phosphate-casein aggregates serve as structure-forming sites to which other caseins can be bound, forming short chains between them.

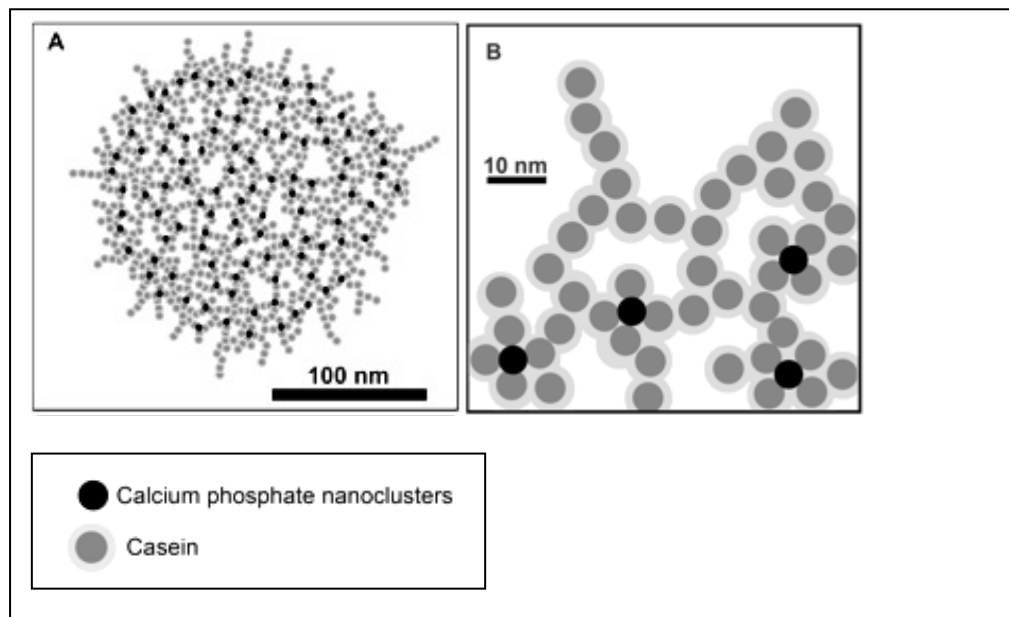


**Figure 3.3.** Schematic diagram of casein micelle with casein-calcium phosphate aggregates. (A) Complete supramolecule, and (B) Portion of the supramolecule periphery.

The model shows a predominance of k-casein on the supramolecule periphery as terminal molecules (or disulfide-linked polymers) with protuberances that can extend into the surrounding environment. The lattice structure is irregular in nature and supports an open structure of the casein micelle, even though the interlocking sites throughout the supramolecule are characterized by a degree of periodicity.

Besides the basic elements, internal forces let microstructure form, connecting micro-components. Hydrophobic interactions as well as calcium bridging play a predominant role for caseins interactions: They are involved in chain formation and are responsible of bonds between caseins and calcium phosphate nanoclusters. Hydrogen bonding and other electrostatic and entropic interactions common to proteins probably also occur to maintain supramolecule integrity. All of these interactions and the interlocking structure give casein micelles elasticity and make them resistant to complete dissociation in case only one interaction is eliminated (McMahon and Oommen, 2008).

Pastorino et al. (2002) explains that structural changes in heated cheese are due to changes in the hydrophobic forces among  $\beta$  caseins. Applied heat raised hydrophobic interactions, and possibly, re-association of  $\beta$ -caseins and calcium with the protein matrix, promoting protein-to-protein interactions. This lets the protein

matrix contract, occupying less cheese matrix area, and microphase separation occurs, causing serum pockets to grow in size, and microstructural heterogeneity to increase. Dissociation of  $\beta$ -casein from the micelle occurs at low temperature as a consequence of weakening of hydrophobic interactions and removal of colloidal calcium phosphate (Pierre and Brule, 1981). This dissociation is reversible and depends on temperature.

Hydrophobic bonds are also liable for holding fat globules among caseins and for micellization (Figure 3.4) of amphiphilic molecules in water, such as the formation of the membranes of lipid bilayers.

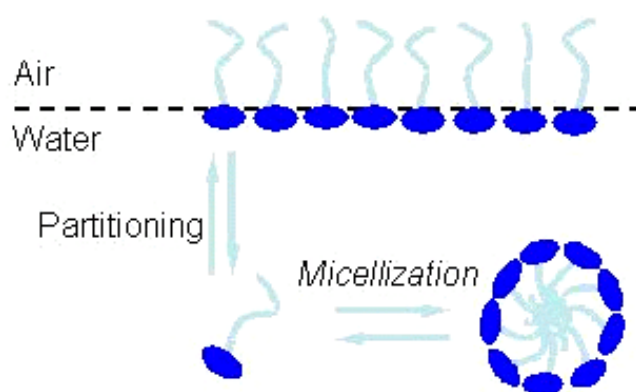


**Figure 3.4.** *Micellization of amphiphilic molecules promoted by hydrophobic forces.*

Hydrophobicity is controlled and quantified from the Gibbs free energy equation and it greatly depends on temperature, especially in the range from 0 to 50°C (Figure 3.5).

$$\Delta G = \Delta H - T\Delta S$$

G is the Gibbs free energy, H is the enthalpy, T is the absolute temperature and S is the entropy. At low temperature (close to 0 °C),  $\Delta H$  for bond formation is positive;  $\Delta S$  is relatively large and positive. The result is that  $\Delta G$  has a relative small negative value, and consequently, bonds are formed. Above a certain temperature, however,  $\Delta S$  starts to decrease, but hydrophobic bonds increase in strength because  $\Delta H$  also decreases.

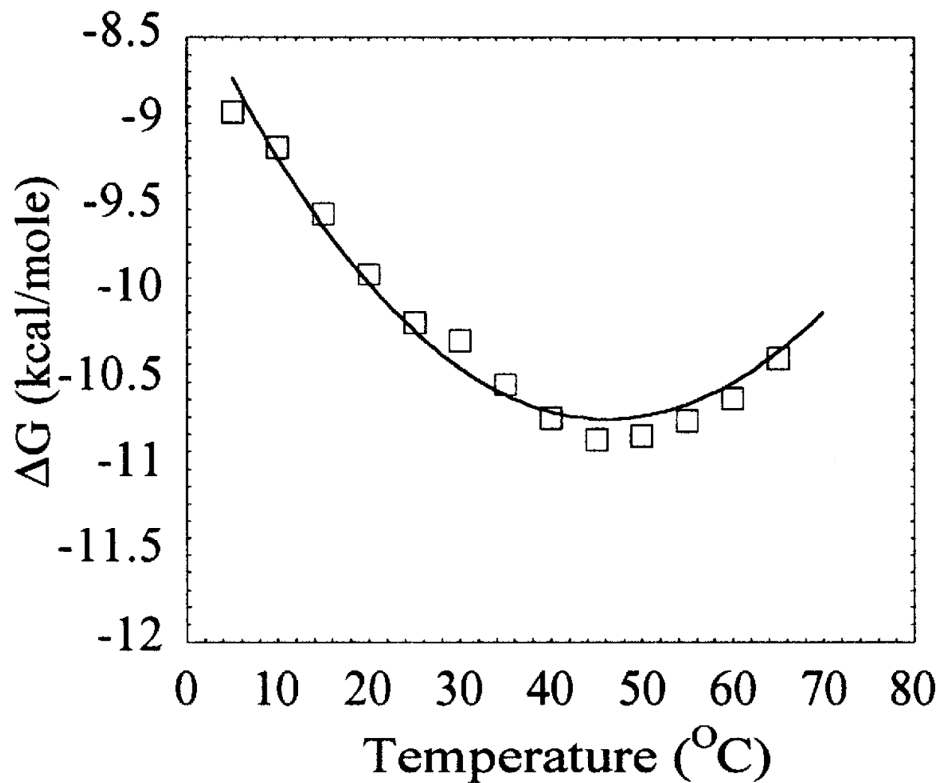


*Figure 3.5. Relation between free energy ( $\Delta G$ ) of formation of hydrophobic bonds and temperature.*

Summarizing, hydrophobicity is a very significant force that control various interactions in cheese structure:

- Interactions among proteins;
- fat globules holding among caseins;
- formation of the membranes of lipid bilayers.

Cheese structure depends on its manufacturing process: Chymosin coagulation of milk gives cheeses with thin protein fibres whereas acid-heat gels will contain thicker fibres (Kalab and Harwalkar, 1973); In stretched cheese, protein fibres appear oriented in parallel with serum channels containing aggregated fat globules, located among the fibres. This orientation is not evident in pressed cheeses, that present an amorphous structure (Guinee, et al., 1999).

Cheese ripening can affect structure, in particular protein organization. Openings in the protein network among caseins, visible after cheese production, decrease in volume over time, due to reduction of expressible serum during maturation (Guinee et al., 2000a) and is most likely due to increased binding water by the protein phase. Hard cheeses have a more defined structure than soft and fresh cheese, whose structure tend to be more unstable.

Changes of basic components of cheese, such as reducing fat, can alter elements aggregation, organization and their interactions (Bryant et al., 1995; Drake et al., 1996). Experiments on reduced fat cheeses have demonstrated that properties such as texture and flavour are deeply influenced by changes in cheese composition (Carunchia Whetstine et al., 2006; Lteif et al., 2009; Martini et al., 2009, McMahon et al., 1993).

Cheese structure is an unstable system, which is subject to changes due to several factors (some of which will be discussed in the next chapters) not only represented by cheese-making processes and cheese composition but also by cheese storage time and conditions.

### *3.3 Manipulating food structure*

The expensive maintenance of using the less well-developed or well-known traditional food products and the new demand of the modern society induce food industry to bet on research of new micro-components to obtain structures that better fit consumers' needs. Nowadays, the investment of introducing new components in foods for a new market is increasing very rapidly.

It is difficult to predict future trends, but once molecular functionalities have been clearly identified, it is easy to operate on them to modify the structure or create a new one.

New sources of polysaccharides have been studied to generate new types of functionality. Several examples can be reported on the application of exopolysaccharides (EPS) in the food industry.

Because EPS<sup>+</sup> strains of *Streptococcus thermophilus* and *Lactobacillus delbrueckii* subsp. *bulgaricus* can reduce syneresis and enhance product texture and viscosity, these types of cultures are commonly used as a substitute for commercial stabilizers in yogurt manufacture (Cerning, 1995). Although use of EPS<sup>+</sup> lactic acid

bacteria (LAB) starters is far less common in cheese manufacture, recent works have shown that EPS<sup>+</sup> *S. thermophilus* (Rhône-Poulenc, Marschall Products, Madison, WI) can improve the functional properties of low fat or part-skim Mozzarella cheese (Perry et al., 1997; Low et al., 1998; Petersen et al., 2000).

Incorporation of EPS or EPS<sup>+</sup> cultures in dairy foods can provide viscosity, stability, and water-binding functions (De Vuyst and Degeest, 1999) that may contribute positively to the mouth-feel, texture, and taste perception of fermented dairy products (Duboc and Mollet, 2001). For many years, European dairy processors have also used EPS<sup>+</sup> starter cultures to control syneresis in yogurt, and this practice is particularly widespread in countries where the addition of plant- or animal-derived stabilizers is prohibited (Cerning, 1995). The latter application is also important if we consider modern consumer preferences for products with lower sugar and fat levels, and with fewer food additives (Broadbent et al., 2003).

Yogurt manufacture remains the most important commercial application for EPS<sup>+</sup> LAB in dairy foods. Some companies have used ropy strains to improve the texture and functionality of cheese (Pruss and Bahrs, 1981). Interest in EPS<sup>+</sup> starters for cheese making has been restricted, however, by the fact that EPS often accumulates in the cheese whey, thereby increasing its viscosity. This outcome is undesirable because it delays the efficiency of membrane processing and slows whey protein concentration and drying processes (Petersen et al., 2000). Consumer demand for reduced-fat foods has created interest in the development and manufacture of reduced-fat, low-fat, and no fat Mozzarella cheese, but fat removal has several undesirable effects on cheese physical properties (McMahon et al., 1993). More specifically, Mozzarella cheese becomes tough and rubbery, more heat is required for melting, and the cheese loses pliability rapidly during cooling (Mistry and Anderson, 1993). Research has revealed that these properties are heavily influenced by cheese moisture level (McMahon and Oberg, 1998). Examination of cheese microstructure shows that in full fat or part-skim Mozzarella cheese, much of the water is contained in channels formed in the protein matrix by entrapped fat globules (McMahon et al., 1993; Oberg et al., 1993). Because there are very few fat globules able to break up the protein matrix in low-fat Mozzarella, the channels become much narrower with less space available for water retention. This results in cheese with a lower moisture level (Oberg et al., 1993) and, as a

consequence, a tough, rubbery texture and poor melt and stretch properties (McMahon and Oberg, 1998).

While the ability to enhance cheese yield (through increased moisture retention) and functionality have strongly boosted the use EPS<sup>+</sup> cultures in Mozzarella cheese, concerns over EPS accumulation in cheese whey continue to limit commercial interest in EPS<sup>+</sup> cheese starters. However, it is important to recognize that while EPS accumulation in cheese whey may be expected from ropy starters, CPS<sup>+</sup> (capsular polysaccharide) bacteria are less likely to affect whey viscosity because the polymer is covalently linked to the cell wall (Deng et al., 2000). Petersen et al. (2000) investigated the effect of capsular and ropy EPS<sup>+</sup> *S. thermophilus* starters on part-skim Mozzarella cheese and whey. They showed that cheese moisture levels were significantly higher in Mozzarella made with EPS<sup>+</sup> versus EPS<sup>-</sup> streptococci, but whey from cheese made with the ropy starter was significantly more viscous than whey from cheeses made with the CPS<sup>+</sup> or EPS<sup>-</sup> strains. More importantly, no significant difference was detected in the viscosity of 5- fold concentrated whey from cheese made with CPS<sup>+</sup> or a commercial EPS<sup>-</sup> starter (Petersen et al., 2000). These findings indicate that CPS<sup>+</sup>, but not ropy, *S. thermophilus* starter bacteria can be used to enhance Mozzarella cheese moisture level, yield, and melt properties without deleteriously affecting whey viscosity.

Understanding of EPS genetics and biosynthesis has increased considerably in recent years. Dozens of basic repeat unit structures have been described, the organization and function of numerous EPS genes have been determined, and the molecular basis for structure-function relationships of EPS in food systems has been elucidated (Broadbent et al, 2003). As this research continues, the dairy industry can expect to see more widespread application of EPS and EPS<sup>+</sup> cultures in ways that provide added value and innovation to milk products for years to come.

### *3.4 Influence of microstructure on rheology*

As described in the previous paragraph, changes at the microscopic level affect the macroscopic properties of foods, the most important being rheology.

To fully understand the rheological and other macroscopic properties of foods, it would be necessary to characterize and define different levels of structure in products, their respective roles and their interactions at different levels. For

instance, fat crystals networks can exhibit structural hierarchy: on super cooling, fats form primary crystals which aggregate or grow into each other; these clusters further interact to form three dimensional networks. All of these levels of structure can affect mechanical properties (Marangoni et al., 2002).

Protein gels can provide good examples of different structures that are created under different processing conditions, usually heating. Microstructure of the network and strands of  $\beta$ -lactoglobulin gels formed at pH 5.3 depended on the heating rate used. Gels formed at fast heating rate (5-10 °C/min) consisted of homogeneous networks with pore sizes of 20-30  $\mu\text{m}$  (Stading et al., 1993). The strands are formed by nearly equal-sized spherical particles linked in a flexible manner. Gels formed at a fast heating rate have higher stress and strain at fracture due to the network structure, whereas those formed at a slow heating rate have a higher storage modulus, ( $G'$ ) due to the microstructure of the strands. The thick strands of particles fused together are stiffer, causing a higher storage modulus than the flexible strands formed at a fast heating rate (Stading et al., 1993).

Combining microscopy with light scattering and laser diffraction, allows to study, quantify, and understand microstructure. In addition to microscopic and size distribution data, fractal dimension has been used to characterize food particles. Fractal dimension indicates the degree to which an image or feature of interest deviates from smoothness and regularity. The characteristic of fractal objects is their “self-similarity”, which means the attribute of features having the same appearance at all magnifications. However, real materials are self-similar only up to a limited range of scales (Marangoni and Rousseau, 1996). A fractal dimension from 1 to 2 indicates the area filled by a convoluted line and a fractal dimension from 2 to 3 describes the volume of a highly rugged surface (Barret and Peleg, 1995). Fractal dimension can be determined using several methods, such as bulk density-particle diameter relation, pore size distribution, viscoelastic behaviour.

### *3.5 Influence of microstructure on flavour*

Flavour is a cognitive response of the brain to a number of nervous signals originating from chemically sensitive nerves in the mouth and nose. The chemicals that stimulate those nerves come from food and beverages before and during consumption. Food structure influences flavours release, altering its

thermodynamics and kinetics. The thermodynamics of release is mainly governed by the volumes and compositions of the various food phases. Foods with a greater affinity for taste and aroma molecules will tend to release fewer of them into the saliva and to the headspace. Under this perspective, changing the structure occurs when an additional “interphase” with different thermodynamic properties is introduced in the already existent phases, thus changing the arrangement of the phases and altering the affinity of food for the flavours. Aroma molecules distribute themselves so that their chemical potential is in equilibrium in all phases, that depend on the affinity of a molecule for each phase. The partitioning of aroma between two phases is described as the ratio of its concentrations in the phases. The partition coefficient between food and headspace gas ( $K_{gp}$ ) is given by

$$K_{gp} = \frac{c_g}{c_p}$$

where  $c_g$  and  $c_p$  are the concentration in the headspace and food phases, respectively. This ratio is important because aroma perception occurs for those molecules that are in the headspace, whereas those entrapped in the food phases will not. The equation describes the thermodynamics of flavour binding: a food product with high affinity for the volatile molecules will have a low  $K_{gp}$  and consequently few aroma molecules will be smelled (Ghosh and Coupland, 2007).  $K_{gp}$  can be affected by temperature as described in Meynier et al. (2003).

As mentioned above, a solvent with great affinity for aroma molecules tend to depress its volatility. As many aroma compounds are non-polar, their headspace concentration will tend to decrease over fatty foods. Lipids are among the major components of food products and therefore influence the food quality by their effect on aroma, taste and mouthfeel. They act as solvent for fat-soluble volatile compounds and are precursors of many volatile compounds. Also, aroma and taste are influenced via the effect that lipids have on phase partitioning and mass transport, whereas mouthfeel is affected by the direct effect of lipids (triglycerides) on texture of a food during eating. Results of in vivo studies indicate that flavour release during consumption is strongly controlled by diffusion. Therefore, release is sensitive to factors that affect mass transport in the product phase, such as content, consistency and particle size of lipids in emulsions. The effect of lipids on the overall flavour is complex due to the interactions between aroma, taste and

mouthfeel (De Roos, 2005). Removal or reduction of lipids leads to an imbalanced flavour, often with a much higher intensity than the original full fat food. According to Ingham et al. (1996), this happens because the non-polar volatiles are no longer dissolved in the lipid phase and released from the food product as soon as eating begins.

Most food are considered as a mixture of oil and water and in these cases aroma compounds will be portioned between these two phases and the vapour phase. Buttery et al. (1973) modelled the portioning of a series of aroma molecules with mass balance equation:

$$\frac{1}{K_{ge}} = \frac{\phi_o}{K_{go}} + \frac{\phi_w}{K_{gw}}$$

where  $K_g$  is the overall gas-emulsion partition coefficient,  $\phi_o$ ,  $\phi_w$  are the volume fraction of lipids, and aqueous phases in the mixture and  $K_{go}$ ,  $K_{gw}$  are the gas-oil and gas water partition coefficients, respectively. This equation is a function of system composition but not of microstructure, so we would expect to see any effects of system microstructure as deviations from the model. Harrison et al. (1997) showed that the Buttery equation gave a good description of the headspace diacetyl concentration in equilibrium with an oil-water mixture, but it was not reliable when the oil and water were emulsified. One consequence on changing structure not considered by the Buttery model is the increase of interfacial area with a decrease of particle size. The chemical environment at the interface changes both for oil and water when emulsification occurs. Indeed the new structure will have more surfactant molecules and the phases will be more attractive for amphiphilic aroma molecules. Many authors (Guyot et al., 1996; Landy et al., 1996; Voilley et al., 2000) showed a change in some volatile compound partitioning whereas no changes occur for other components. Buttery equation is independent from particle size, thus a reversible surface binding model can be adopted, where the partition coefficient decreases with decreasing of particle size. The new equation can be written as follow:

$$\frac{1}{K_{ge}} = \frac{\phi_o}{K_{go}} + \frac{\phi_w}{K_{gw}} + \frac{A_s K_{iw}^*}{K_{gw}}$$

where  $A_s$  is the interfacial area per unit volume of an emulsion and  $K_{iw}^*$  is the apparent surface binding coefficient, given by  $\Gamma_i / c_w$ , where  $\Gamma_i$  is the surface load of aroma compound (i.e. volume of aroma compound adsorbed per unit interfacial area) and  $c_w$  is the aroma concentration in the aqueous phase (Gosh et al 2006).

The equation above is reversible. However if the aroma compounds form covalent irreversible bonds with the adsorbed emulsifier at the interface, volatile partitioning into the headspace would be affected by the amount of free aroma molecules in the emulsion (Meynier et al., 2004).

Aroma compounds are not in equilibrium and their distribution changes with time. The concentration of volatile molecules reaching the aroma-sensitive receptors in the nose will change over time depending on both the thermodynamics of binding and on the barriers to mass transport (De Roos, 2005). The rate of mass transfer is given by the Fick's first law that relates the diffusive flux to the concentration field, assuming that the flux goes from regions of high concentration to regions of low concentration, with an extent that is proportional to the concentration gradient (Smith, 2004). A path taken by a volatile compound moving from an oil droplet in a food emulsion to the headspace gas is limited by the movement in the oil phase, the movement in the aqueous phase and the movement across the oil-water interface or the food-air interface. In literature various theories can be found modeling flavors release. The most interesting works combine instrumental measurements with those of evolving food structure into human mouth (Buettner and Schieberle, 2000a, 2000b; Buettner et al, 2002).

## Conclusions

Most foods can be considered dispersed systems, in which two or more kinds of structural elements, connected by various interaction forces, can be distinguished. Bonds among elements have an overriding effect on the properties of dispersed systems, and these forces can even be considered as being part of the structure.

The existence of a physical structure affects many properties such as viscosity, elasticity, consistency and fracture properties. Because of the physical inhomogeneity of foods, some kinds of physical instability can occur, which are usually undesired. Food systems are characterized by compartmentalization of basic chemical components, which may affect their mutual reactivity and, as a

consequence, the chemical stability of the food product. Compartmentalization also tends to affect flavour.

An important point is whether the various structural elements can be said to constitute phases or not. If not, they are called lyophilic systems, which are in equilibrium. In most foods, structural elements do constitute phases, which implies that they have phase boundaries in which the free energy is accumulated. They are known as lyophobic systems and are inherently unstable, due to an excess of free energy.

Foods structure determines products behaviour, and some of their properties (e.g. rheological and sensory). Studying microstructure has revealed useful to relate nano-feature arrangement and distribution to rheological and sensory properties of food. Structure depends on manufacturing and storage history and, for natural food, on growth conditions. Microscopy is extensively used to study food structure. Such knowledge can lead to improve food quality and to produce food with desirable structure and rheology. The challenge is to establish a link between the macroscopic rheological properties with changes at the microscopic level.

Applications of exopolysaccharides in the food industry is an example of changing microstructure to produce the desired functionality in food products. Due to their ability to reduce syneresis and enhance product texture and viscosity, these types of cultures are commonly used as a substitute for commercial stabilizers in yogurt manufacture.

Food structure also influences flavour release, altering its thermodynamics and kinetics. Thermodynamically, flavours molecules bounded tightly to the food phase are unavailable to the receptors in the mouth and nose, then their presence will be not perceived.

The kinetics is dependent on time and temperature and flavour release is affected by structure that provide great resistance to mass transport of the flavour.

Besides the nature of the structural elements, other factors can influence flavour distribution, such as particle size. Dispersions with small particles are in most instances far more stable than those with large ones. External forces applied to a system have a stronger effect on large particles than on small ones, which has direct consequences for their separation.

Finally, the oral processing of food products is essential to understand the relationship between food microstructure and sensory perception. Approaches that

make a product very stable on the shelf can result unacceptable to the mouthfeel. Therefore, the optimum would be making stable food products that maintain their taste once eaten.

# Chapter 4

## Image processing

### Introduction

In recent years, the analysis of digital images has become a relevant tool not only in food science but also in many other fields. Today, food microstructure can be easily accessed by many different imaging techniques and their importance in improving and understanding food behaviour is unquestionable. However, the real value of images relies on the quantitative information and numerical data that can be extracted from them. The following chapter describes image analysis techniques used in the characterization of food microstructure.

### *4.1 Image analysis process*

Image Processing involves a series of image operations that enhance the quality of an image in order to remove defects such as geometric distortion, improper focus, repetitive noise, non-uniform lighting and camera motion. Image Analysis is the process of distinguishing the objects (regions of interest) from the background and producing quantitative information. The general methodology used in digital image processing and analysis is usually divided into different consecutive steps (Aguilera and Briones, 2005; Du and Sun, 2006a):

1. **Pre-processing** of the raw image is carried out to produce an improved version of the original image that facilitates the subsequent analysis steps. It usually involves the correction of geometric distortions, noise-removal (denoising), grey level correction, deblurring.
2. **Image segmentation** involves partitioning the digital image into non-overlapping regions. This step is the most important operation because the subsequent measurements are highly dependent on its accuracy. It can involve the conversion of colour images into greyscale images.
3. **Feature extraction** involves the application of different algorithms to generate quantitative data based on information contained in the image (e.g.,

geometric properties such as area, perimeter and form factor). The greyscale image may also serve to produce global measurements associated with the general information content of the image, such as colour and texture.

4. **Recognition and interpretation** of the extracted image features, and their classification into different categories, which can be considered a processing step of higher level of abstraction.

#### *4.2 Image Preprocessing*

Image pre-processing consists in a series of corrections of the image, such as colours adjustment, contrast and brightness correction, image alignment, and removal of non-uniform illumination. The mathematical nature of digital images makes it relatively easy to enhance, process and analyze with several mathematical operators, functions and transformations (Aguilera and Briones, 2005).

Adjustments to correct colours can be performed using a wide variety of coordinate systems. The HSV model, based on hue, saturation and intensity, is more powerful than the RGB model (red, green, and blue) because it corresponds more closely to how people perceive colours. Global manipulation of the pixel values is better understood by using histograms as a guide. Maximising contrast either for the entire image or for just a portion of it, or varying the brightness value, can improve the visibility of structures of interest.

Problems of image distortions can be solved by measurement of the distortion or from knowledge of the optics.

Removal of non uniform illumination can be required to easier detect features in the image.

The goal of these procedures is to correct defects of the image so that the best image possible is provided to the next step of image analysis (Russ, 2005).

#### *4.3 Noise removal*

Noise can be described as part of the image signal that does not represent the observed specimen, but has been introduced by the system. Many kind of noise can be detected in the image, such as salt and pepper, and white Gaussian noise.

A common strategy to reduce noise is to filter the image by spatial averaging. This method simply takes the average of the pixel values. However, it can blur edges or alter position and shape of objects. A better approach is to use Gaussian smoothing, where a weighted mean is used to favour central pixels, resulting in a bell-shaped function centred at the central pixel. Gaussian smoothing gives better results but does not completely eliminate edge blurring.

The two operations above are linear filters because the resulting value is a combination of the pixels in the neighbourhood. Non linear filters, such as ranking filters, can also be applied. These filters are based on listing the values of the pixels in the neighbourhood in brightness order. The result is obtained by choosing the darkest, lightest or median value from the list. The median value is usually the best choice for speckle noise (i.e salt and pepper) removal, it can effectively reduce noise with any edge blurring.

#### *4.4 Image segmentation*

Segmentation is one of the most important steps in image processing and refers to the process of extracting the desired object of interest from the background.

Let  $R$  represent the entire spatial region occupied by an image. We may view image segmentation as a process that partitions  $R$  into subregions,  $R_1, R_2, \dots, R_n$ , such that

- a.  $\cup R_i = R$
- b.  $R_i$  is a connected set,  $i = 1, 2, \dots, n$
- c.  $R_i \cap R_j = \emptyset$  for all  $i$  and  $j$ ,  $i \neq j$
- d.  $Q(R_i) = \text{TRUE}$  for  $i = 1, 2, \dots, n$
- e.  $Q(R_i \cup R_j) = \text{FALSE}$  for any adjacent regions  $R_i$  and  $R_j$

Condition a. indicates that the segmentation must be complete, which means every pixel must lie in a region. Condition b. requires that points in a region be connected in some predefined sense. If our interest is focused on phases, point b. does not need to be satisfied. Condition c. indicates that the regions must be disjoint. Condition d. deals with the properties that must be satisfied by the pixels in a segmented region, for example,  $Q(R_i) = \text{TRUE}$  if all pixels in  $R_i$  have the same

intensity level. Finally, condition e. indicates that two adjacent regions  $R_i$  and  $R_j$  must be different in the sense of the predicate  $Q$ .

In more intuitive terms, the fundamental problem in segmentation is to partition an image into regions that satisfy certain conditions.

Most of the segmentation algorithms are based on one or two basic properties of intensity values: discontinuity and similarity. In the first category, the approach is to partition an image based on abrupt changes in intensity, such as edges. The main approaches in the second category are based on partitioning an image into regions that are similar according to a set of predefined criteria. Thresholding, region growing, and region splitting and merging are examples of methods in this category (Gonzales and Woods, 2008). Thresholding-based and region-based methods are preferred in food sciences (Du and Sun, 2004).

#### ***4.4.1 Edge detection***

Edge detection is a widely-used approach that highlights pixels lying on edges between different regions. Non-edge pixels that form connected regions are then allocated to the same category. Since edges are local features, they are determined based on local information. Many edge detection methods are available, some very simple others more advanced, that take into account factors such as image noise and the nature of edges themselves (Gonzales and Woods, 2008). Edge models are classified according to their intensity profiles. A *step edge* involves a transition between two intensity levels occurring ideally over a distance of 1 pixel. Step edges occur in images generated by a computer for use in areas such as solid modelling and animation. In practice, edges in real images are blurred and noisy, depending on the limitation in the focusing mechanism and the electronic components of the imaging system. Real edges are thus modelled by an intensity *ramp* profile. In this model, the edge point is any point contained in the ramp and the edge segment would be a set of such point that are connected. A third model of an edge is the *roof edge*. It models lines through a region, with the base of a roof edge being determined by the thickness and sharpness of the line (Figure 4.1).

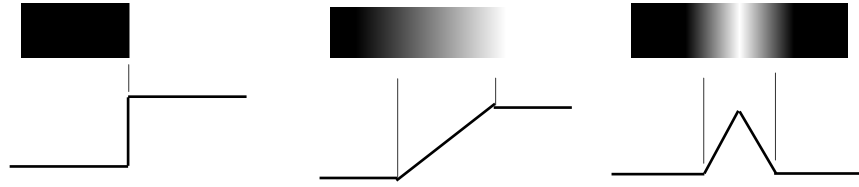


**Figure 4.1.** *Ideal representations of models of a step, ramp and roof edge detection and their corresponding intensity profiles.*

There are three fundamental steps performed in edge detection:

1. Noise reduction.
2. Detection of candidate edge points.
3. Edge localization.

The first point aims to prepare the image for edge detection, the second point extracts from an image all points that are potential candidates to become edge points and the third one selects from the candidates edge points only those that are true members of the set of points comprising an edge.

#### **4.4.2 Threshold-based segmentation**

Because of its simplicity of implementation, and interactive computational speed, thresholding is the most used segmentation technique in food science. This method consists in partitioning images directly into regions based on intensity values. It transforms a greyscale image into a binary one in which all pixels that form part of the features or structures (foreground) are set to white (0) while the background pixels are set to black (1). In other words, the segmented image,  $g(x, y)$ , is given by

$$g(x, y) = \begin{cases} 1 & \text{If } f(x, y) > T \\ 0 & \text{If } f(x, y) \leq T \end{cases}$$

where,  $f(x, y)$  is the intensity of image pixels and  $T$  is the threshold value.

Choosing a threshold value is not simple and it can be done manually or automatically. In the last case, the brightness threshold value is defined based on the information contained on the intensity histogram. When the image is made of

several classes with different surface characteristics, multiple thresholds can be used for segmentation (Scalon and Zghal, 2001).

Thus, points  $(x_i, y_j)$  belong to the background if  $f(x_i, y_j) < T_1$ , to one object class if  $T_1 < f(x_i, y_j) \leq T_2$  and to another object class if  $f(x, y) > T_2$ .

The segmented image is given by

$$g(x, y) = \begin{cases} I_1 & \text{If } f(x, y) > T_2 \\ I_2 & \text{If } T_1 < f(x, y) \leq T_2 \\ I_3 & \text{If } f(x, y) < T_1 \end{cases}$$

where  $I_1, I_2, I_3$  represent three distinct intensity values.

Figure 4.2 show the results of segmenting the individual features by thresholding images.

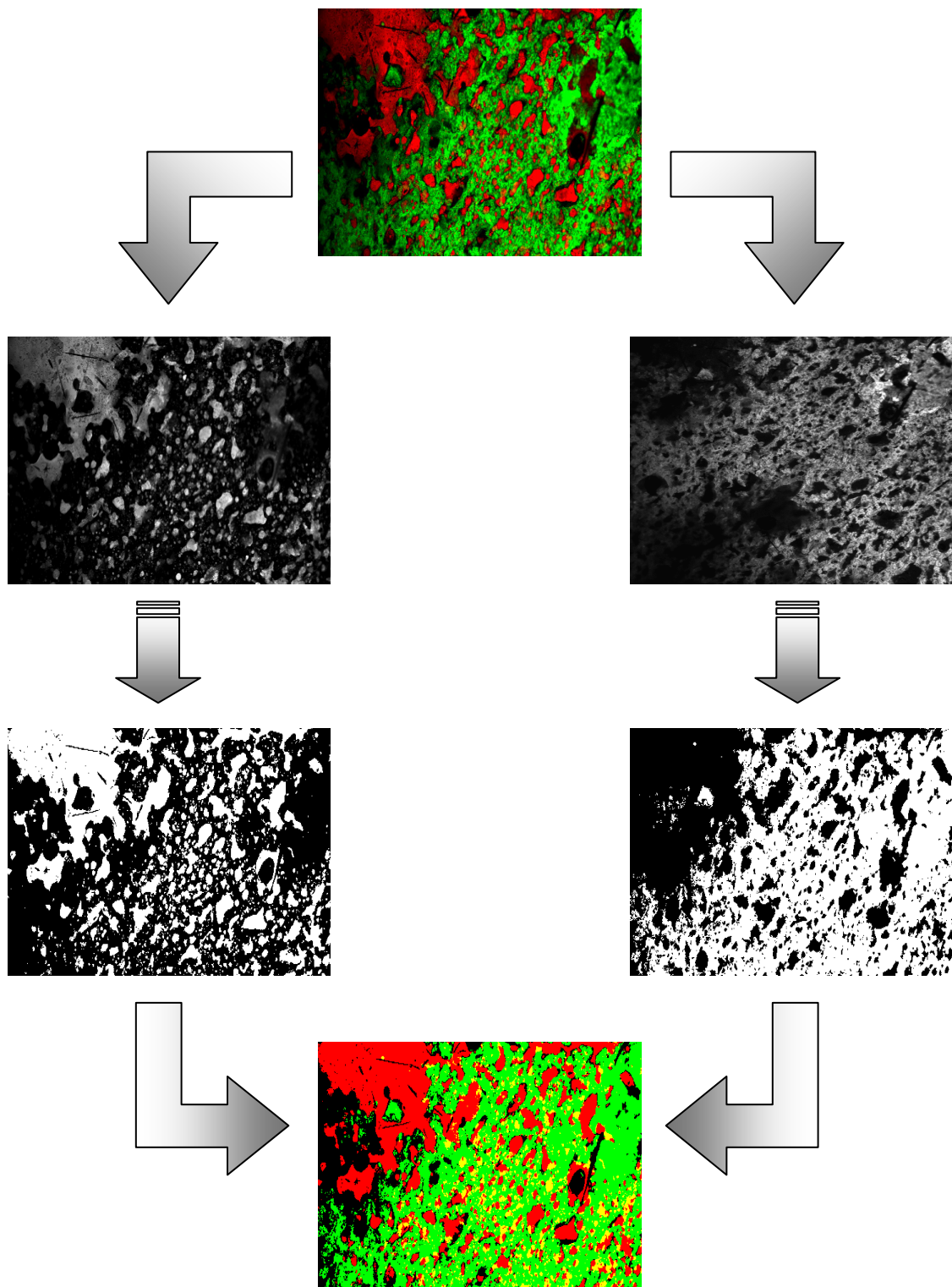


*Figure 4.2. Thresholding-based segmentation.*

Finally, based on the preceding discussion, the success of intensity thresholding is directly related to the width and depth of the valley separating the histograms modes. The key factor affecting the properties of the valley are: the separation between the peaks, the noise content in the image, the relative size of object and background, the uniformity of the illumination source and the uniformity of the reflectance properties of the image.

Segmentations requiring more than two thresholds are difficult and better results are usually obtained using other methods such as the region growing (Gonzales and Woods, 2008).

#### ***4.4.3 Region-based segmentation***

Region-based methods use algorithms to group adjacent pixels having similar values and to divide groups of pixels that have dissimilar values. They can be grouped in two different classes, region growing and splitting-and-merging (Du and Sun, 2004).

As its name implies, region growing is a procedure that groups pixels or subregions into larger regions according to a set of predefined criteria for growth. The basic approach is to start with a set of “seed” points and from these grow regions by appending to each seed those neighbouring pixels that have predefined properties similar to the seed (such as specific ranges of intensity or colour) (Gonzales and Woods, 2008).

The region splitting and merging procedure subdivide an image initially into a set of arbitrary, disjoint regions and then merge and/or split the regions attempting to satisfy the conditions of segmentation (Gonzales and Woods, 2008). Region-based methods are able to utilize several image properties simultaneously in determining the final boundary location.

#### ***4.4.4 Segmentation using morphological watersheds***

The watershed algorithm is a segmentation algorithm based on the topology of the image. Segmentation by morphological watersheds embodies many of the concepts of the previous approaches, and often produce more stable segmentation results, including connected segmentation boundaries. The concept of watersheds is

based on visualizing an image in three dimensions: two spatial coordinates versus intensity. Supposing to flood the surface from its minima and, preventing the merging of the waters coming from different sources, the image will be partitioned into two different sets: the catchment basins and the watershed lines.

Applying this transformation to the image gradient, the catchment basins should theoretically correspond to the homogeneous grey level regions of this image (Gonzales and Woods, 2008).

#### *4.5 Measurement of object characteristics*

The result of the segmentation process is an image where the objects have been properly identified. The next step is to quantify those objects by measuring their characteristics, such as size and shape.

The size of object can be identified by three parameters: area, perimeter and diameter. Area is the most used and it is determined by counting the number of pixels that are part of the object. Perimeter is very useful to discriminate between objects with simple and complex shape.

Shapes features can be measured by combining size measurements. Some of the most common features used in food science are roundness, elongation and compactness.

Roundness is the ratio between the area of the object and that of a circle having the same perimeter. Its value lies in the [0, 1], being 1 a perfect circle.

$$\text{Roundness} = 4 \pi \frac{\text{Area}}{\text{Perimeter}^2}$$

Elongation represent the ratio between the major axis length and the minor one in the object.

$$\text{Elongation} = \frac{\text{Major axis}}{\text{Minor axis}}$$

Compactness indicates the ratio between the diameter of the circle that has the same surface area as the object and the object's major axis length.

$$\text{Compactness} = \frac{\sqrt{4\text{Area}/\pi}}{\text{Major axis length}}$$

## **Conclusions**

CLSM can provide structural information that can be qualitatively related to food material properties such as taste release and mechanical properties. However, it is often desirable to quantitatively determine structural quantities using image analysis and to relate these quantities to other measurements of different physical quantities using multivariate statistics and experimental design.

Three-dimensional volume rendering software is a very useful tool to exploit the information in the two-dimensional image stacks acquired through confocal microscopy. In recent years, a vast array of software programs have been developed to help microscopists, many of which are open-source and freely available but not specific for CLSM images. Imaris (produced by Bitplane, Zurich, Switzerland) was used for our confocal micrographs. It is a commercial software that, having eight modules individually combined, offers a very powerful and versatile 3D imaging analysis software solution.

Most structures are formed during continuous processing and gradients in the processing have an impact on the structures that are being formed. Thus, it is possible to control the structure and related properties kinetically. Dynamic measurements are essential for several aspects of engineering of food structures. Information is needed from dynamic measurements to find how different flow and temperature conditions affect the structure. The chance to combine microscopy and image analysis leads to better understanding of the mechanism involved in structure formation.

Image analysis of CLSM images combined with modelling and simulation offers new possibilities for determining and understanding kinetic processes in the structure.

## Part II: CLSM Applications

### *Summary*

During my three years of PhD at CoRFiLaC, I had the opportunity to participate to different research projects in the dairy science field involving CLSM and other facilities and laboratories of the research centre, notably:

- Three dimensional reconstruction of Pecorino cheese micrographs: fat globules evaluation
- Imaging of Ragusano and Pecorino cheese for structure characterization
- Automatic labelling of CLSM images.
- Heating treatments effects on milk and its products
- Observation of Tina biofilm.

The aim of this second part is to give an overview on different applications, in which CLSM and digital image processing tools can be of great help.

The first example describes 3D reconstruction process of 2D slices of Pecorino cheese. Qualitative and quantitative analysis were performed on the three dimensional representation.

The second case compares microstructure of Ragusano and Pecorino cheeses, focusing on the manufacture process effects and on their geometrical and morphological characteristics.

The third application concerns the automatic detection of CLSM features by an algorithm developed on purpose. It will be shown the capabilities of this image processing tool to reveal various features in cheese microstructure, such as defects, helping the optimization in the manufacturing process.

The fourth experiment illustrates the effects of heating treatments on milk and cheeses structure in order to characterize their feature distribution and aggregation.

The fifth research study deals with observation of biofilm in traditional wooden vat (*tina*). Bacteria hereby represent the autochthonous microflora that make Ragusano cheese unique and inimitable in its flavour and taste.

# Chapter 5

## Applications to cheese structure

### **5.1 Three dimensional reconstruction of Pecorino cheese micrographs: fat globules evaluation**

#### **Introduction**

Microstructure has been defined as a complex organization of chemical components under the influence of internal and external forces (Stanley, 1987). Microstructure influences cheese functional properties such as melting, stretching, browning, free oil development and expressible moisture. The prediction and control of these properties requires an understanding of where the components of cheese are located in relation to each other, and how they interact and change during ripening.

Observation of cheese microstructure and changes in it with perturbations of composition or physical forces can reveal parameters directly related to texture. For example, poor texture and poor flavour in cheese are two consequences of low fat content.

There are several ways to study cheese microstructure. The choice depends on the microscopic features of interest and the level of resolution required (Vodovotz et al, 1996). Electron microscopy offers the advantage of high resolution (3nm) but sample preparation and procedures are long and may lead to artefacts. Most published papers on cheese microstructure are based on two-dimensional (2-D) evaluations (Melilli et al., 2005; Fallico et al., 2006; Pastorino et al., 2003) but, since cheese microstructure is three-dimensional, we need to explore 3D microstructure to extract more accurate information about microstructural characteristics in the inner part of the sample.

Confocal laser scanning microscope offers the possibility to observe food structure and acquire digital data with high resolution (2 $\mu$ m) and without any disturb to the internal structure. It allows to penetrate the surface and visualize internal thin layers. The single slices can be used to study the 2D microstructure and

they can also be combined using an appropriate algorithm to have a 3D representation (Gunasekaran and Ding, 1999). This study aimed to construct 3D images of Pecorino cheese, to visualize three-dimensional distribution of its fat globules, and to provide some information about those microstructural features.

### **CLSM observation**

Pecorino cheese was made according to the traditional technique (Campo and Licitra, 2006). A thin slice (8x4x1mm) was sampled and prepared for examination by CLSM. Cheese sample was soaked in 0.20 g/ml Nile Red (Sigma-Aldrich, Inc.) in dimethylsulfoxide (Sigma-Aldrich, Inc.) for 10 min in darkness to stain lipids. It was rinsed twice in deionized water and stained with 0.050g/ml Fluorescein Isothiocyanate (FITC, Sigma Aldrich, Inc.) in acetone:water (1:1) solution for staining proteins. The stained sample was mounted on standard microscope slide, enclosed with cover-slip, sealed with glycerine jelly and placed on the Nikon C1si inverted microscope (Calenzano, Firenze-Italy) with an Argon Ion Laser 457-514nm 40mW, He/Ne Laser (543 nm) 2,0mW, and He/Ne Laser (640nm) 1,5mW. FITC was excited at 488 nm and Nile Red at 568 nm, while their emission wavelengths were 520 and 630 nm, respectively. The so prepared sample was then observed using a 20X objective. After the optimization of the acquisition process, a z-stack was made of 51 adjacent slices (Figure 5.1), which resulted in a total depth of 40  $\mu$ m.

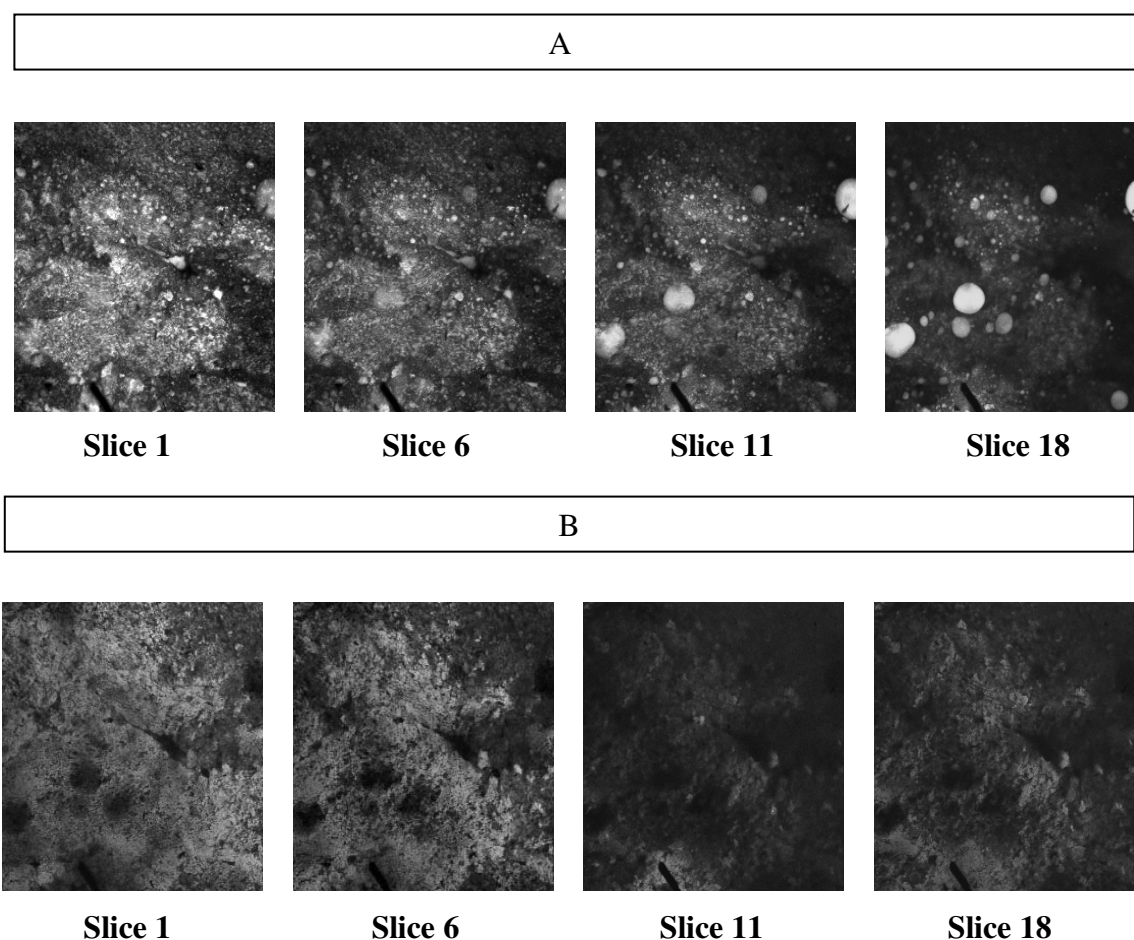


**Figure 5.1.** Two dimensional slices of Pecorino cheese. **A)** Fat distribution. **B)** Proteins distribution.

The z-stack was processed with the *Imaris* software (Bitplane, Zurich, Switzerland) to obtain the corresponding volume rendering and to obtain statistical data of the three-dimensional image and its components, that were artificially labelled green (proteins) and red (lipids).

The software has revealed to be a very powerful of image analysis software. It allowed real time visualization of original and derived data, which could quickly be rendered in a 3D image to discover relationships among the micro-components that were otherwise hidden. Volumes and objects were visualized in real time using various rendering modes (Figure 5.2 A, B, C).

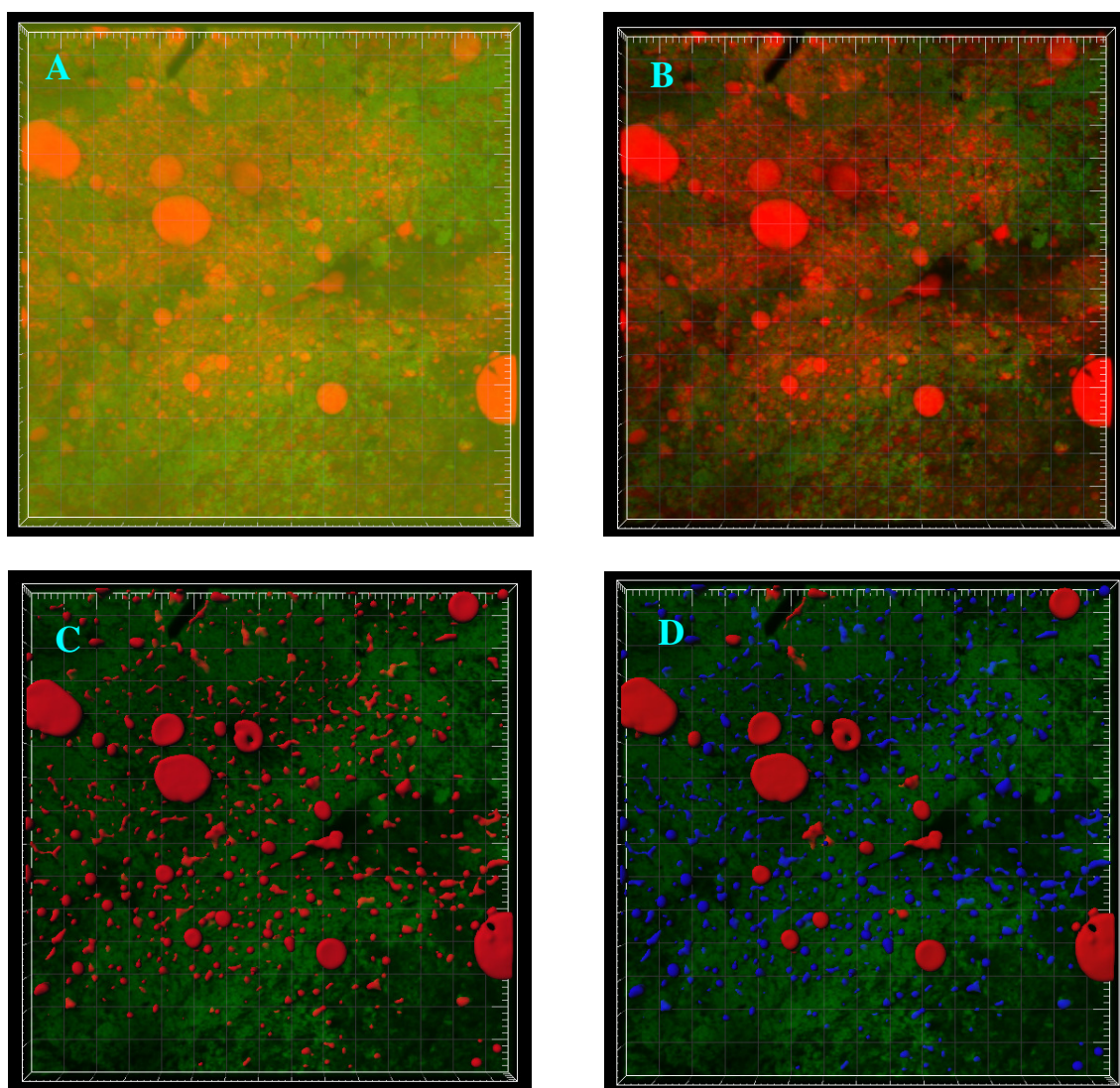


**Figure 5.2.** Volumes obtained using various rendering modes. **A)** The same intensity value was given to proteins and lipids. **B)** Lipids were emphasized, giving a lower intensity value to the proteins. **C)** Features extraction. Identification of lipids was performed, based upon their morphology. **D)** Features extraction. Lipids were discriminated upon their size. Bigger fat drops were labelled in red whereas fat droplets were coded in blue.

Since we intend to focus the attention on fat, the software was used to identify, separate, and visualize lipids areas through the “Iso-Surface” module. The “Surface Object” is a computer-generated representation of a specified region of interest (ROI) in the data set. The selected feature (in this case lipids) was visualized as an artificial solid object, and allowed to interactively verify the accuracy of segmentation against the original data. Lipids were automatically identified, and

their discrimination was based on morphology and size (Figure 5.2 C and D, Figure 5.3).

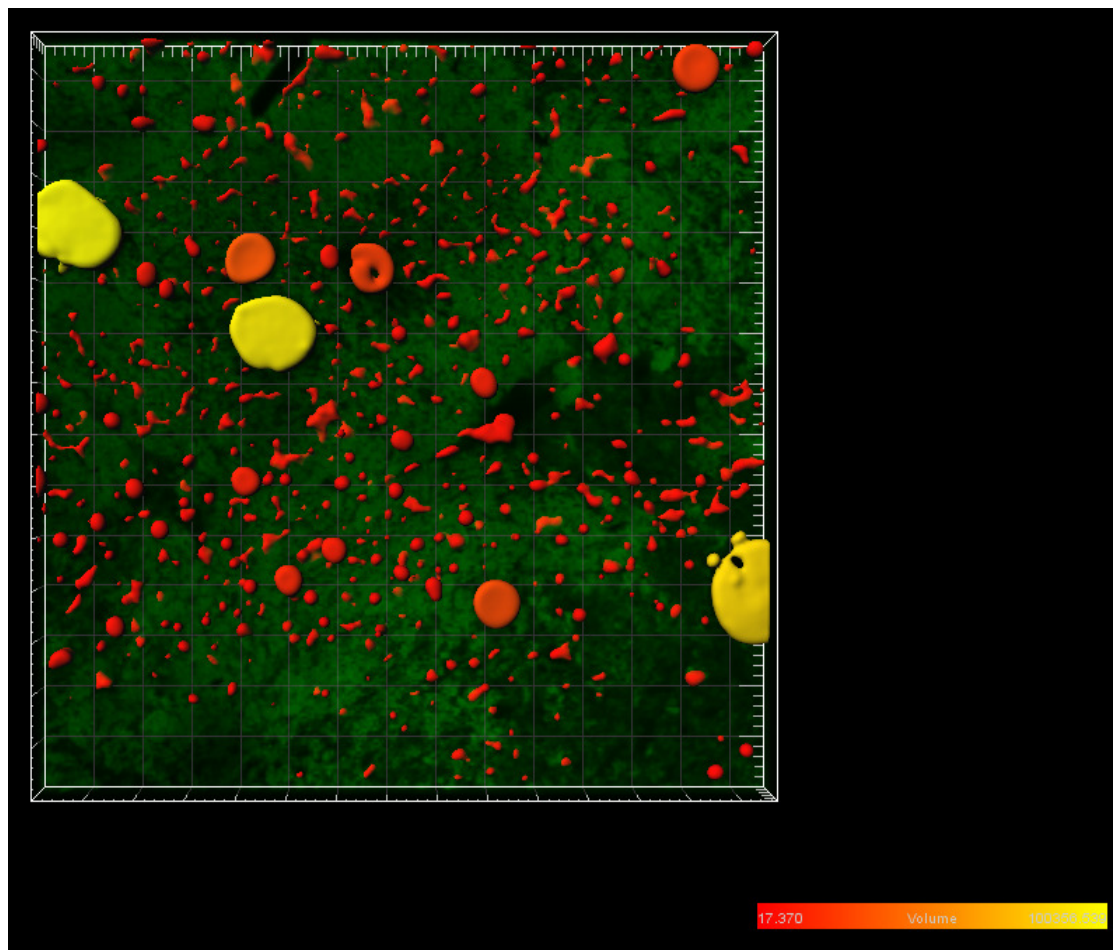


**Figure 5.3.** Identification of fat globules. Lipids were coded using different colors depending on their volume size.

As shown in Figure 5.4, the 3D image obtained could be rotated and watched from any angle. Using *Imaris*, various kinds of movies of sample rotations could be created, with part of the image being turned on and off or cut away.

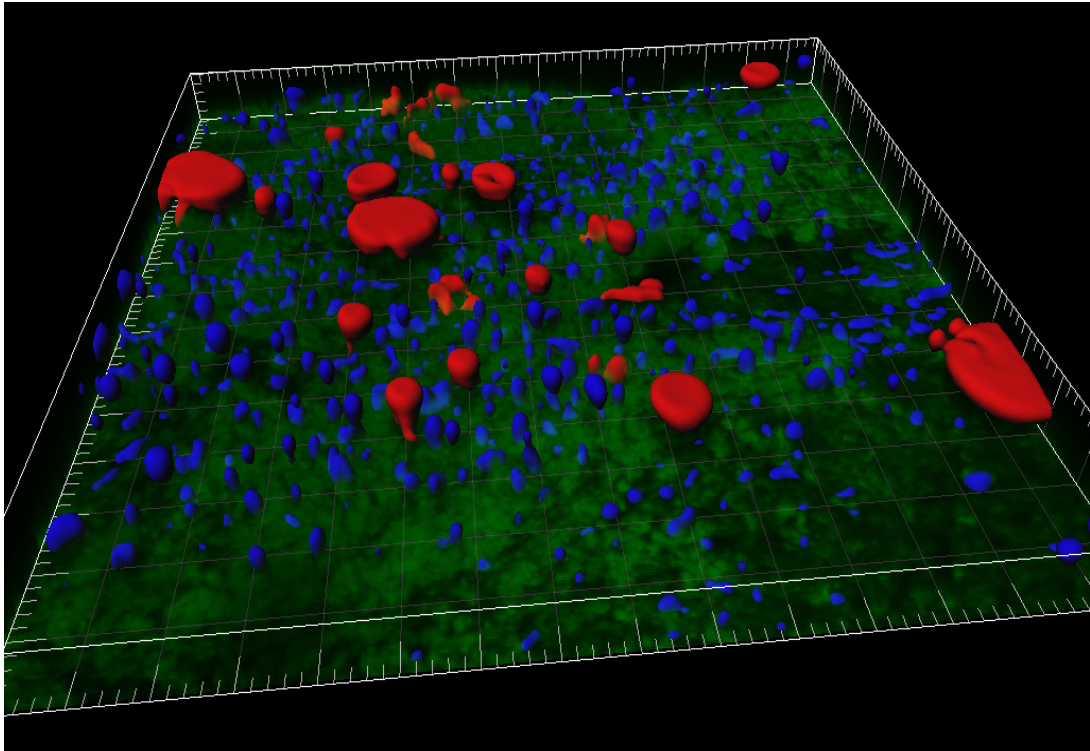


**Figure 5.4.** Visualization of Pecorino cheese 3D microstructure while rotating.

The “Oblique Slicer” module selectively cut away objects on one side of the plane, focusing on an ROI. It could be freely moved and rotated in the scene and enabled to look inside any object at any depth (Figure 5.5 A, B, C, D).

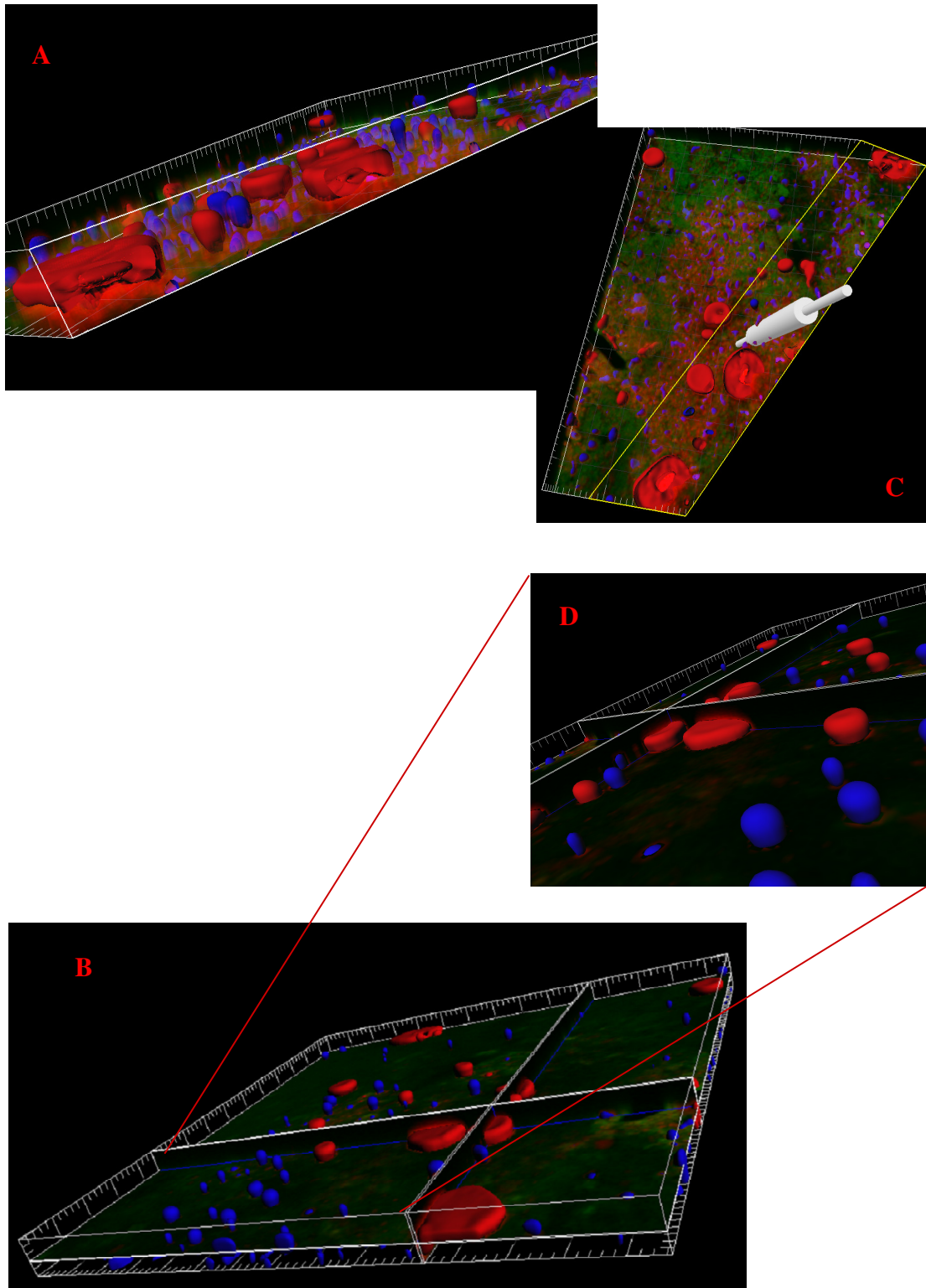


**Figure 5.5.** *A) and B) Volume viewing and detection of a region of interest (ROI). C) Cropping image in the space. The images was resized down to the ROI, making the handling faster, and the viewing of the ROI easier. D) Detail of an ROI.*

## Structure measurements

The surface object acted as a container from which statistics were performed with the “Measurement-Pro” module. The total number and percentage of lipidic structures in the examined Pecorino cheese sample are presented in Table 5.1. The number of small fat droplets was much greater than that of the large fat globules. This can be due to the homogenization treatment applied to the milk used to make Pecorino cheese. Homogeneous distribution of little fat droplets makes the whole cheese uniformly tasteful.

Variable	Large lipids	Small
Total	23.00	518.00
Percentage of lipids	13.95%	15.71%

*Table 5.1. Statistical data corresponding to large and small lipids.*

Although the number of large lipids was noticeably lower than the number of small fat globules, their percentages were comparable (Figure 5.6) because the area occupied by a large fat globule is similar to that occupied by many small lipid droplets. Then, many small droplets are needed to have the same area of a bigger one.

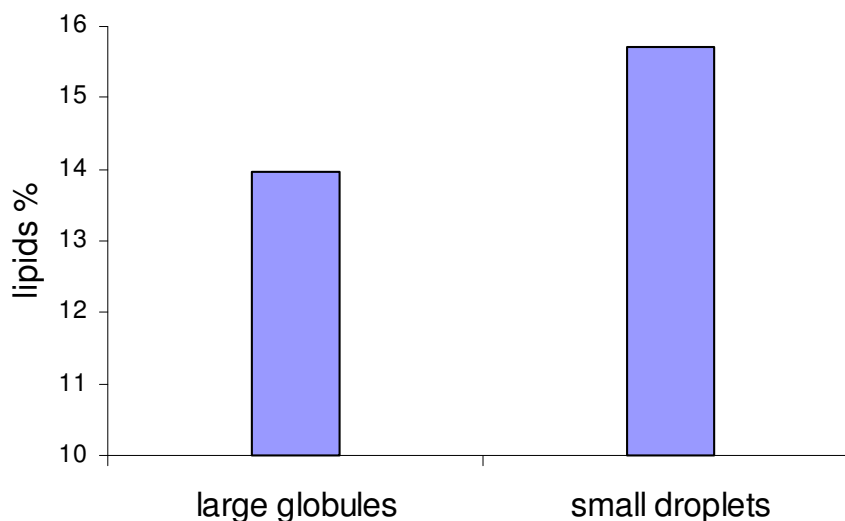


*Figure 5.6. Percentages of large fat globules and small fat droplets.*

Fat shape was analyzed on the digitally reconstructed image. Most of the lipid structures were close to a regular sphere shape. This means that globules did not coalesce and did not cluster, and that the oiling-off process was kept down.

## **Conclusions**

CLSM is a useful tool to analyze 3D microstructure. Studying 3D image gives more information than the bi-dimensional analysis, since the 2D image does not consider the z axis. A large number of 2D slices should be analyzed to obtain the same amount of information. Because cheese microstructure is related to cheese sensory properties, quantification of three-dimensional features in cheese micrographs could help to evaluate the corresponding cheese making process effects and quality of cheese.

## **5.2 Imaging of Ragusano and Pecorino cheese for structure characterization**

### **Introduction**

Sicilian cheese-making tradition counts a large variety of artisanal products, made according to different techniques of processing and ripening. Traditional manufacture processes are one of the most important factors of biodiversity of Sicilian cheeses and play the main role in determining cheese structure which, in turn, affects cheese sensory properties such as texture (firmness, softness, elasticity, crumbliness), and flavour. Therefore, knowing of how cheese structure is produced and develops during brining and ripening is of great importance.

Cheese microstructure is determined from the spatial arrangement among caseins, that join to form a protein network, and fat globules, moisture, and minerals (Lucey et al., 2003). Cheeses have different structure characteristics, affected by factors such as milk and cheese chemical composition, cheese-making procedure, heat treatments of milk and curd, rate and extend of acid development, maturation conditions, and rate of proteolysis (Lucey et al., 2003). These factors control and modify the nature and the strength of the micro-components interactions, their size and shape.

In this experiment, samples of two different traditional Sicilian cheeses were observed by confocal laser scanning microscope (CLSM). Ragusano and Pecorino cheeses were chosen as representatives of two curd processing methods during cheese-making: *Pasta Filata* (or stretched) and *Pasta Pressata* (or pressed) cheeses.

### **Material and Methods**

Ragusano and Pecorino cheeses were produced according to traditional cheese making processes (Campo and Licitra, 2006). One slice of each was taken to be stained for the CLSM observation. Cheese samples were soaked in 0.20 g/ml Nile Red (Sigma-Aldrich, Inc.) in dimethylsulfoxide (Sigma-Aldrich, Inc.) for 10 min in the dark to stain lipids. They were rinsed twice in deionized water and stained with 0.050g/ml Fluorescein Isothiocyanate (FITC, Sigma Aldrich, Inc.) in acetone:water (1:1) solution for staining proteins. The stained samples were mounted on standard microscope slide, enclosed with cover-slip, sealed with glycerine jelly and placed

on the Nikon C1si inverted microscope (Calenzano, Firenze-Italy) with an Argon Ion Laser 457-514nm 40mW, He/Ne Laser (543 nm) 2,0mW, and He/Ne Laser (640nm) 1,5mW. FITC was excited at 488 nm and Nile Red at 568 nm, while their emission wavelengths were 520 and 630 nm, respectively. Micrographs were taken using a 20X lens.

## **Results**

Pasta Filata cheese micrographs showed a fibrous structure as expected. During the cheese making process, the hot water stretching step transformed the amorphous protein matrix of the curd into a complex network of long parallel-aligned uniformly oriented protein strands (Figure 5.7A),. Consequently, whey and fat globules (Figure 5.7B) accumulated in longitudinal channels among the casein strands, resulting in a partial alignment of fat and serum phases within the cheese (Joshi et al., 2004). The cooking and the stretching process helps to confer a plastic appearance to the curd and the formation of a fibrous structure (Lucey et al, 2003). During the early stages of cheese maturation, the casein fibres will lose their identity.

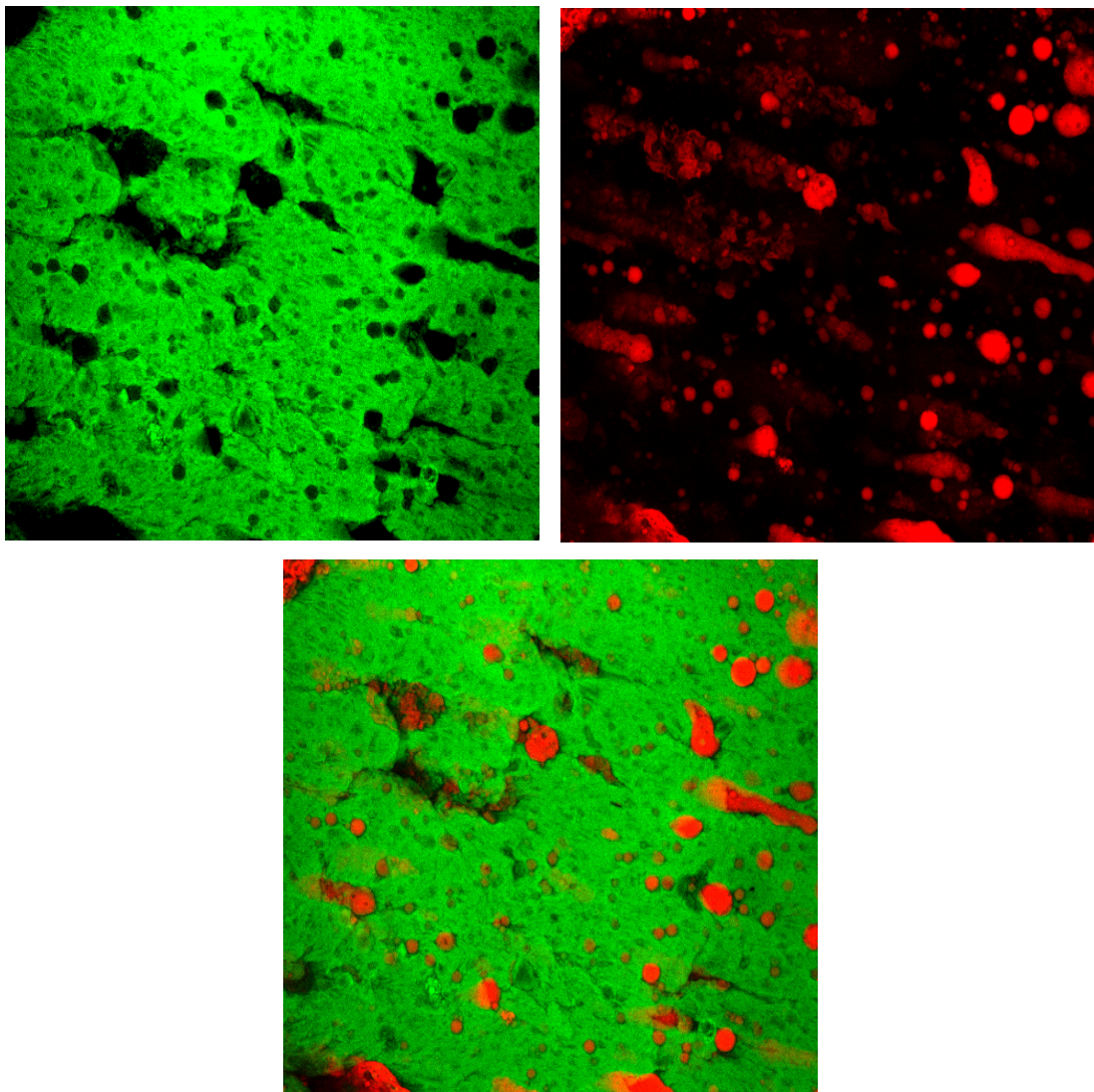


**Figure 5.7.** *Confocal micrographs of Ragusano Cheese. A) Protein matrix stained with FITC. B) Fat globules treated with Nile Red. C). Merged image of protein and fat phases.*

Pressed cheese micrographs resulted to be characterized by a sponge-like structure (Figure 6.8). In the pressed cheese-making process, curd was cut into small granules using a wooden staff (Ruotula). This granular structure was kept during the stirring and first cooking steps, letting fat globules and whey to uniformly disperse within the cheese protein matrix. Casein micelles joined together forming clusters with no specific orientation (Jack and Paterson, 1992) and imparting to the cheese an amorphous texture. At the end of pressing, the cheese already loosed the spongy structure, formed by large casein clusters, that transforms

in a more compact and homogeneous spongy structure during ripening (Figure 5.8 A, B, and C).

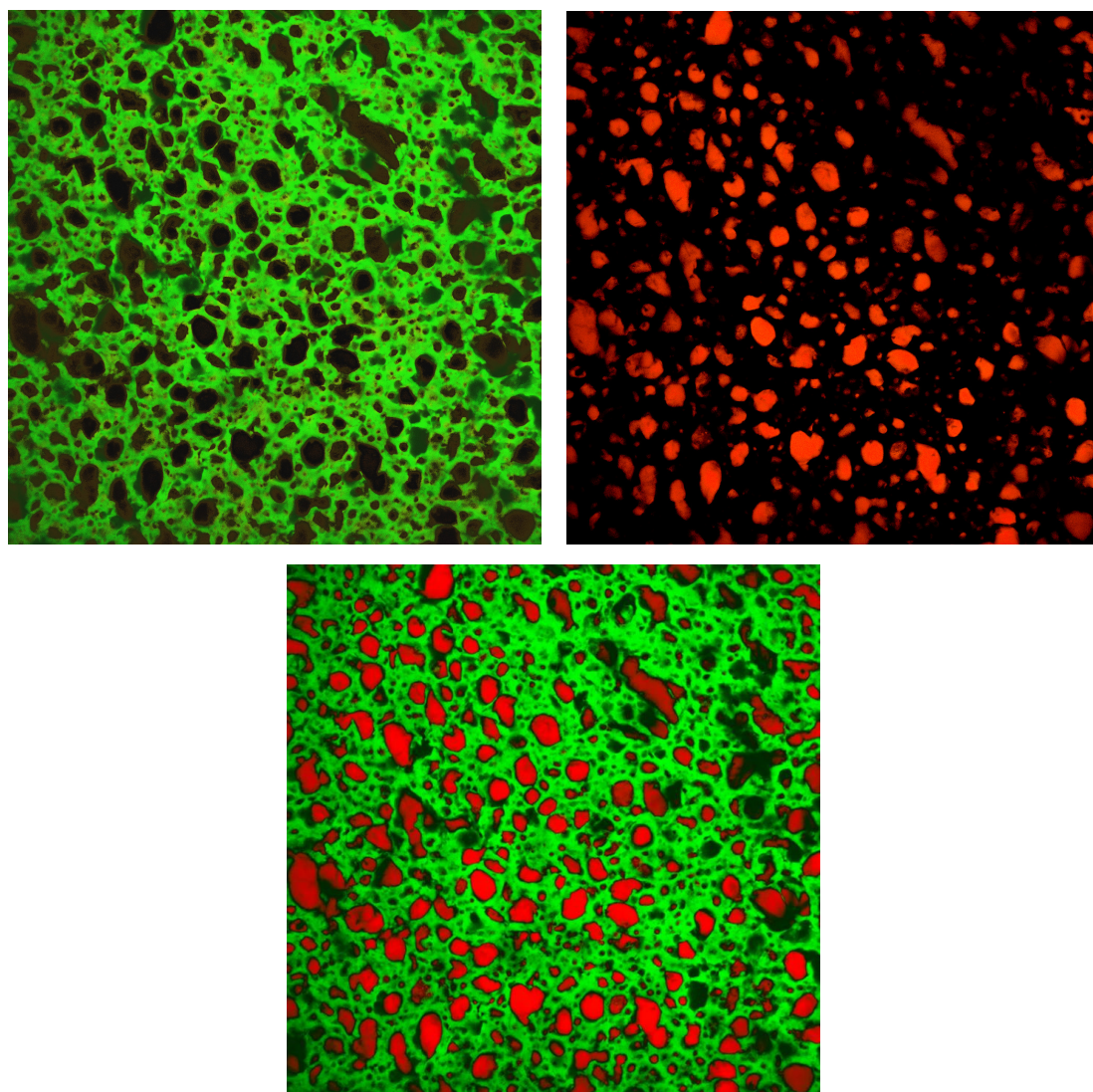


**Figure 5.8.** Confocal micrographs of Pecorino cheese. *A) Protein matrix stained with FITC. B) Fat globules treated with Nile Red. C) Merged image of protein and fat phases.*

As already mentioned above, microstructure affects cheese properties. In all kinds of cheeses, one or two days after the manufacture, some free serum can be observed when the cheese is cut. However, the watering-off process differ among various cheeses. Pecorino cheese-making is made of several steps that promote syneresis and lead to a final product poorer of water. First, the coagulum is cut into small curd particles. Then, high temperature is used and the curd blocks are laid on a tilted board, placed on reed baskets and pressed. Cheese results with a low water content, as required for pressed-cheeses. Conversely, Ragusano cheese has a greater water holding capacity, due to the protein hydration as water is absorbed into the

protein matrix from the original serum channels or pores, formed during the stretching process (McMahon et al., 1999). Water holding capacity affects directly the rigidity of the matrix, and thus cheese softness.

## Particle Size Analysis

The naked eye observation of Ragusano and Pecorino cheeses micrographs provided qualitative information about their microstructures. To support and confirm qualitative analysis, particle size analysis was performed using specific tools of ImageJ (<http://rbs.info.nih.gov/ij>) software.

The method was used to determine circularity, area, max and min diameters of fat particles of the two different cheeses (made with different manufacturing processes). Values of circularity were grouped in 10 ranges, normalized (Table 5.2) and then graphically interpreted from the histogram below (Figure 5.9).

	0-0.1	0.11-0.2	0.21-0.3	0.31-0.4	0.41-0.5	0.51-0.6	0.61-0.7	0.71-0.8	0.81-0.9	0.91-1	
Pecorino	0	1	9	16	33	51	46	58	49	19	282
Normalized values	0	0.35	3.19	5.67	11.70	18.09	16.31	20.57	17.38	6.749	100
Ragusano	1	7	11	18	10	13	14	9	25	46	154
Normalized values	0.65	4.55	7.14	11.69	6.49	8.44	9.09	5.84	16.23	29.87	100

**Table 5.2** *Circularity of fat particles in Pecorino cheese.*

Most of the fat particles of Pecorino cheese micrograph have values between 0.5 and 0.9, whereas Ragusano cheese has many particles roughly spherical (0.91-1), and many others elongated (0.11-0.4).

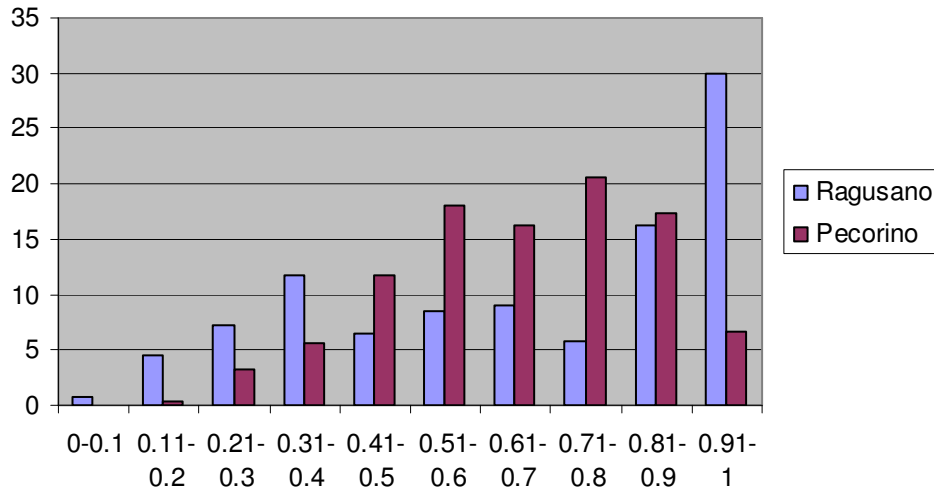


**Figure 5.9** Histogram of circularity for Ragusano and Pecorino cheese.

Since the histogram showed many circular fat particles in Ragusano cheese and not lots of spherical particles in Pecorino cheese, the qualitative comments made previously have been contrasted. Then, a more accurate analysis was performed.

A pairwise correlation was used to estimate correlations among the 4 parameters calculated for each cheese image (Area, Major, Minor, and Circularity). A complete matrix with correlations (4 × 4) was obtained, where correlations were estimated using the restricted maximum likelihood (REML) approach (Table 5.3).

Ragusano Cheese				
	Area	Major	Minor	Circularity
Area	1***	0.94***	0.88***	-0.53**
Major	0.94***	1***	0.78***	-0.63***
Minor	0.88***	0.78***	1***	-0.42***
Circularity	-0.53***	-0.63***	-0.42***	1***

\*\*\*  $P < 0.001$

**Table 5.3** Pairwise correlations in Ragusano cheese.

For Ragusano cheese, moderate inverse correlation factors (statistically significant,  $P < 0.001$ ) were found between circularity and area (-0.53), and circularity and major axis (-0.63), which means that the smallest particles were those closest to the perfect sphericity; and the biggest had an elongated shape. Our data explained that just the bigger particles were affected by the stretching process, whereas the smaller ones escaped to that and maintained their spherical shape.

Moreover, it is well known that only smallest fat crystals can be roughly spherical and that larger crystals often show rounded edges of elongated shapes (Walstra, 2003).

In Pecorino cheese any strong correlation was found among the calculated parameters (Table 5.4). Circularity was weakly inversely correlated to area (-0.17) and major axis (-0.30). Correlations were statistically significant ( $P < 0.001$ ).

Pecorino Cheese				
	Area	Major	Minor	Circularity
Area	1***	0.94***	0.91***	-0.17**
Major	0.94***	1***	0.84***	-0.30***
Minor	0.91***	0.84***	1***	-0.01
Circularity	-0.17**	-0.30***	-0.01	1***

\*\*\* $P < 0.001$

\*\* $P < 0.01$

**Table 5.4** Pairwise correlations in Pecorino Cheese.

The reason of our results is found in the cheese making process. Indeed, the pressure applied to Pecorino cheese squeezes fat particles and gives them an irregular shape. Anyone of them can escape to the pressure, justifying that their size does not influence the shape. For this reason the most fat particles of Pecorino cheese have a circularity value between 0.5 and 0.9 and just some of them are close to the perfect sphericity.

## Conclusions

Differences of the final cheese texture between the *Pasta Filata* and *Pasta Pressata* processes is in general due to the compression force versus the torsional force. Deformations of the curd particles occur through a totally different mechanism. In the Ragusano cheese (*Pasta Filata*), there is substantial curd movement and high sheering forces resulting in channels in which whey can flow from the cheese curd. In the *Pressed Cheese*, there is only slight movement of curd particles during pressing, with whey being forced out without substantial curd movement. During these profoundly different processes many microstructural changes occur. The *Stretched Cheese* has a very fine texture and proteins have directional alignment. The pressed curd has distinct curd boundaries, less

stretchability, and a looser texture. Lucey et al. (2003) asserts that it is the different water holding capacity that makes *Pasta Filata Cheese* softer than *Pressed Cheese*.

Quantitative analysis on Pecorino and Ragusano cheeses micrographs was performed to investigate correlations among circularity, area, major and minor diameters.

In Pecorino cheese, area and circularity were not strongly correlated, that is particles size of fat particles does not weigh on their shapes.

In Ragusano cheese, circularity and area are high-moderate inversely correlated, which explains that small particles are nearly spherical and that bigger fat particles veer off the sphericity, as also showed from the image, and appear elongated. We can deduce that only bigger fat masses undergo the stretching treatment, whereas small particles escape that just because of their size.

Conversely, in Pecorino cheese all the globules feel the pressing process, even the smallest. Indeed, looking at the histogram, most of the globules are not perfectly round, they have medium values of circularity, because the pressing process has squeezed all of them, regardless of their size.

### **5.3 Automatic labelling of CLSM images**

#### **Introduction**

Quality control in food research is often carried out by careful evaluation of microstructural features such as holes, protein, and fat of food samples. Indeed, the microstructural arrangement of basic elements of a complex food product affects its macroscopic behaviour and properties.

Microscopy combined with quantitative analysis is used to find out the relationships between food properties and its microstructure. Reliable quantitative analysis of microscopic features can be automatically accomplished only if a high-quality segmentation is computed beforehand. The measurements computed on binary images are deeply influenced by the segmentation accuracy, especially when shape descriptors of features are involved (Impoco, 2006). General-purpose segmentation methods fail with most classes of microscopy images due to several reasons. Segmentation of biological data is mostly concerned with detection of macroscopic structures. The extent of published work on segmentation and analysis of microscopy images is lower compared to the macroscopic world. The rationale of this phenomenon can be found in a number of causes: the large diversity of imaging approaches, the lack of a priori knowledge on the image content, the lack of common evaluation procedures, the large variety of imaged objects for different disciplines (Nattkemper, T.W.,2004). Most of the literature in this field is dedicated to biomedical data (e.g., analysis of cells) or to the study of bacteria in biological images. The segmentation of structural features in food images is mostly carried out with time-consuming user interaction, by means of techniques as simple as thresholding and basic morphological operators (Russ, 2004).

A statistically-founded algorithm was set up for the classification of cheese microstructure features from confocal laser scanning micrographs. A statistical Image Processing algorithm was developed for automatic detection, requiring no user intervention. The chosen method is based on image statistics of pixel neighbourhoods at different scales. Its robustness is shown to be sufficiently to assure reliable estimation of porosity. This work demonstrates that segmentation based on image statistics is a promising approach for dependable quantitative analysis.

Ten sample of Ragusano *pasta-filata* cheese were prepared for CLSM observation. Cheese was cut into slices of 10x5x1mm, which were treated with different dyes. Proteins were stained with Fluorescein Isothiocyanate (FITC) and lipids with Nile Red. The samples were incubated for 30 min in a dark room and then mounted on glass slides, enclosed with cover-slip and sealed with the appropriate gel. Ten CLSM double-stained micrographs were acquired using a 10x objective and displayed with the colour coding: red for fat, green for protein, and black for serum phase, voids and any gas. The main microstructural features of the images were gathered into morphologically-meaningful classes: fat globules, void, gas and protein matrix.

Then, the micrographs were manually labelled for training for a new type of cheese. A simple ad-hoc tool was used to help the operators during manual labelling. The operative stage required no user intervention at all.

Because pixel intensities alone are not sufficient to detect specimen structures, since they are not strictly related to useful properties of looked-for features, we employed multiscale detectors to encode information about the neighbourhood of interest structures. Four circular neighbourhoods were defined around each pixel, with increasing radius. Each neighbourhood was divided into four sections along the N,S,E,W directions to capture possible typical orientation of structures.

The multiscale statistical description employed is depicted in Figure 5.10. Here, for example,  $N_i$  identifies the  $i$ -th neighbourhood in the North direction.  $C$  refers to the value of the central pixel.

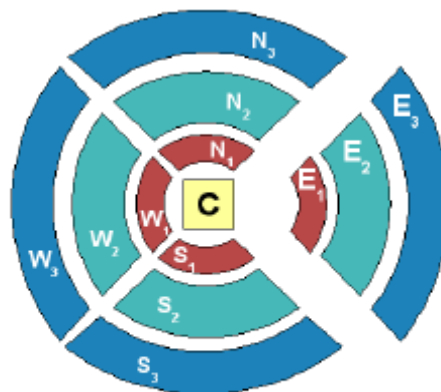


**Figure 5.10** Multiscale statistics.

In more formal terms, for each scale  $s$ , we employed a circular annulus of radius  $r_s$  centred around the interest pixel.

We define

$$v_s(x) = (F_{s,N}(x), F_{s,E}(x), F_{s,S}(x), F_{s,W}(x))$$

as functions of pixel values for four sectors in the surrounding window: North (N), East (E), South (S), and West (W) (see Figure 6.9), where  $x$  is a pixel. We use the intensity value of the interest pixel ( $x$ ) together with feature vectors  $v_s$ . For each pixel, statistics were gathered for the colour of surrounding pixels.

A probability density function (PDF) was generated for each area for each class, in four directions, plus the central pixel. Micrographs were analysed using pixel neighbourhoods and the PDFs generated during the learning stage. The posterior probability of a pixel belonging to a certain phase was computed using the Bayes' Theorem and using the PDFs as conditional probabilities.

The automatic detection made by our algorithm resulted acceptable even though not accurate (Figure 5.11).

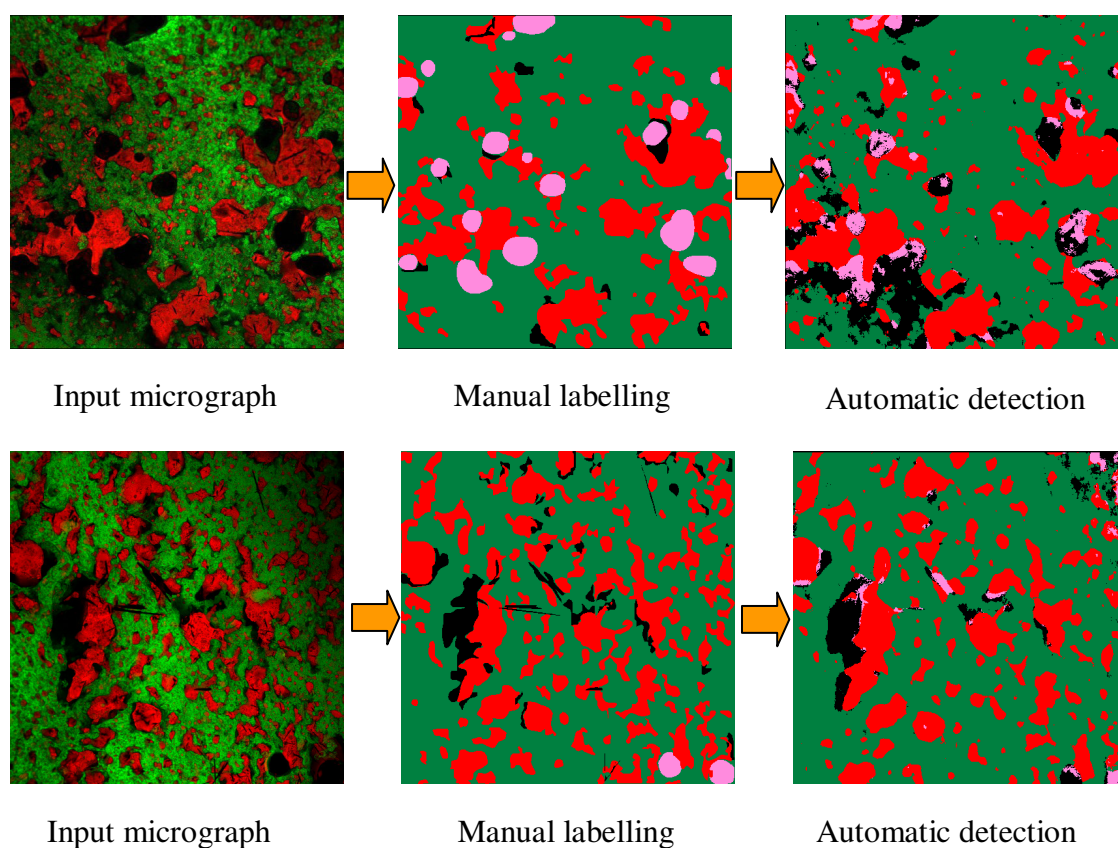


**Figure 5.11.** Automatic classification of features based on pixel neighbourhoods and the PDFs generated during the learning stage.

Protein matrix, voids and gas holes were well detected. However, many little lipids were not found at all. Moreover, statistical analysis suggested that in the observed images gas holes lay close to fat with high probability (Technical report, Impoco et al., 2009). These results suggest to use the algorithm combined with one more algorithm based on geometric properties of features.

# Chapter 6

## Application to milk

### 6.1 Heating treatments effects on milk and dairy products

#### Introduction

In the dairy industry, thermal treatments of milk aim at increasing shelf life and at improving food safety of the final product. Milk for cheese manufacture is usually pasteurized at 73 °C for 15 sec. The effects of heating treatments have been considered for their potential of improving cheese yield through incorporation of whey proteins into cheese curd (Lucey, 1995), even though higher temperatures provoke longer coagulation times, weaker gels (Guinee et al., 1997; Singh and Waungana, 2001), and affect curd syneresis, promoting higher cheese yield (Rynne et al., 2004).

Milk is also often subject to homogenization. This is performed to break milk fat globules into fine droplets, in order to prevent cream separation, therefore increasing stability and shelf life of milk. Although homogenization has damaging effects on curd forming properties (Emmons et al., 1980), and curd syneresis (Green et al., 1983), it improves rennet action and cheese yield due to better fat recovery (Jana and Upadhyay, 1992).

We aimed to evaluate the effects of heat treatments and homogenization on milk and Provola cheese microstructure.

#### Treatments of milk

Raw bovine milk was taken from a local dairy farm and was divided into 6 portions (A to F). The first part (A) was maintained raw and was not submitted to any treatment. The other 5 parts were homogenized and then subject to 5 different heat treatments. B milk was pasteurized at 73°C for 13.75 sec (HTST) by Ragusa

Latte (a dairy plant in Ragusa – Italy); C, D, E, and F milk were heated at 73 °C for 30 sec, 5, 10, and 15 min respectively by the dairy laboratory at CoRFiLaC.

HTST milk and raw milk were then used to produce Provola cheeses (named, Pr and Pt) at CoRFiLaC dairy plant. Cheese samples were examined after 1, 6, 13 and 20 days of brining. The experiment was performed in triplicate: each replication was carried out one week after from the previous.

### **CLSM observation**

Microstructural analysis of milk and Provola cheese samples was carried out using confocal laser scanning microscope (CLSM). Samples were previously treated with 0.20 g/ml Nile Red (Sigma-Aldrich, Inc.) in dimethylsulfoxide (Sigma-Aldrich, Inc.) for 10 min in darkness to stain lipids. After double rinse of the excess of dye with deionized water, 0.050g/ml Fluorescein Isothiocyanate (FITC, Sigma Aldrich, Inc.) in acetone:water (1:1) solution was used for marking proteins. The stained samples were mounted on standard microscope slides, enclosed with cover-slip, and placed on the Nikon C1si inverted microscope (Calenzano, Firenze-Italy) with an Argon Ion Laser 457-514nm 40mW, He/Ne Laser (543 nm) 2,0mW, and He/Ne Laser (640nm) 1,5mW. FITC was excited at 488 nm and Nile Red at 568 nm, whereas their emission wavelengths were 520 and 630 nm, respectively. Provola cheese samples were examined using 10X and 20X lenses to have the general view of components distribution, whereas milk samples were observed using 40X lens because of fat globule size.

### **Results**

CLSM images revealed that heating treatments did not induce any significant difference in the microstructure among Provola cheese samples. Micrographs showed high variability in the microstructure both within each sample and among different cheeses. As it has been explained in the Chapter 3, fat is found in cheese in the form of small droplets, of fat globules aggregates or of large pools of free fat that do not bind the proteins. Figure 6.1 shows that fat globules were finely dispersed in the protein matrix, but also present as free fat pools among the caseins both in the Pr and the Pt samples at 1 day of brine.

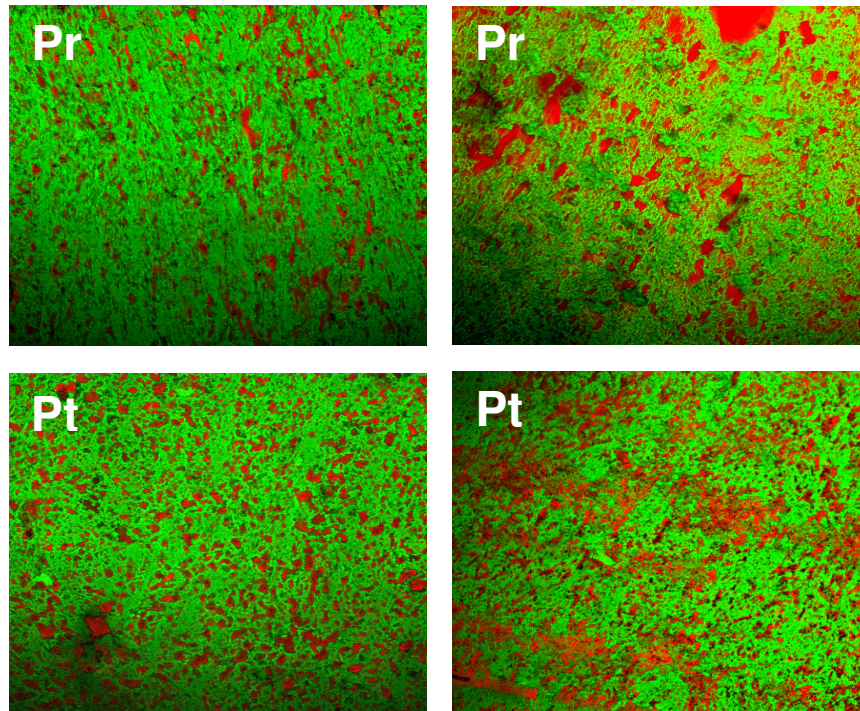
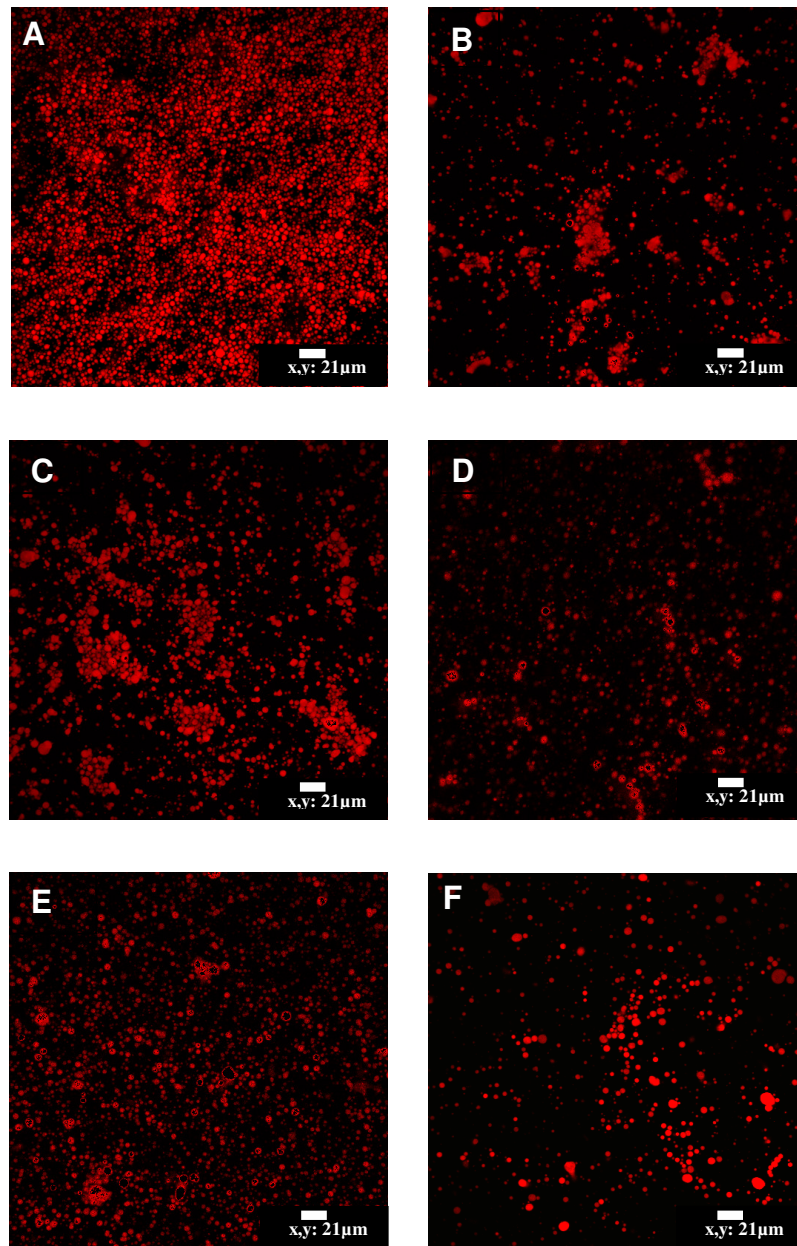


**Figure 6.1.** (Pr) “Provola” at 1 day of brine made from raw milk BI, (Pt) “Provola” at 1 day of brine made from pasteurized milk.

Confocal micrographs displayed some differences among milk samples (Figure 6.2). Image of raw milk sample (Figure 6.2 A) illustrated that the fat globules were uniformly dispersed, had the same shape and were of the same order of size. Conversely, the other pictures showed that fat globules were organized into clusters and were not uniformly scattered (Figure 6.2 B, C, D, F). We conclude that heat treatments and homogenization of milk modified milk fat globules, dashing the membrane, modifying their surface and sometimes decreasing their size.



**A ≠ B, C, D, E, F**

**Figure 6.2.** *A) Raw milk. B) Pasteurized milk at 73 °C for 13, 75sec. C) Heated milk at 73 °C for 5sec. D) Heated milk at 73 °C for 30sec. E) Heated milk at 73 °C for 10min. F) Heated milk at 73°C for 15 min.*

Heat treatments and homogenization induced changes in lipid membrane. Fat globule membrane contains about 40 - 50% of proteins (about 1% of the total protein in milk) and 30 % of phospholipids. It is also the site of trace elements, about 10 enzymes, and carotene. The main ultrastructure element is a bilayer membrane that surrounds fat globules and its inner and outer layers (Keenan et al., 1983). The inner protein layer possesses a paracrystalline array and separates the

membrane from the triglyceride core. This paracrystalline array is modified by the heating or cooling of raw milk and by changes in ionic strength (Buchheim, 1986). According to Corredig and Dalgleish (1998b), during heating treatment a more resistant membrane was developed outside the globules, probably due to the interaction of the outer layer of the membrane with other proteins ( $\beta$ -lactoglobulins), generating a polymerized new surface that is more resistant to coalescence. However, heating as well as homogenization enhanced the possibility of partial coalescence among fat globules. The phenomenon, extensively studied, is quite complex and is encouraged by the following mechanisms:

- a) The encounter frequency which is proportional to the velocity gradient (shear rate).
- b) The chance that a protruding crystal does reach the film between two globules, greatly enhanced by the globules rolling over each other.

When a fat globule is disrupted, the new area is covered with the hydrophobic part of casein particles, generating a new membrane for the fat globule with a different composition and binding mainly casein micelles with other fat globules (Tosh an Dalgleish, 1998). Part of the original MFGM remains on the globule but is insufficient to cover the new surface and prevent formation of clusters (Figure 6.2 B and C).

A more accurate analysis of the Figure 6.2 reveals that the sample “E” differed from the other treated samples: it was characterized by fat globules almost uniformly distributed. The sample “E” was heated at 73 °C for 10 min. Looking at its microstructure, it can be a good time-temperature compromise to obtain the ideal structure, however we must consider other milk parameters, such as sensory properties. It is well known that heating milk for long time can induce protein denaturation and vitamins loss. Thus, other analysis are needed to verify the effectiveness of this time-temperature combination.

## **Conclusions**

Heat treatments and homogenization are very useful processes to maintain milk safety and to extend milk shelf life, however they can induce some changes in milk components and their structure.

Physical stability of fat globules against aggregation, coalescence, and oleification processes are largely connected to membrane properties of fat globules. Temperature and some mechanisms connected to the homogenization process, such as encounter frequency, can damage MFGM and promote partial coalescence of milk fat globules. Thus, the best combination of temperature and time of heating treatment and homogenization is necessary to obtain a safe, and high quality product at the same time. Moreover, the combined effect of heat and homogenization of milk can improve cheese-making properties inducing changes to the protein–fat structures.

# Chapter 7

## Application to wooden tools

### 7.1 Bacteria biofilm in inactive Tina wooden vats

#### Background

Ragusano cheese is made in the Hyblean region of Sicily from raw milk using traditional wooden tools, without commercial starters. In the cheese making process of this brine-salted pasta filata cheese, raw milk is directly placed in traditional wooden vat (*tina*) and lactic acid is produced by natural milk flora and desirable flora from the biofilm of the internal surface of the *tina*. The respective contributions of these two bacterial sources, raw milk and Tina biofilm, as well as the ecosystem in the biofilm are still not completely elucidated. Licitra et al. (2007) demonstrated the predominance of lactic acid bacteria in the biofilm, and in particular *S. thermophilus*, the presence of thermophilic lactobacilli, lactococci and of a few high GC% microorganisms such as coryneform bacteria. The PCR-Temperature Temporal Gradient Electrophoresis (TTGE) profiles showed some variability among *tinas* coming from 5 different farms of the Hyblean region (2 to 10 co-dominant species), which represents a valuable source of biodiversity. Moreover, each molecular profile was shown to be stable in time at least for the dominant species. Raw milk spontaneous acidification before and after a few minutes of contact with the *tinas* was accelerated in 80% of the cases clearly supporting the idea of lactic acid bacteria inoculation via the Tina biofilms. One more experiment on *tina* biofilm was performed by Lortal et al. (2009), who assessed the safety and efficiency of this natural inoculation system. They showed the predominance of thermophilic lactic acid bacteria, low counts of yeasts in a few *tinas* and the total absence of *Salmonella*, *Listeria monocytogenes*, and *Escherichia coli* O157:H7. Also, micropieces taken from four *tinas* were observed by confocal and scanning electron microscopy. The biofilm covered almost entirely the surface of the wood and polysaccharides were detected around bacteria in the four *tinas*. In three of the latter, cocci were predominant in the ecosystem whereas in the other one, cocci, bacilli, yeasts and moulds were observed.

Since the traditional cheese making season spans from October to June, in this research project we intended to assess the presence of biofilm in inactive *tinas* and to further describe *tina* biofilm composition and organization through Confocal Laser Scanning Microscopy.

### **CLSM observation**

In October, *tina* samples (not used by the farmers for the entire summer time) were collected from the inner surface of the wooden vat. The wood splinters were taken from *tinas* of four local farms. By using a sterile blade, three small wood splinters were removed (15×5×1 mm), at about 20 cm from the bottom.

The samples were treated with 5 µL of LIVE/DEAD® *BacLight*<sup>TM</sup> Bacterial Viability Kits stain (Invitrogen L13152), added directly to the wood for microorganisms detection and 5 µL of Concanavalin A linked with Alexa Fluor 633 (Invitrogen 21402) for polysaccharides detection. The samples were incubated for 15 min in darkness and observed at different magnifications (4x, 10x, 20x, 40x and 60x), with an excitation wavelength of 488 nm or 638 nm, and an emission wavelength range from 500 to 530 nm or over 650 nm, respectively.

Micrographs showed that inactive *tinas* were still almost entirely covered by the biofilm, as illustrated on Figure 7.1. Biofilm was rich of bacteria colonies surrounded by an exopolysaccharides matrix. In the Figure 7.1, biofilm layer covering the wood surface is indicated in green.

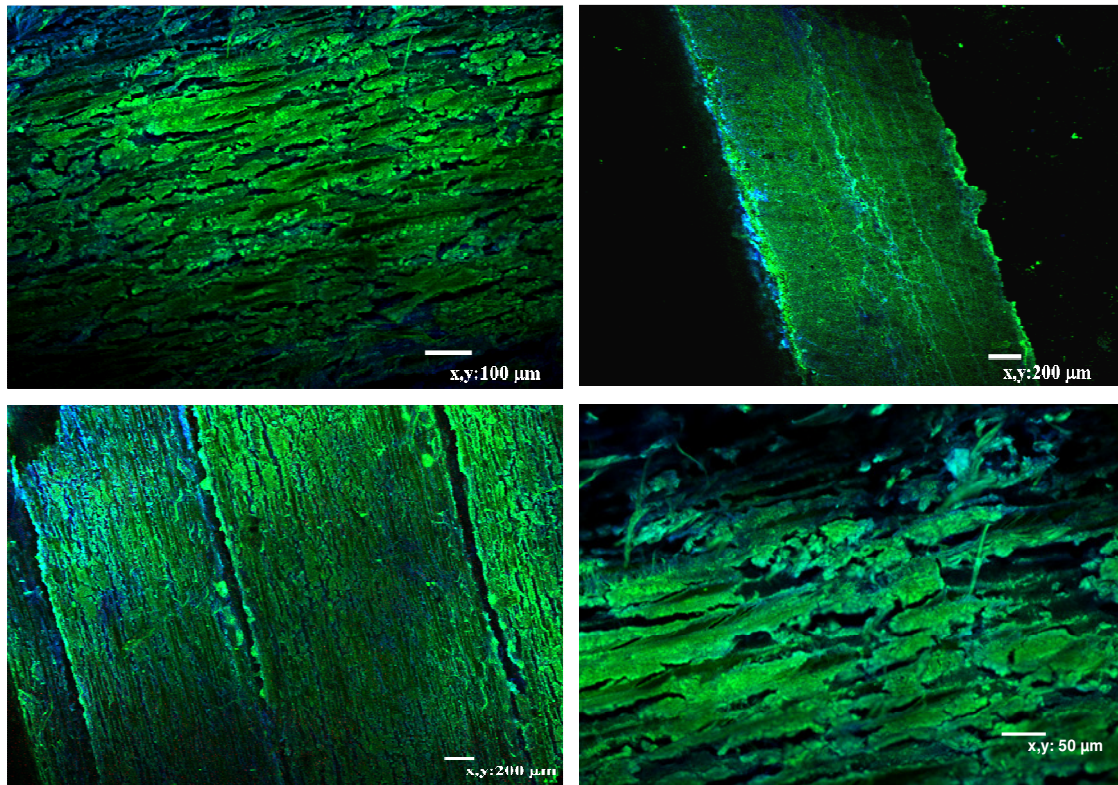


**Figure 7.1.** Confocal microscopy observations of tina biofilm at different magnifications. Biofilm (in green) almost entirely covers the surface.

Bacteria colonies were found being both on the internal surface and within the deeper layers of the wood splinters (Figure 7.2). Below, the yellow stain represents microbial population growing among inner wood fibers.

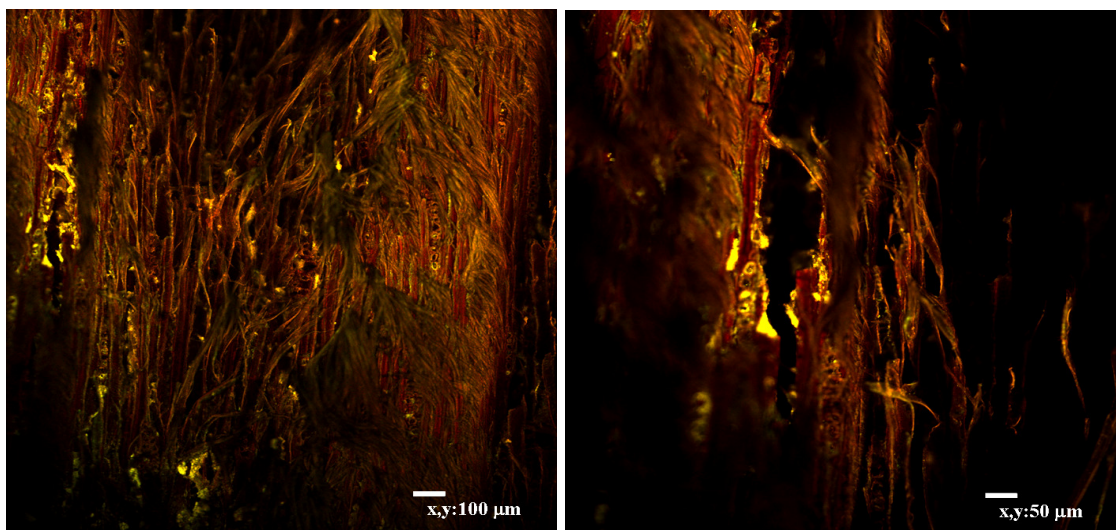


**Figure 7.2.** Bacteria colonies dispersed within the deeper wood layers. Microorganisms are coded in yellow, wood fibers appear in brown.

Wood probably maintains a percentage of humidity even in summer time (when *tina* is not used) and lets bacteria survive. They were especially found to gather around vessels perimeter (Figure 7.3), due to the greater availability of moisture and nutrients. Indeed, during the cheese making process, a certain amount of milk is absorbed from wood. Milk flows trough these wood channels leaving some of its nutrients. Then, bacteria will tend to group on the edges of vessels.

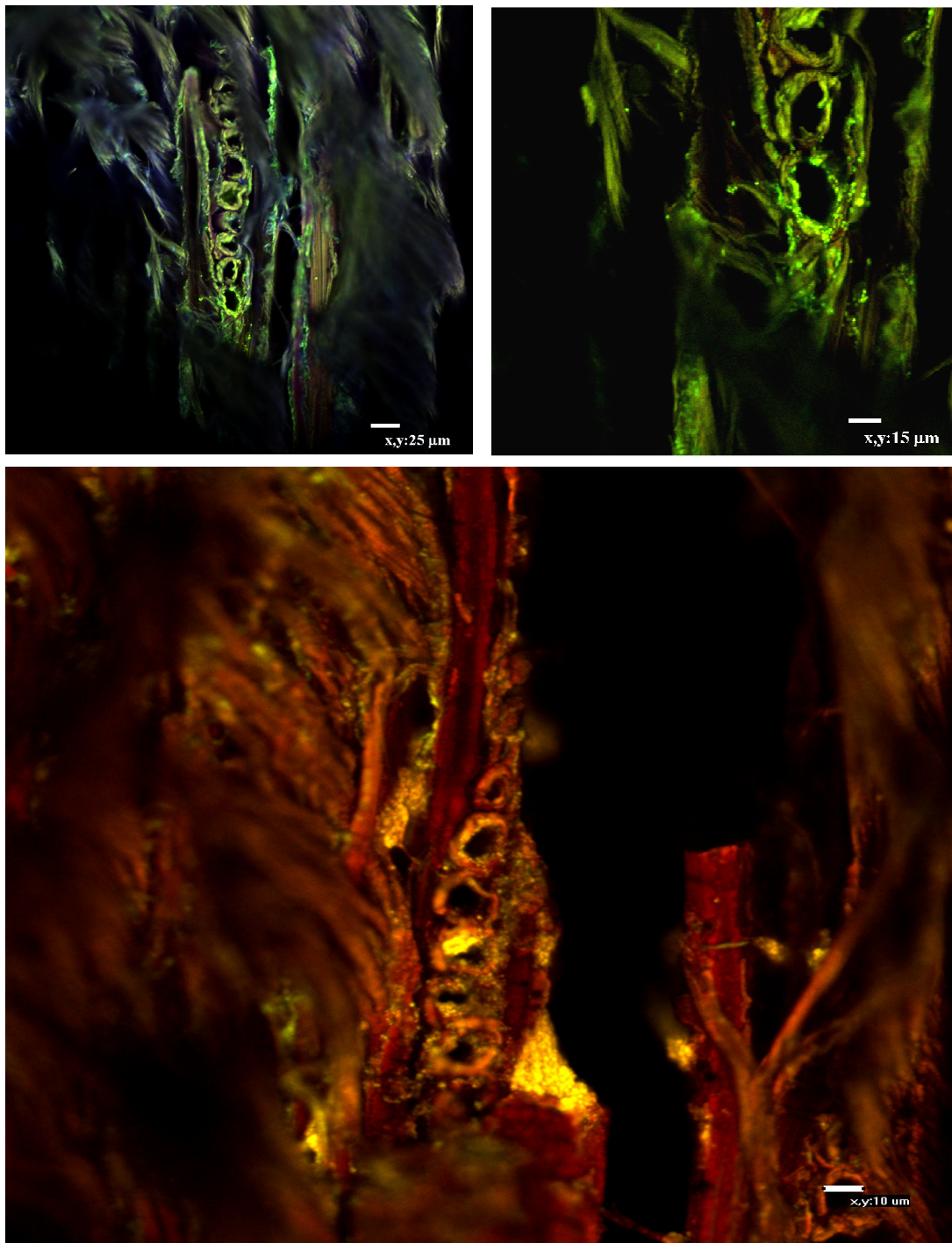


**Figure 7.3.** Detail of bacteria distribution in wood splinters of tina. Bacteria colonies are gathered around vessels perimeter.

Thanks to the dye used to stain microorganisms, we could discover that biofilms, in inactive *tinas*, were mainly made of living bacteria (Figure 7.4). The LIVE/DEAD® BacLight™ Bacterial Viability Kits employs two nucleic acid stains: green-fluorescent SYTO® 9 and red-fluorescent propidium iodide. These dyes differ in their ability to penetrate healthy bacterial cells. When used alone, SYTO® 9 labels both living and dead bacteria. In contrast, propidium iodide penetrates only bacteria with damaged membranes, reducing SYTO® 9 fluorescence when both dyes are present. Thus, live bacteria with intact membranes fluoresce green, while dead bacteria with damaged membranes fluoresce red. Since, both alive and dead bacteria are present in biofilm, the green fluorescence can result to be yellow.

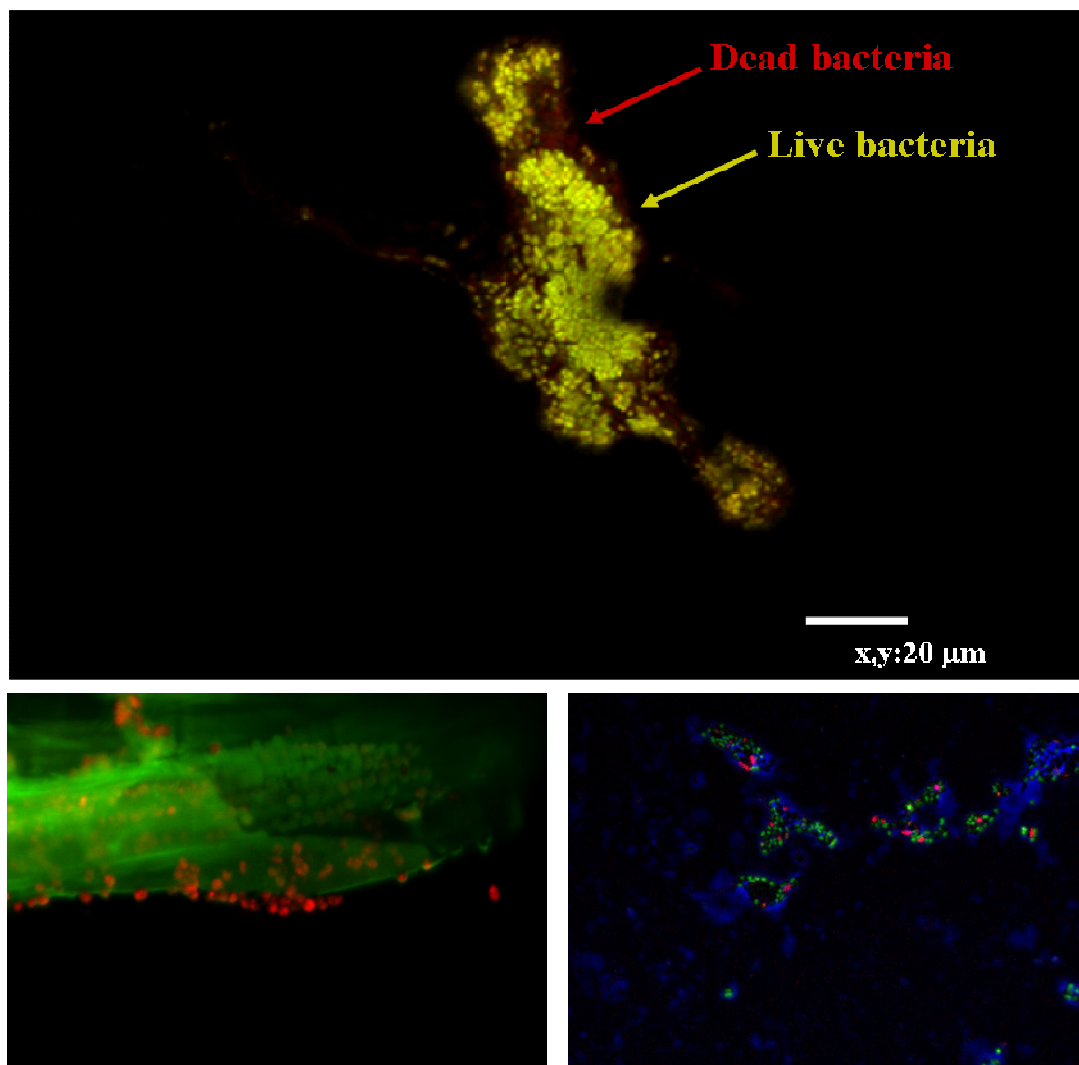


**Figure 7.4.** Biofilm population. **A)** Bacteria colony are mostly made of alive microorganisms (coded in yellow), and few dead microorganisms (coded in red). **B)** colonies made of dead (red) and alive (green) cells are enclosed from exopolysaccharides (blue). **C)** Cocci consortium. Just few dead bacteria are present, while most of the cells are showed to be alive (green).

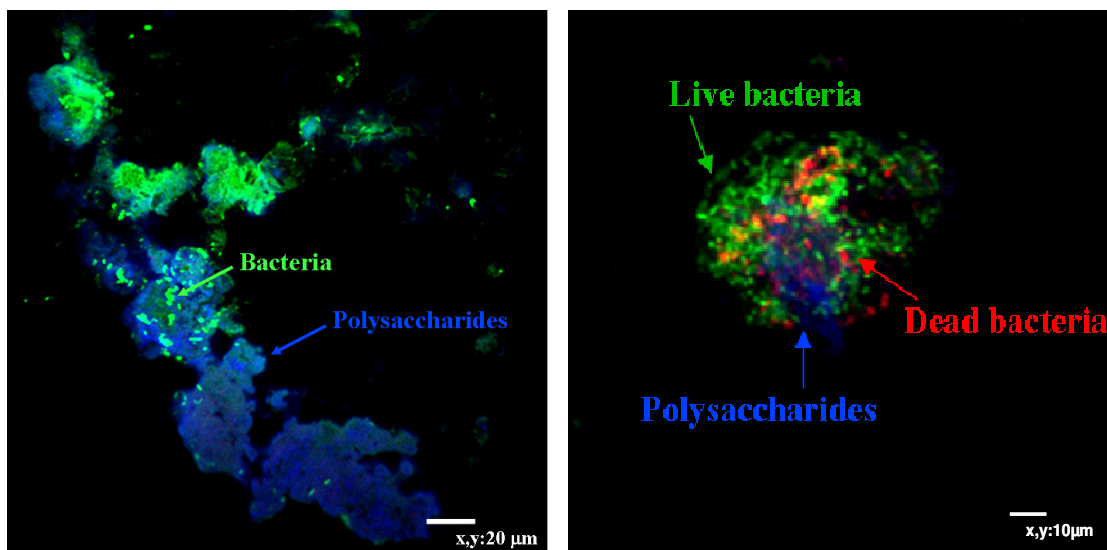


**Figure 7.5.** *A) Bacteria (green) surrounded by exopolysaccharides matrix coded in blue. B) Consortium, made of alive and dead bacteria, and exopolysaccharides.*

Staining with Concanavalin A dye allowed us to ascertain the presence of an exopolysaccharide layer on the biofilm (Figure 7.5), which provides nutrients to bacteria and protects them from the external environment.

## Conclusions

Biofilms are densely packed multicellular communities of microorganisms attached to a surface or interface and covered by a hydrated polymeric matrix. Microbial biofilms can represent valuable source of biodiversity.

Biofilm found on the surface of traditional wooden vats used to produce Ragusano cheese have been demonstrated to be safe and mainly composed of lactic bacteria.

Here, CLSM observations confirmed the presence of biofilm on inactive *tinas* and demonstrated that bacteria survive in dried vats. Bacteria colonies were found not only on the surface but also within the internal layers of the wood micropieces. The greater availability of nutrients and moisture close to vessels let bacteria gather on their perimeter. Moreover, bacteria were marked with a specific staining procedure that allowed us to distinguish living microorganisms from dead

cells. CLSM micrographs displayed colonies mainly made of living bacteria and just few dead cells. As already found, an exopolysaccharides matrix was observed around colonies, as a protection from environmental conditions.

The experiment will be repeated next season both to continue to verify the presence of colonies and to evaluate differences among the species.

## *Conclusion and Perspectives*

Visualization of the inner microstructural features of food is a facet of relevant interest for a wide range of scientific and industrial applications. Confocal Laser Scanning Microscopy (CLSM) is a powerful non-destructive technique capable of satisfying these needs.

Food microstructure is related to many other properties of foods, i.e. texture, appearance, shelf life, and taste perception. Knowledge of microstructure offers ways to improve existing products or to design new ones.

Qualitative and quantitative analysis of microstructure is essential. Digital image processing tools, image analysis software or custom developed algorithms, obtain exhaustive geometrical, morphological and topological description of the features inside the volume, or extract other particular parameters of interest (i.e. porosity, protein aggregation, fat distribution, bacteria amount).

The overall objective of this dissertation has been to define a non-destructive procedure suitable to the microstructural characterisation of dairy products and wooden tools exploiting the Confocal Laser Scanning Microscopy.

This globally required the acquisition of different competences:

- first, the set up of the CLSM facility dedicated to acquire different substrates (i.e. cheese, milk, and wood);
- then, the development of specific tools for the quantitative analysis of the acquired data, in order to extract their peculiar microscopic properties.

The structure of this dissertation has been subdivided in two main parts which correspond to the chronological development of the work.

In the first part, working at the microscopy laboratory of CoRFiLaC, I improved my theoretical knowledge about microscopy imaging and, at the same time, I learnt about image analysis and processing. I practiced about the existent SEM facility and also with the  $\mu$ -CT (computed microtomography) at the Syrmep beamline at Elettra, synchrotron of Trieste and I worked for the realization of some algorithms aimed at the quantitative description of the microstructure of our samples.

As already mentioned in previous chapters, microstructure can be studied with different instruments, up to the resolution and details we want to achieve. Besides my practise on SEM and  $\mu$ -CT, in order to add more information about microstructure, CoRFiLaC decided to let me specialize on Confocal Laser Scanning Microscopy at the Utah State University.

At CoRFiLaC, CSLM was set up to achieve the best results on our food samples. We worked on an ad hoc method of staining food samples, deeply different from biological specimens. We have also pointed out the main aspects that contribute to the deterioration of image quality (i.e., laser beam hardening), experimenting specific methods to avoid or at least to reduce their impact.

In the second part, I mainly dedicated my efforts to the observation and analysis of different substrates. Particularly, I investigated three different matters: cheeses, milk and wood.

The results proved clearly enough the potential and the capabilities of CLSM to discern and define the microstructures inside the investigated samples. We demonstrated that CLSM, coupled with digital image processing, can be considered as a valid approach to obtain the measurement of those nano-features of geometrical and topological nature. The microscope is a complementary tool to the conventional analysis in order obtain a correlation between microstructure and other food properties, such as sensory properties.

The aspects related to digital image processing and 3D representation have been discussed in this study, providing a correlation between the microstructure and the macroscopic behaviour of the observed samples.

Representative examples of studies carried out with the described methods have been used to demonstrate the application of CLSM, combined with the developed image processing tools, to food science: Three dimensional reconstruction of Pecorino cheese micrographs for fat globule evaluation, imaging of Ragusano and Pecorino cheese for structure characterization, automatic labelling of CLSM images, heating treatments effects on milk and its products, and bacteria biofilm in inactive Tina wooden vats.

The activities presented in this dissertation open the way to a large extent of scientific and industrial applications. The possibility of deriving the physical properties from the 3D digital microstructure is very attractive. The state-of-the-art facilities available represent an ideal tool to investigate several phenomena

involving the microstructure of food products. On the other hand the computational power of modern calculators allows the rapid examination of huge amount of data.

I trace here just few key-aspects in order to address possible future activities:

- The existent CLSM set-up could be further upgraded, for instance, combining different type of mechanical stages (time-temperature, tensile, controlled atmosphere) to run new experiments.
- Digital image processing methods need to be tailored for a wide range of applications, each one requiring its own customization. This means that new specific algorithms suited, for example for multiphase systems, will be more and more essential. Furthermore, the developed algorithms necessitate to be optimized for speed and efficiency, in order to be able to manage more details.
- Several applications could be afford through direct simulation on the digital data as the lattice Boltzmann method (for example, the investigation of materials behaviour under stress, the multi-phase fluid flow study inside porous media, etc.).
- The study of biofilm in “*tinas*” could continue to distinguish bacteria species, using specific antibodies by immunolabelling and Fluorescence In Situ Hybridization (FISH) technique. FISH with rRNA-targeted probes provides unique possibilities to visualize uncultured microorganisms. It is also a powerful tool for analyzing structure and organization of biofilms in their natural environment. Preparing nucleic acid probes for one species and performing FISH would allow us to visualize the distribution of the species of interest within the biofilm. If the interest is for two species in the bacteria community, two probes prepared in two different colors provide to visualize and study their co-localization, and can be useful in determining the fine architecture of the biofilm.

# Appendix

## CoRFiLaC and its facilities

### Introduction

"CoRFiLaC" (Consorzio Ricerca Filiera Lattiero-Casearia) is a Dairy Research Center located in Ragusa and founded in 1996. Its main activity is studying traditional Sicilian dairy products, geared towards the methods of small and medium traditional cheese-makers, to create a link between the world of research and the world of production and consumers.

The Consortium works towards the greater goal of elevating the production of historic cheeses, made according to traditional methods, to the status of "works of art."

CoRFiLaC (Figure I) aims to improve the quality of life of the rural world in a socio-economical context based on solidarity and equal opportunities, while respecting the environment, the historic and cultural heritage and all those traditions that allow man and his values to find the proper role in the society.



**Figure I** CoRFiLaC. Consorzio di Ricerca Lattiero Casearia located in Ragusa.

The mission is to observe the rural world in order to project studies to support and to better coordinate all the different steps behind Ragusano cheese and the other Sicilian traditional products. The purpose is to demonstrate scientifically that the traditional production systems are not only an historical testimony or a piece of memory, but Nature's great expression in tune with the environment where man is the harmonizing element, essential in guaranteeing respect and integrity of the biological cycles. Nature and its many specific expressions, called bio-diversity factors, make these products unique. Bio-diversity factors studied by CoRFiLaC belong to three main research fields:

- Healthy properties of dairy products.
- Food safety
- Traditional systems of production of Sicilian historical cheeses.
- Aromatic and sensorial profiles of traditional cheeses.

CoRFiLaC commits itself both to help forming the operators of the "Filiera", and to start operations of experimental marketing, with the aim of increasing the value of traditional niche production, by monitoring and studying market and consumers' needs.

Last but not least, CoRFiLaC is also a Certification agency for the two Sicilian P.D.O. cheeses: Ragusano and Pecorino Siciliano (Gazzetta Ufficiale Repubblica Italiana, 1995).

Since CoRFiLaC works with scientific partners of great international relevance, knowledge about microstructure was improved at the Nutrition and Food Science Department by the Utah State University (Utah-USA). CoRFiLaC includes a series of laboratories, an experimental cheese plant and an aging centre.

### *I Microscopy laboratory*

Among all the laboratories, the attention will be focused on the microscopy laboratory. This houses a Scanning Electron Microscope and a Confocal Laser Scanning Microscope for studying the microstructure of dairy products. In Italy, CoRFiLaC is a pioneer in analyzing food microstructure. Scanning Electron Microscopy and Confocal Laser Scanning Microscopy allow to monitor the effects of the main factors of the cheese-making process on cheese microstructure

and to visualize the spatial arrangement of casein micelles and of all the other structural components. Also, these analysis allow to identify the main chemical components using specific labelling techniques, making qualitative and quantitative evaluations of the microstructure possible. Computer vision techniques are applied to digital micrographs, supplying numerical data about, for instance, porosity, dimension and shape of the pores among the casein matrix, and so on.

Knowing cheese microstructure and the factors influencing its constitution enables to develop peculiar strategies aimed to both control and improve cheese quality.

Furthermore, Scanning Electron Microscopy and Confocal Laser Scanning Microscopy analyses are performed to support the important role that traditional wooden tools play in the production of high quality cheese. Our studies have showed that a rich microflora totally immersed in a polysaccharide extracellular matrix grows on the internal surface of the wooden vat (Tina), used to collect and acidify milk to make cheese. Thus, Tina plays an important role in milk acidification because it enriches the original microflora of the whole raw milk with a natural starter from its internal surface, promoting the process of acidification of curd and characterizing cheese ripening.

## *II NIKON D-Eclipse C1si*

As forefront technology in food science, confocal microscope allow to have food microstructure images with high resolution and with any damage to the internal structure of the sample. CLSM can observe the specimen in depth, can obtain numerous and consecutive slices, ready to be reassembled by appropriate software to elaborate 3D images. Moreover, as it has been already discussed in the previous chapters, unlike the standard epifluorescence, CLSM removes the out of focus light, allowing the observation of thick specimens. This is very important for matrices (like food samples) which are difficult to cut in thin slices with a microtome.

In this context, CoRFiLaC had bet on *Nikon D-Eclipse C1si* confocal microscope (Figure II). The innovative C1si Confocal Microscope System gives a level of flexibility, speed and spectral capability not available in conventional

confocal systems, with detectors for both traditional fluorescence and spectral imaging in a wide range of applications. The C1si is a revolutionary true spectral imaging confocal laser microscope system with the amazing capability to acquire 32 channels of fluorescence spectra over a 320 nm wide wavelength range in a single pass.

By cleanly unmixing overlapping spectra of different fluorescent labels, the C1si improves dynamic observations of live cells and facilitates the acquisition of detailed data.

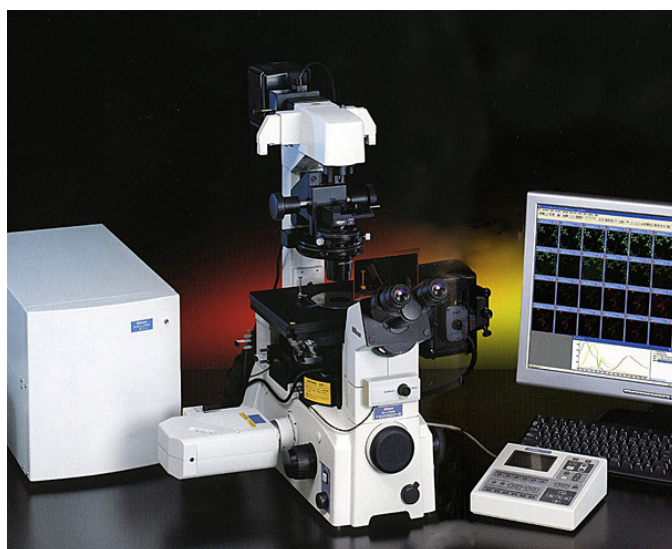


**Figure II.** Nikon D-Eclipse C1si. Main components.

### ***III.II.1 Significant reduction in image acquisition time***

The C1si boasts a multi-anode PMT (PhotomMultiplier) with 32 channels, the top for confocal microscopes. Innovations such as multiple high-speed digital conversion circuits and LVDS (Low Voltage Differential Signal) high-speed (approximately 2 sec) serial transmission technology allow a full 32 channels of spectral images to be obtained from a single scan. This allows for a dramatic reduction of imaging time and real-time observation. In the other systems, this acquisition should take too much time (several minutes), making impossible the experiment running.

Nikon D-Eclipse C1si comes with three lasers, allowing to detect fluorescence of almost all the fluorochromes. In particular, with the use of the

Krypton – Argon laser, three discrete wavelengths of light are produced simultaneously within the laser beam: 488nm, 568nm, 647nm. Thus, with the selection of the appropriate fluorescent dyes, multiple components of the sample can be labelled and identified simultaneously and a full range of 320 nm can be obtained in a single pass, a capability unmatched by previous spectral imaging systems.

Spectral images over a broad wavelength range can be obtained with only a single laser excitation. Therefore, adjustment of laser intensity and PMT gain is simple and quick, and there is no need to make multiple scans to acquire a broad spectrum, keeping fluorescence fading and specimen low damage.

### ***III.II.II True spectral imaging***

C1si allows observation of specimens in True Colour. Peak wavelengths and spectral shapes obtained in the C1si image closely match those obtained by the probe manufacturer (Figure III).

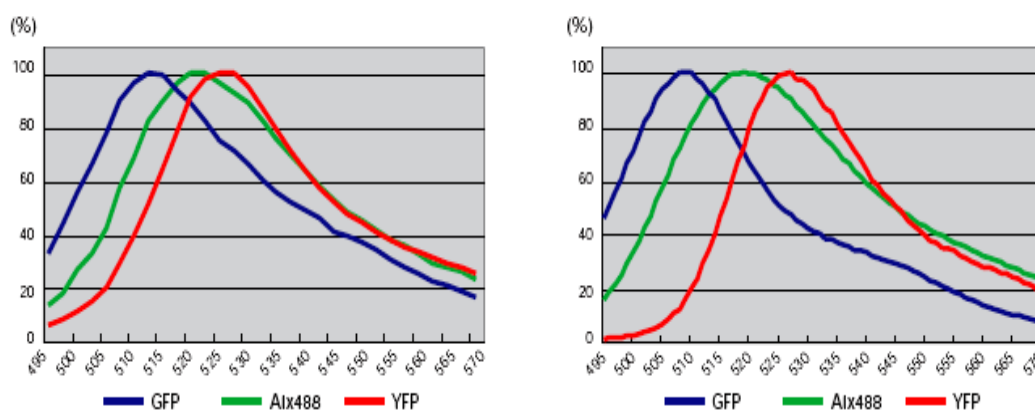


**Figure III.** Comparison between Spectral data from C1si (on the left) and those from the probe manufacturer (on the right)

Accuracy of spectra is maintained with highly precise correction technologies, including wavelength correction using emission lines and luminosity correction utilizing a NIST (National Institute of Standards and Technology) traceable light source.

Multi-anode PMT sensitivity correction technology (Nikon property) allows correction of sensitivity error and wavelength transmittance properties on a per-channel basis, allowing researchers to minimize measurement errors and deviations among different equipments.

### ***III.II.III Spectral imaging focusing on brightness***

Signal loss has been minimized by use of optics that very efficiently transmit fluorescence emission photons to the detector and the signal processing circuitry that digitizes for the full pixel period. Also, C1si system has two patented functional modes to optimize high quality images acquisition:

- Diffraction Efficiency Enhancement System (DEES) for polarization control has been adopted in the spectral detector of the C1si to maximize brightness. A prism splits the laser light in its two components (S and P). The P component, usually lost, is recovered on a S2 plane and focused with S1 on the detector. By co-aligning the direction of polarization, the efficiency of the diffraction grating is optimized, resulting in exceptionally clean images.

- Dual Integration Signal Processing (DISP) technology has been implemented in the image processing circuitry to improve electrical efficiency, preventing signal loss while the digitizer processes pixel data and resets. The signal is monitored for the entire pixel time resulting in an extremely high S/N ratio.

Moreover, the spectral imaging detector utilizes a newly developed laser shielding mechanism. Coupled with the wavelength resolution-independent of pinhole diameter, this mechanism prevents the reflected laser beam from noisy data. The blocking mechanism can be moved freely with software allowing users to block any laser wavelength, making the C1si compatible with virtually any laser selection. In addition, the ends of the fluorescence fibres and detector surfaces use a proprietary anti-reflective coating to reduce signal loss to a minimum, achieving a high optical transmission.

### ***III.II.IV Unmixing of images with no crosstalk***

It has always been difficult to cleanly separate fluorescences of multi-stained specimens with greatly overlapping wavelengths with a confocal microscope. By mathematically processing the spectral data of closely overlapping probes such as CFP, YFP, RFP, and Alexa 488, the C1si cleanly separates emissions from each,

yielding clear images with no cross-talk. This is particularly useful in observations of multi-stained specimens with localized protein molecules, and in FRET experiments. Spectral separation of probe signals from autofluorescence is also possible. Since the laser can be precisely pointed at ROI to photobleach only a specific area of cells, it is possible to observe the fluorescence recovery process (FRAP) as the molecules move over time.

### ***III.II.V CFI Plan Apochromat***

*NIKON D-Eclipse CIsi* mounts top of the line objectives that achieve both full correction of chromatic aberration in the visible range and high peripheral resolution. They are perfect for digital imaging, which requires uniform resolution from the image center to the periphery. These objectives remove aberrations in the peripheral visual field and also eliminate shading, resulting in images that are sharp all the way to the edges, a necessary feature when stitching images together.

The lenses boast exceptional optical performance in brightfield, DIC, and multi-stained fluorescence observations. In addition to the chromatic aberration correction range (435-660 nm) of the previous Plan Apo series, axial chromatic aberration has been corrected up to 405 nm, making this series appropriate for confocal observations. Moreover, these lenses have the highest NA (numerical aperture) ever within the Nikon objective lens line, with nearly complete aberrational correction. Their powerful optical capabilities are perfectly suited to multi-wavelength observations, and they can be used with normal cover glasses and immersion oils.

The 60x oil immersion lens utilizes the world's first temperature correction mechanism. Changes in the refraction index of the immersion oils resulting from changes in temperature affect image quality. With a 60x lens, this change can be easily modified with a correction ring in the range of 23 °C (room temperature) to 37 °C (incubation temperature). The correction ring is also effective in improving visualization of fine structures in DIC and epi-fluorescence microscopy, making this lens optimal for laser tweezers microscopy as well. Improving observation quality on a consistent basis is possible, as this lens allows for correction of the slight optical degradations that arise from temperature and coverglass thickness changes, (Nikoninstruments, 2006).

## Conclusions

CoRFiLaC is a dairy research centre which has bet on Sicilian capacities to improve the quality of life of the rural world and to elevate the value of their production. Born as “Progetto Ibleo”, it has almost a twenty-yearly experience on doing research. Its last bet is “food microstructure”, which is studied by two powerful microscopes: SEM and CLSM. *NIKON D-Eclipse Clsi*, the last purchase, is a cutting edge instruments to research food microstructure.

# Bibliography

Abramowitz M, Davidson MW (2007). "Introduction to Microscopy". *Molecular Expressions*.

Aguilera J.M and F. W. Stanley. 1999. Microstructural Principles of food processing and Engineering, 2<sup>nd</sup> ed. Aspen, Gaithersburg, MD.

Aguilera J.M. and V. Briones. 2005. Computer vision and food quality. *Food Aust*, 57 (3), 79-87.

Allan E. 2000. Protein Localization by Fluorescence Microscopy: A Practical Approach. The Practical Approach Series, Oxford University Press, Oxford, United Kingdom, 231 pages.

Art J. 1995. Photon detectors for confocal microscopy. In: Handbook of Biological Confocal Microscopy, 2<sup>nd</sup> edn. (ed. J. Pawley), Plenum Press, New York, pp. 183-196.

Auty M. A. E., M. A. Fenelon, T.P. Guinee, C. Mullins, and D.M. Mulvihill. 1999. Dynamic confocal scanning laser microscopy methods for studying milk protein gelation and cheese melting . *Scanning*, 21, 299-304.

Barret A. H. and M. Peleg. 1995. applications of fractals analysis to food structure. *Lebensm Wiss U Technol* 28, 553-563.

Bastiaens, I. H., A. Squire. 1999. Fluorescence lifetime imaging microscopy: spatial resolution of biochemical processes in the cell. *Trend Cell. Bioloby*, 9, 48-52.

Blonk J.C.G. and H. Van Aalst. 1993. Confocal scanning microscopy in food research. *Food Research International*, 28 297-311.

Broadbent J. R., D. J. McMahon, D. L. Welker, C. J. Oberg, and S. Moineau. 2003. Biochemistry, Genetics, and Applications of Exopolysaccharide Production in *Streptococcus thermophilus*: A Review. *J. Dairy Sci.* 86:407–423.

Buettner A. and P. Schieberle. 2000a. Changes in concentration of key fruit odorants induced by mastication. In: *Flavour release*. Roberts D.D. and Taylor A.J. Washington, DC, American Chemical Society, 87-98.

Buettner A. and P. Schieberle. 2000b. Influence of mastication on the concentrations of aroma volatiles – some aspects of flavor release and flavor perception. *Food Chemistry*, 71 (3), 347-354.

Buettner A., A. Beer, C. Hannig, M. Settles and P. Schieberle. 2002. Physiological and analytical studies on flavor perception dynamics as induced by the eating and swallowing process. *Food Quality and Preference*, 13 (7-8), 497-504.

Burke M.D., J.O. Park, M. Srinivasarao, S.A. Khan. 2000. diffusion of macromolecules in polymer solutions and gels: a laser scanning confocal microscopy study. *Macromolecules*, 33 (20), 7500-7507.

Campo P., G. Licitra. 2006. *I Formaggi Storici Siciliani*. Monografia del CoRFiLaC. ISBN 88-87562-01-6.

Cardullo R. A., V. and Parpura. 2003. Fluorescence resonance energy transfer microscopy: Theory and Instrumentation., *Methods in Cell Biology* 72: 415-430.

Cerning, J. 1995. Production of exocellular polysaccharides by lactic acid bacteria and dairy propionibacteria. *Lait* 75:463–472.

Carunchia Whetstine M. E., M. A. Drake, B. K. Nelson, and D. M. Barbano. 2006. Flavor Profiles of Full-Fat and Reduced-Fat Cheese and Cheese Fat Made from Aged Cheddar with the Fat Removed Using a Novel Process. *J Dairy Sci.* 89: 505-517.

Corredig, M., and D. G. Dalgleish. 1998b. Characterization of the interface of an oil-in-water emulsion stabilized by milk fat globule membrane material. *J. Dairy Res.* 65:465–477.

Deng, L., D. L. Kasper, T. P. Krick, and M. R. Wessels. 2000. Characterization of the linkage between the type III capsular polysaccharide and the bacterial cell wall of group B *Streptococcus*. *J. Biol. Chem.* 275:7497–7504.

De Roos K.B. 2005. How lipids influence flavour perception. In: Food lipids- Chemistry, Flavour and Texture. Shadidi F. and Weenen H. Vol 920 ACS Symposium Series, Washington, DC, American Chemical Society.

De Vuyst, L., and B. Degeest. 1999. Heteropolysaccharides from lactic acid bacteria. *FEMS Microbiol. Rev.* 23:153–177. *Journal of Dairy Science* Vol. 86, No. 2, 2003.

Duboc, P., and B. Mollet. 2001. Applications of exopolysaccharides in the dairy industry. *Neth. Milk Dairy J.* 11:759–768.

Diaspro, A. 2002. Confocal and Two photon Microscopy: Foundations, Applications and Advances. Wiley-Liss, New york.

Du C.J. and D.W. Sun. 2004. Recent developments in the applications of image processing techniques for food quality evaluation. *Trends Food Sci Technol*, 15 (5), 230-249.

Du C.J. and D.W. Sun. 2006a. Learning techniques used in computer vision for food quality evaluation: a review. *J Food Eng*, 72 (1), 39-55.

Elumalai, P., Atkins, P., de Paula, J. *Atkins' Physical Chemistry*, Oxford University Press, 2002.

Emmons, D. B., M. Kalab, and E. Larmond. 1980. Milk gel structure. X. Texture and microstructure in Cheddar cheese made from whole milk and from homogenized low-fat milk. *J. Texture Stud.* 11:15–34.

Everett D. W., and N. F. Olson. 2003. Free Oil and Rheology of Cheddar Cheese Containing Fat Globules Stabilized with Different Proteins. *J Dairy Sci* 2003 86: 755-763.

Everett D. W., M. A.E Auty. 2008. Cheese structure and current methods of analysis. *Int. Dairy Journal*, 18 759-773.

Fallico V., L. Tuminello, C. Pediliggieri, J. Horne, S. Carpino and G. Licitra. 2006. Proteolysis and Microstructure of Piacentinu Ennese Cheese Made Using Different Farm Technologies. *J. Dairy Sci.* 89:37-48.

Gazzetta Ufficiale Repubblica Italiana n. 133 del 9 Giugno 1995. D.M. del 2 Maggio 1995. 6.

Ghosh S., D. G. Peterson, J. N. Coupland. 2006. Effects of droplet crystallization and melting on the aroma release properties of a model oil-in-water emulsion. *Journal of agricultural and food chemistry*, 54 (5), 1829-1837.

Ghosh S. and J. N. Coupland. 2007. Influence of food microstructure on flavours interactions. In: *Understanding and controlling the microstructure of complex foods*. (D.J. McClements, Ed), Woodhead Publishing Limited, Abington, Cambridge, England. pp.425-444.

Gonzales R.C., R.E. Woods. 2008. Image segmentation. In: *Digital image processing*. 3<sup>rd</sup> ed. Pearson education international, pp.689-692.

Gratton, E., and M.J. Van Deven. 1995. Laser sources for confocal microscopy. In: *Handbook of Biological Confocal Microscopy*, 2<sup>nd</sup> ed. (ed. J. Pawley), Plenum Press, New York, pp. 69-90.

Green, M. L., R. J. Marshall, and F. A. Glover. 1983. Influence of homogenization of concentrated milks on the structure and properties of rennet curds. *J. Dairy Res.* 50:341–348.

Greenspan, P., E.P. Mayer and S.D. Fowler. Nile red: a selective fluorescent stain for intracellular lipid droplets. *Journal of Cell Biology*, Vol 100, 965-973.

Guinee, T. P., C. B. Gorry, D. J. O'Callaghan, B. T. O'Kennedy, N. O'Brien, and M. A. Fenelon. 1997. The effects of composition and some processing treatments on the rennet coagulation properties of milk. *Int. J. Dairy Technol.* 50:99–106.

Guinee, T. P, M. A. E. Auty, C. Mullins, M.O. Corcoran, and E.O. Mulholland. 2000. Preliminary observations on effects of fat content and degree of fat emulsification on the structure–functional relationship on cheddar-type cheese. *Journal of texture studies*, 31, 645-663.

Gunasekaran S., and K. Ding. 1999. Three dimensional characteristics of fat globules in Cheddar cheese.

Guyot C., C. Bonnafont, I. Lesschaeve, S. Issanchou, A. Voilley and A.E. Spinnler. 1996. Effect of fat content on odor intensity of three aroma compounds in model emulsions: d-decalactone, diacetyl, and butyric acid. *J. Agric and Food Chem*, 44, 2341-2348.

Harrison M., B.P. Hills, J. Bakker, and T. Clothier. 1997. Mathematical models of flavour release from liquid emulsions. *Journal Of Food Science*, 62 (4), 653-658.

Haugland R. P., J. Gregory, M. T. Z. Spence, I. Johnson, and E. Miller. 2002. Introduction to fluorescence techniques. In: *Handbook of Fluorescent Probes and Research Products.*, Molecular Probes, Inc., Eugene, Oregon.

Heim R., A. Cubitt, R. Tsien. 1995. "Improved green fluorescence". *Nature* 373 (6516): 663–4.

Hess S.T., S. Huang, A.A. Heikal, W.W. Webb. 2002. biological and chemical applications of fluorescence correlation spectroscopy: a review. *Biochemistry*, 41, 697-705.

Jana, A. H., and K. G. Upadhyay. 1992. Homogenization of milk for cheesemaking – A review. *Aust. J. Dairy Technol.* 47:72–79.

Keenan et al., 1983 T.W. Keenan, T.W. Moon and D.P. Dylewski. 1983. Lipid globules retain globule membrane material after homogenisation, *Journal of Dairy Science* 66, pp. 196–203.

Kimber A.M., B.E. Brooker, D.G. Hobbs and J.H. Prentice. 1974. Electron microscope studies of the development of structure in Cheddar cheese. *J. Dairy Res.* **41**, pp. 389–396.

Impoco G., S. Carrato, M. Caccamo, L. Tuminello. 2006. Quantitative analysis of cheese microstructure using SEM imagery. In: SIMAI 2006. Minisymposium: Image Analysis Methods for Industrial Application.

Impoco G., L. Tuminello, N. Fucà, M. Caccamo, and G. Licitra. 2009. Automatic Detection of Microstructural Features Using a Statistical Image Processing Method. ADSA Annual Meeting. Montreal, Canada.

Ingham K. E., A.J. Taylor, F.F.V. Chevance and L.J. Farmer. 1996. Effect of fat content on volatile release from foods. In: *Flavour Science: Recent Developments*. Taylor A.J. and Mottram D.S. London, Royal Society Chemistry, 386-391.

Keller H.E. 1995. Objective lenses for confocal microscopy. In: *Handbook of Biological Confocal Microscopy*, 2<sup>nd</sup> edn. (ed. J. Pawley), Plenum Press, New York, pp. 111-126.

Jack F.R., and A. Paterson. 1992. Texture of hard cheeses. *Trends in Food Science & Technology* 3, pp. 160–164.

Jonkman J., E. Stelzer. 2002. resolution and contrast in confocal and two-photons microscopy. In: Confocal and Two-Photn Microscopy: Foundations, Applications and Advances. (ed. A. Diaspro). Wiley , New York pp.101-125.

Joshi N.S., K. Muthukumarappan and R.I. Dave. 2004. Effect of calcium on microstructure and meltability of part skim Mozzarella cheese. J Dairy Sci 87 (7) pp. 1975–1985.

Lakowicz, J.R. 2006. Principles of Fluorescence Spectroscopy, Third Edition, Plenum Press, New York.

Lakowicz J.R., and H. Szmazinski. 1996. Imaging Applications of Time-Resolved Fluorescence Spectroscopy. In: Fluorescence Imaging Spectroscopy and Microscopy. Vol. 137. (X.F. Wang and B. Herman, Eds.), John Wiley & Sons, Inc. Publishers. pp. 273-311.

Landy P., J.L. Courthaudon, C. Dubois and A. Voilley. 1996. Effect of interface in model food emulsions on the volatility of aroma compounds. J. Agric. Food. Chem., 44 (2), 526-530.

Licitra G., G. Portelli, P. Campo, G. Longombardo, G. Farina, S. Carpino, D. Barbano, 1998. Technology to produce Ragusano cheese: a survey. Journal of Dairy Science 81, 3343–3349.

Licitra G., J.C Ogier, S. Parayre, C. Pediliggieri, T.M. Carnemolla, H. Falentin, M.N. Madec, S. Carpino, S. Lortal, 2007. Variability of the bacterial biofilms of the “*tina*” wood vat used in the Ragusano cheese making process. Applied and Environmental Microbiology 73, 6980–6987.

Lippincott-Schwartz J., N. Altan-Bonnet, G.H. Patterson. 2003. Review: photobleaching and photoactivation: following protein dynamics in living cells. Nature Cell. Biology, 5 S7-S14.

Lorén N., M. Langton and A.M. Hermansson. 2007. Confocal fluorescence microscopy (CLSM) for food structure characterization. In: Understanding and controlling the microstructure of complex foods. (D.J. McClements, Ed), Woodhead Publishing Limited, Abington, Cambridge, England. pp.232-257.

Lortal S., A. Di Blasi, M.N. Madec, C. Pediliggieri, L. Tuminello, G. Tanguy, J. Fauquant, Y. Lecuona, P. Campo, S. Carpino, G. Licitra. Tina wooden vat biofilm: A safe and highly efficient lactic acid bacteria delivering system in PDO Ragusano cheese making. 2009. International Journal of Food Microbiology. 132, 1–8.

Low D., J. A. Ahlgren, D. Horne, D. J. McMahon, C. J. Oberg, and J. R. Broadbent. 1998. Role of *Streptococcus thermophilus* MR-1C capsular exopolysaccharide on cheese moisture retention. Appl. Environ. Microbiol. 64:2147–2151.

Lucey, J. A. 1995. Effect of heat treatment on the rennet coagulability of milk. Pages 171–187 in Heat induced changes in milk. 2nd ed. P. F. Fox, ed. International Dairy Federation, Brussels, Belgium.

Lteif L., A. Olabi, O. Kebbe Baghdadi, and I. Toufeili. 2009. The characterization of the physicochemical and sensory properties of full-fat, reduced-fat, and low-fat ovine and bovine Halloumi. J Dairy Sci 92: 4135-4145.

Lucey J. A., M. Jonhson and D. S. Horne. 2003. “Perspectives on the basis of the rheology and texture properties of cheese”. J. Dairy Sci., 86:2725-2743.

Marangoni A.G. and D. Rousseau. 1996. Is plastic fat governed by the fractal nature of the fat crystals? J Am Oil Chemists Soc 73 (8), 991-994.

Marangoni A.G. 2002. The nature of fractality in fat crystal networks. Trends Food Sci. and Tecnol. 13 (2), 37-47.

Martini S., J. E. Thurgood, C. Brothersen, R. Ward, and D. J. McMahon. 2009. Fortification of reduced-fat Cheddar cheese with n-3 fatty acids: Effect on off-flavor generation. *J Dairy Sci* 2009 92: 1876-1884.

McMahon, D. J., C. J. Oberg, and W. McManus. 1993. Functionality of Mozzarella cheese. *Aust. J. Dairy Technol.* 48:99–104.

McMahon, D. J., and C. J. Oberg. 1998. Influence of fat, moisture, and salt on functional properties of Mozzarella cheese. *Aust. J. Dairy Technol.* 53:98–101.

McMahon D. J., Robert L. Fife, and Craig J. Oberg. 1999. Water Partitioning in Mozzarella Cheese and Its Relationship to Cheese Meltability. *J Dairy Sci* 82:1361-1369.

McMahon D. J., and B. S. Oommen. 2008. Supramolecular Structure of the Casein Micelle. *J. Dairy Sci.* 2008. 91:1709-1721. doi:10.3168/jds.2007-0819.

Melilli C., D. Carcò, D. M. Barbano, G. Tumino, S. Carpino, and G. Licitra. Composition, Microstructure, and Surface Barrier Layer Development During Brine Salting. *J Dairy Sci* 2005 88: 2329-2340.

Meynier A., A. Garillon, L. Lethuaut and C. Genot. 2003. Partitioning of five aroma compounds between air and skim milk, anhydrous milk fat or full fat cream. *Lait*, 83, 223-235.

Meynier A., V. Rampon, M. Dalgarrondo and C. Genot. 2004. Hexanal and t-2-hexenal form covalent bonds with whey proteins and sodium caseinate in aqueous solution. *International Dairy Journal*, 14 (8), 681-690.

Mistry, V. V., and D. L. Anderson. 1993. Composition and microstructure of commercial full-fat and low-fat cheeses. *Food Str.* 12:259–266.

Moter, A., Göbel, U., 2000. Fluorescence in situ hybridization (FISH) for direct visualization of microorganism. *J. Microbiol. Methods* 41, 85–112.

Muzi P., M. Bologna. 1999. Tecniche di immunoistochimica. Caleidoscopio. Medical System SPA Ed. Genova. pp.23-54.

Nath J., K.L. Jonsson. 2000. A review of fluorescence in situ hybridization (FISH): current status and future prospects. *Biotech. Histochem.*, 75 (2), 54-78.

Nattkemper T.W. 2004. Automatic segmentation of digital micrographs: a survey. *Studies in health technology and informatics* 107 (2) 847- 851.

Navratil M., G.A. Mabbott, E.A. Arriaga. 2005. Chemical microscopy applied to biological systems. *Analytical Chemistry*, 78 (12), 4005-4020.

Oberg, C. J., W. R. McManus, and D. J. McMahon. 1993. Microstructure of Mozzarella cheese during manufacture. *Food Str.* 12:251–258.

Ormö M., A. Cubitt, K. Kallio, L. Gross, R. Tsien, S. Remington. 1996. Crystal structure of the *Aequorea victoria* green fluorescent protein. *Science* 273 (5280): 1392–5.

Pastorino A. J., R. I. Dave, C. J. Oberg, and D. J. McMahon. 2002. Temperature effect on structure-opacity relationships of nonfat Mozzarella cheese. *J. Dairy Sci.* 85:2106–2113.

Pastorino A. J., C. L. Hansen, and D. J. McMahon. 2003. Effect of Salt on Structure-Function Relationships of Cheese. *J Dairy Sci* 86: 60-69.

Prasad J.V., D. Semwogerere and E.R. Weeks. 2007. Confocal microscopy of colloids. *J. Phys.: Condens. Matter*, 19 113102 (25pp).

Perry D. B., D. J. McMahon, and C. J. Oberg. 1997. Effect of exopolysaccharide-producing cultures on moisture retention in low-fat Mozzarella cheese. *J. Dairy Sci.* 80:799–805.

Petersen, B. L., R. I. Dave, D. J. McMahon, C. J. Oberg, and J. R. Broadbent. 2000. Influence of capsular and ropy exopolysaccharide-producing *Streptococcus thermophilus* on Mozzarella cheese and cheese whey. *J. Dairy Sci.* 83:1952–1956.

Pierre, A., and G. Brule. 1981. Mineral and protein equilibria between the colloidal and soluble phases of milk at low temperature. *J. Dairy Res.* 48:417–428.

Pruss, H.-D., and L.-W. Bahrs. 1981. Preparation of cheese with ropy lactic acid bacteria. US patent 4243684.

Rynne, N. M., T. P. Beresford, A. L. Kelly, and T. P. Guinee. 2004. Effect of milk pasteurization temperature and in situ whey protein denaturation on the composition, texture and heat-induced functionality of half-fat Cheddar cheese. *Int. Dairy J.* 14:989–1001.

Russ J.C. 2005. *Image Analysis of Food Microstructure*. 4<sup>th</sup> ed. Boca Raton, FL, CRC Press LLC.

Shaner N, Steinbach P, Tsien R (2005). "A guide to choosing fluorescent proteins". *Nat Methods* 2 (12): 905–9.

Sheppard C.J.R., D.M. Shotton. 1997. *Confocal Laser Scanning Microscopy*. Bios Scientific Publisher, Royal Microscopical Society, UK.

Singh, H., and A. Waungana. 2001. Influence of heat treatment of milk on cheesemaking properties. *Int. Dairy J.* 11:543–551.

Slavik J. (1996). *Fluorescence Microscopy and Fluorescent Probes*, 1. Plenum Press, New York, 306.

Smith W.F. 2004. *Foundations of Materials Science and Engineering* 3<sup>rd</sup> ed., McGraw-Hill.

Sprague B.L., J.G. McNally. 2005. FRAP analysis of binding: proper and fitting. *Trends in Cell Biology*, 15 (2), 84-91.

Spring KR, M.W. Davidson. "Introduction to Fluorescence Microscopy". 2008. *Nikon MicroscopyU*.

Stading M, M. Langton and A.M. Hermasson. 1993. Microstructure and rheological behavior of particulate beta-lactoglobulin gels. *Food Hydrocolloids* 7(3), 195-212.

Stanley D. W. 1987. Food texture and microstructure. In: *Food Texture: Instrumental and sensory Measurement*. Moskowitz, H. R. Ed. Marcel Dekker, Inc, New York, NY.

Tsien R. 1998. "The green fluorescent protein". *Annu Rev Biochem* 67: 509–44.

Vodovotz Y., E. Vittadini, J. Coupland, D. J. McClements, and P. Chinachoti. 1996. Bridging the gap: use of confocal microscopy in food science.

Voilley A., M.A. Espinoza Diaz and P. Landy. 2000. Flavour release from emulsion and complex media. In: *Flavour release*. Roberts D.D. and Taylor A.J. Washington, DC, American Chemical Society, 142-152.

Walstra, P. 1995. Physical chemistry of milk fat globules. In: *Advanced Dairy Chemistry Vol. 2: Lipids*, 2 ed., Fox, P. F., ed. Chapman & Hall, London.

Walstra P. 2003. *Physical Chemistry of Foods*. Ed. By Marcell Dekker, Inc.

Weinbreck F., H.S. Rollema, R.H. Tromp, C.G. De Kruif. 2004. Diffusivity of whey protein and gum Arabic in their coarcervates. *Langmuir*, 20, 6389-6395.

Yang F., L. Moss, G. Phillips. 1996. The molecular structure of green fluorescent protein. *Nat Biotechnol* 14 (10): 1246–51.

Yuste R. 2005. Fluorescence microscopy today. *Nat Methods* 2 (12): 902–4.